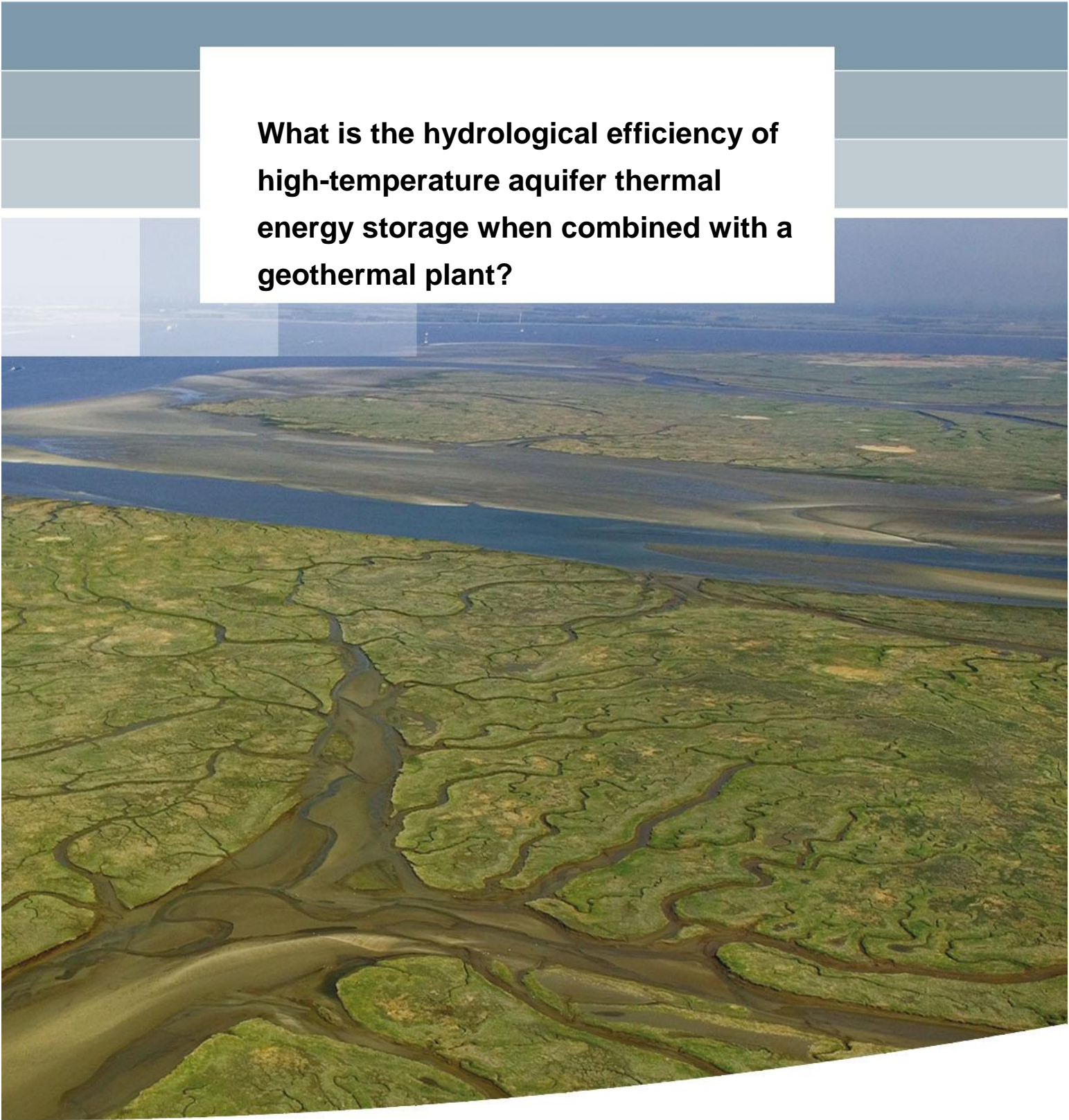


**What is the hydrological efficiency of high-temperature aquifer thermal energy storage when combined with a geothermal plant?**





**What is the hydrological efficiency of high-temperature aquifer thermal energy storage when combined with a geothermal plant?**

Clothilde Pineaud

1209489-002



**Title**

What is the hydrological efficiency of high-temperature aquifer thermal energy storage when combined with a geothermal plant?

Project	Reference	Pages
1209489-002	1209489-002-HYE-0003	96

**Keywords**

High-temperature aquifer thermal energy storage, aquifer heterogeneity, heat transport modelling, density-driven flow

**Summary**

During this five months internship, consideration has been given to the efficiency of a system that combines deep geothermal system (about 2 km depth) with a high-temperature heat storage system at shallower depth (about 200m depth). The idea is to run the geothermal plant continuously throughout the year, and to store in an aquifer (Maassluis Formation) the excess heat produced during summer which is not needed for the glasshouses and to extract it back when needed in winter. The study is based on a pilot project in Vierpolders, next to Brielle.

The combination of production and storage of heat becomes interesting if enough energy can be recovered after being stored for one season. This study investigates this process, which is governed by the geology and the hydrogeology of the storage aquifer and by the design of the system. The heterogeneity of the aquifer plays a major role that is emphasized during the study. One part of the work consisted in collecting data to assess this heterogeneity and understand its spatial structure. Grain-size analyses were performed and other types of data such as gamma-ray logs, core analysis or lithology cross-sections permit to determine the correlation lengths of the hydraulic parameters. Then numerical modeling was used to answer those questions, through stochastic modeling.

Version	Date	Author	Initials	Review	Initials	Approval	Initials
	Sep. 2014	Clothilde Pineaud	<i>CP</i>	Jasper Griffioen	<i>JG</i>	Hilde Passier	<i>HP</i>

**State**  
final



## Contents

<b>1 Introduction</b>	<b>7</b>
<b>2 Study area</b>	<b>11</b>
2.1 Geology	11
2.2 Hydrogeology	17
2.3 ATES system design	20
<b>3 Aquifer architecture and properties characterization</b>	<b>23</b>
3.1 Methodology and data	23
3.1.1 Initial data analysis	23
3.1.2 Hydraulic conductivity estimation	30
3.1.3 Stochastic simulation	30
3.2 Results	34
3.2.1 Results of the TGA and comparison of the different grain-size measurements	34
3.2.2 At the core scale	37
3.2.3 At the borehole scale	40
3.2.4 At the local scale: close wells	43
3.2.5 At the regional scale	46
3.2.6 Summary	51
<b>4 Model exercise</b>	<b>53</b>
4.1 Model construction	53
4.1.1 Simulation domain and boundary conditions	55
4.1.2 Flow parameters	59
4.1.3 Thermal parameters	61
4.1.4 Output treatment	62
4.2 Model results	63
4.2.1 Reference case and comparison with the effect study results	63
4.2.2 Impact of the heterogeneity	70
4.2.3 Density effect	76
4.2.4 Impact of the ATES design: different storage temperature	79
4.2.5 Impact on the overlying aquifer	80
4.2.6 Summary	81
4.3 Discussion	82
<b>5 Conclusion</b>	<b>85</b>
<b>6 Bibliography</b>	<b>87</b>
<b>Appendix 1. Detailed description of core H0637 and photographs</b>	<b>91</b>
<b>Appendix 2. Original photographs of the core H0537</b>	<b>93</b>
<b>Appendix 3. Original core descriptions of H0537 and D0227</b>	<b>95</b>
<b>Appendix 4. TGA results</b>	<b>97</b>





## Acknowledgements

Foremost, I would like to express my sincere gratitude to my supervisor, Jasper Griffioen, for the continuous support and precious advice throughout my internship, for giving time to review and comment at the different steps of the study and for a particularly pleasant welcome in the Netherlands. I can say I learnt a lot from his knowledge and experience.

I also want to thank Wijnb Sommer, for providing help and enthusiasm, and time to find hidden bugs in the scripts. Thank for sharing his experience in ATES systems.

A general thank you to the entire Deltares team, to Rob van Galen for its help in the laboratory, to Miranda for its help with administrative details, to the BGK department for helpful responses, in particular Johan Valstar, for the Deltares team of interns and juniors that made my stay really pleasant. Also thank you to the TNO members that also provided help, in particular Wim Westerhoff, Ronald Vernes, Ronald Harting, Marcel Bakker and Alex Klomp for his welcome in the core house.

Finally, thank you to my teacher François Larroque, the supervisor of this internship and university lecturer in ENSEGID, being available during the internship period.

## Table of figures

Figure 2.1:	Cross-section west of the Roer Valley Graben. The site is located in the middle part of the cross-section. Source: Digital Geological Model v2.2.....	12
Figure 2.2:	Paleogeographical maps showing the development of the Rhine-Meuse and Eridanos fluvio-deltaic systems in the Southern North Sea Basin during the early Pleistocene. The Roer Valley Graben is indicated with black lines. The site location is indicated by a red cross. Source: Westerhoff, 2009.....	13
Figure 2.3:	A) Schematic map of a tide-dominated estuary. B) Longitudinal variation of the intensity of the three main physical processes and the resulting directions of net sediment transport. C) Longitudinal variations of the grain-size and sediment concentration. Source: Dalrymple and Choi, 2007.....	16
Figure 2.4:	Thickness map of the Maassluis Formation. The lighter the colour the thicker the formation is. Along the coastline the thicknesses of 300m are reached while along the eastern margins of the area it reaches several meters. Red lines represent faults which were active in the Maassluis Formation. The site location is indicated with a red cross. Source: Noorbergen, 2013.....	17
Figure 2.5:	Temperature log from a well located 20 km from the site (well coordinates: X: 92461, Y: 437430).....	20
Figure 2.6:	Operation condition of the aquifer thermal energy storage system during injection (summer) and withdrawal (winter) periods. The colours of the arrow correspond to the relative temperature difference in the doublet. Modified picture from Buik & Godschalk, 2011.....	21
Figure 2.7:	Variation of temperature in the hot and cold wells over two years according to the values of the study effect (Buik & Godschalk, 2011).....	22
Figure 3.1:	Map locating the boreholes used in the study. The cross-sections presented in section 3.2 are also located.....	24
Figure 3.2:	Schematic representation of Monte Carlo simulation applied for uncertainty analysis in hydraulic conductivity in groundwater modelling. (From Earth Surface Hydrology) .....	31
Figure 3.3:	Different types of variograms with corresponding distribution of a given parameter along the vertical dimension. (from www.stations.com) .....	32
Figure 3.4:	Correlation between difference in $d(0.5)$ between treated and untreated samples and other parameters .....	36
Figure 3.5:	Grain-size distribution for the sample D113 from the borehole B37D0228, both treated and untreated. The arrows show the effect of the treatment. ....	37
Figure 3.6:	Grain size-distribution of the 1 meter cores samples from cores D0227 and H0537 .....	38
Figure 3.7:	Percentage of clay, silt and sand along the core length, according to the grain-size analysis for cores D0227 and H0537, the blue dots correspond to the fraction above 2 mm that was removed from the samples prior to the measurements, it gives an approximation of the shells contents."Lutum" means "clay". .....	39

Figure 3.8. Grain-size distribution of the 59 samples from well D0228 along the Maassluis Formation ..... 40

Figure 3.9. A) Percentage of clay, silt and sand along the Maassluis Formation, according to the grain-size analysis, for well D0228, the red dots correspond to the fraction above 2 mm that was removed from the samples prior to the measurements, it gives an approximation of the shells contents.”Lutum” means “clay”. B) Lithological log of well D0228. Clay is represented in green (5 different clayey textures) and the different sand textures in yellow. .... 41

Figure 3.10. Variograms of 8 wells and exponential model variogram that fits the best. Values were normal transformed to be compared. .... 42

Figure 3.11. Variogram of the well B37B0172, showing the different spatial structures. A trend is visible in this variogram, as well as cyclicity. The red dashed line shows the variance of the gamma-ray values. .... 43

Figure 3.12 . Comparison of the variograms of the pair of wells B3807 and B3808 ..... 44

Figure 3.13 . Comparison of the gamma-ray logs of the pair of well B3807 and B3808..... 45

Figure 3.14 . Comparison of the lithological logs of the pairs of a) H2651 and H2652 and b) 5437 and 5439. .... 46

Figure 3.15. Lithological cross-section A-A’ including gamma-ray logs in blue and spontaneous potential in grey. The Maassluis Formation boundaries, indicated in grey, are determined from the DGM. Clay layers are distinguished from sand layers by a different colour. Sand layers themselves are individualized by the width of the layers according to their coarseness. The symbol ø indicates the presence of shell-rich layers (sand containing more than 30% of shells above 2 mm). See Figure 3.1 for the location ..... 47

Figure 3.16. Lithological cross-section B-B’ including gamma-ray and spontaneous potential logs. See figure 3.15 for legend and Figure 3.1 for the location. .... 48

Figure 3.17 . Lithological cross-section C-C’ including gamma-ray logs. See figure 3.15 for legend and Figure 3.1 for the location. .... 49

Figure 3.18. Lithological cross-section D-D’ including gamma-ray logs. See figure 3.15 for legend and Figure 3.1 for the location. .... 50

Figure 4.1. Schematized domain of model 1. Not to scale. .... 56

Figure 4.2. Schematized domain of model 2. Not to scale. .... 57

Figure 4.3. Schematized domain of model 1. Not to scale ..... 58

Figure 4.4. Example of one stochastic realization, with a maximum horizontal correlation range of 1000 m. The logarithm of hydraulic conductivities in meter per days. .... 60

Figure 4.5. Cross-section of the resulting temperature difference with initial temperature in model 1, at t=1800 days. The green scale represents hydraulic conductivity. .... 64

Figure 4.6. Plan views showing resulting temperature of model 1 at t=1620 and t=1800, using the same scale, at a depth between 130 and 145 m. The dashed line shows the location of the cross-section (figure 4.4)..... 65

Figure 4.7. Temperature influence (difference with initial temperature) results from the effect study (Buik & Godschalk, 2011). Top figures show the plume at the end of the winter season and bottom ones at the end of summer, after 5 years of exploitation. ....	66
Figure 4.8. Temperature variation in a hot and a cold well through the five years of exploitation. ....	67
Figure 4.9. Operation conditions according to the effect study ((Buik & Godschalk, 2011).....	67
Figure 4.10. Drawdown in meters in the storage aquifer at a depth between 130 m and 140.5 m after an injection period after 5 years of exploitation (t = 1620).....	68
Figure 4.11 Drawdown in meters in the storage aquifer at a depth between 130 m and 140.5 m after an extraction period after 5 years of exploitation (t = 1800).....	69
Figure 4.12. Hydraulic influence in the storage aquifer at the end of winter (top figure) and at the end of summer (bottom figure) according to the effect study (Buik & Godschalk, 2011).....	70
Figure 4.13. Extent of thermal plume for the four different types of model after 5 years of exploitation (t = 1800d). The green scale indicates the hydraulic conductivity.....	71
Figure 4.14. Cross-sections of the resulting temperatures for the five different realizations with a horizontal correlation range of 1000 m (model 3a) .....	73
Figure 4.15. Cross-sections of the resulting temperatures for the five different realizations with a horizontal correlation range of 100 m (model 3b).....	74
Figure 4.16. Thermal recovery for the hot well the different types of model with injection temperature 84C .....	75
Figure 4.17 . Thermal recovery for the cold well the different types of model with injection temperature 84C .....	76
Figure 4.18. Energy balance ratio for the different types of model with injection temperature 84C .....	76
Figure 4.19. Comparison between no density effect (top figure) and density effect included (bottom figure). The red zones indicates the supplementary thermal plume extent. ....	78
Figure 4.20. Difference in hydraulic heads between the runs with and without density effect....	78
Figure 4.21. Difference in resulting temperature between the runs with and without density effect for model 1 and 3a. ....	79
Figure 4.22. Thermal recoveries and energy balance ratio for the different types of model and different injection temperature. The same legend is used for the four figures.....	80
Figure 4.23. Thermal recovery of the hot well for the homogeneous aquifer (model 1) and for the heterogeneous (model 3a) for two different injection temperatures (84C and 15C). In both cases, density-effect is included.....	82
Figure 4.24. Thermal recoveries for the different types of model for injection temperature = 15C .....	83

## 1 Introduction

In the Netherlands, the use of geothermal energy started in the early eighties and since that has developed considerably. This development is alimeted by a specific context: energy demand is rising on a global scale, resulting in energy security and independence concerns, and awareness of climate change leads to new policies aiming at reducing greenhouse gas emissions. As a result, production and use of renewable energies increase. Geothermal energy is one of them. Aside from replacing natural gas based on traditional heating system, it has numerous advantages. The variety of geothermal systems is large and it can be adapted to various contexts and needs, from the individual housing heating to the production of electricity in specific contexts. Besides being a non-greenhouse gas emitting energy, it is a domestic energy resource that supports local economic development and has low ground coverage. It is available year round and independent of seasonal fluctuations and weather conditions.

To be efficient and competitive, geothermal energy has to be well understood and its consequences and environmental impacts to be grasped and controlled. Numerous studies have been performed to quantify these impacts, to weight and to classify them (environmental, physical, chemical, biological, hydrological, thermal, and microbiological). Different tools have been used for this purpose: modeling, life-cycle analysis and calculation of indicators as subsurface footprint, energy return on investment, CO<sub>2</sub> balance or water demand. Within the global comprehension of geothermal energy effects, one of the most challenging aspects concerns groundwater issues. Indeed, groundwater constitutes often a major drinking water resource and brings important ecosystem services, calling for a good protection both qualitatively and quantitatively. In a broader perspective, geothermal energy might interfere with other subsurface uses as gas storage, urbanization infrastructures or drinking water, and must be fully integrated with those. The evolution of geothermal energy has always been closely related to oil and gas production and prices, e.g. the rapid development during the eighties after the oil shock. The recent renewed interest in geothermal energy calls for the setting of a proper policy framework, based on sustainable management strategies, risk consideration and established limits and indicators.

Geothermal energy exists at different scales, following the natural geothermal gradient of the Earth: the use of the shallow ground to heat and cool buildings through a heat pump (Ground Source Heat Pump and Ground Water Heat Pump), the storage of heat in the ground (Aquifer Thermal Energy Storage and Borehole Thermal Energy Storage systems), the production of heat directly from hot water present in deeper layers and the production of electricity with even deeper geothermal systems. The project studied in this report combines in a unique way in the Netherlands high-temperature aquifer thermal energy storage (ATES) with a deeper heat production aquifer. This combination will provide heat to greenhouses that represent a large heat demand in the South Holland province.

Aquifer thermal energy storage knows a revival of interest in the Netherlands these last decades. The country is now pretty well experienced concerning energy storage in the ground, with the first implementation in the early eighties and with the presence of about 1500 ATES systems and 43 000 BTES (closed storage system in boreholes) in 2011 (Heekeren & Bakema, 2013). The advantage of the low topography in the country results in a low hydraulic gradient that prevents temperature dispersion in the surroundings. The interest for direct use of geothermal energy from

deeper layers in the Netherlands is more recent, the first exploration wells being drilled in 2006-2007 in a Lower Cretaceous aquifer in the West Netherlands basin (Vis et al., 2010).

This development comes in the context of a commitment made by the government to achieve 14 % of renewable energy by 2020. This experience leads to a “National Action Plan for Geothermal Energy”, published in 2011, but also to the setting of a specific regulation that had to be build up from scratch. All the systems down to 500 meters deep are concerned by the Water Act while the deeper systems depend on the Mining Act. A permit is required for ATES installations. In the Netherlands, an energy balance in the soil throughout the year is required and storage with temperatures higher than 30°C is not permitted.

ATES does not provide energy but only stores it. Then an external heat source has to be found. For most of the project, this energy come from solar heat, waste heat (industrial and process heat, waste incineration, data centers...) or heat and power cogeneration (HPC). For this study, the heat source lies in the ground itself, produced via a deep geothermal wells system. It is hot groundwater of 85°C that is injected in the aquifer storage. It obtained therefore a specific permission from the Province of South Holland as a pilot project. The combination of high-temperature heat production and storage is interesting because the ATES system acts as a buffer. With a high enough temperature difference, there is no need of heat pump, which implies less external energy input. Furthermore, the storage permits to optimize the geothermal installation, which is associated with a high energy investment in terms of drilling and equipment. The plant can be run year-round without a high loss of energy and thus be fully exploited, with a lower pumping rate needed. When compared to natural gas-based heat systems, the use of geothermal energy and high temperature storage permits to reduce the CO<sub>2</sub> emissions by 25,7 tons/year, according to the effect study (Buik & Godschalk, 2011).

In order to compete with fossil fuel based energies, geothermal energy still needs to prove its reliability and efficiency by the mean of numerous studies and different questions still has to be answered. One useful tool to investigate these issues is numerical modeling. Models help to understand these specific processes and to test different scenarios that are not feasible at the field scale and this for a low cost. The success of modeling is highly dependent on the knowledge of the spatial distribution of the aquifer hydraulic properties, which is usually partial, non-exhaustive and sometimes of poor quality. Beside this deficiency in the data, the heterogeneity of the aquifer architecture makes the task even more complex. Representing heterogeneity in the models remains a major challenge. Even more when the heterogeneity is intended to be represented in a realistic way, taking into account the sedimentological controls. Another challenge that plays a major role in the modeling exercise is the scale dependence of the hydraulic properties, varying between process scale, measurement scale and management scale.

Stochastic modeling is used for this study. Considering hydraulic properties as stochastic variables permits the modeler to cope with the lack of knowledge of the deterministic variables distribution and to describe the uncertainties related to them. This method is based on the probability distribution of the hydraulic properties. It requires estimating the spatial correlation of these variables from a limited amount of measurements. This can be done when it is assumed that a parameter value at a specific location depends on its spatial coordinates and neighbors locations values. The aim here is to generate different realizations of 3D field representative of the aquifer structure in order to incorporate them in the model. The different realizations can then be tested statistically.

Within this study, the efficiency of such a combined project is closely studied. Indeed, the combination of production and storage of high temperature heat becomes interesting if enough energy can be recovered after being stored for one season. This study investigates this process that is governed by the geology and the hydrogeology of the storage aquifer and by the design of the system. The heterogeneity of the aquifer plays a major role that is emphasized during the study. During this study, the impact of two different factors driving the system efficiency is investigated:

- The heterogeneity of the aquifer. Indeed during the modeling exercise of the study effect, the aquifer was considered homogeneous, as it is done in most of the studies. But different studies showed that heterogeneity in hydraulic properties affect the heat distribution and then the efficiency of the storage (Bridger & Allen, 2010; Sommer, et al., 2013).
- The impact of the density effect, i.e. the impact of variation of temperature on density and thus on groundwater flow. This will be assessed with different injection temperatures and the models will be run both with and without incorporating the density-effect.

A real effort is put on understand the geology and integrate it in the model. The interest in such a study lies in the multi-disciplinary approach that can bring a new understanding of complex problems.

After introducing the project and its context in the first chapter, the second chapter presents the data collection and analysis that lead to the characterization of the aquifer properties. In the third chapter, the methodology used for the model development is explained, based on the results of the first part, and the results of the geohydrological modeling are then presented. These results are discussed in the light of others researches in the fourth chapter.





## 2 Study area

The pilot project GeoMEC-4P is used as a study case to study how efficient the storage of high temperature thermal energy coming from a deep geothermal system can be.

The field site is situated in Vierpolders, in the municipality of Brielle, in South Holland, at about 10 kilometers of the coast. This area, in the island of Voorne-Putten, at the mouth of the New Maas, is characterized by the strong presence of greenhouses. The project is designed to heat 60 hectares of glasshouses. The project combines two systems:

- A deep geothermal plant, that runs throughout the year and pump water out of a 2200 meter deep aquifer;
- A high-temperature aquifer thermal energy storage system (ATES), that acts as a buffer. It can store the excess heat from the geothermal plant when there is less demand, mainly in summer. The stored energy can be exploited again when demand increases and cannot be supplied by the geothermal plant. The aimed aquifer lies at 200 meters deep.

This study focuses on the latter. The ATES system consists of three doublets, i.e. three hot wells and three cold wells each for which groundwater can be extracted or infiltrated. The distance between the cold and the hot wells is approximately 100 meters.

### 2.1 Geology

The aquifer of concern belongs to the Maassluis Formation. This geological formation corresponds to shallow marine deposits from the Lower Pleistocene, with alternations of shell-containing sand and clay layers. Until recent studies, not so many data were available about these horizons. Indeed, relative large depths and high groundwater salinity hampered hydrogeologists' interests while the exploration wells for oil and gas purpose focused on larger depths. Nowadays, the geological unit is investigated more precisely. A regional mapping for hydrogeological and geothermal research is being made, as well as an inventory of available data to incorporate them in the DINO database.

In the area of the project, the Maassluis Formation rests on the Oosterhout Formation (Figure 2.1). These marine deposits consist of sands, sandy clays and clays with a relatively high content of glauconite. Marine molluscs and bryozoans occur frequently. The formation gradually changes into the overlying Maassluis Formation. This gradual transition is characterized by an upward increase in grain size and the disappearance of glauconite minerals.

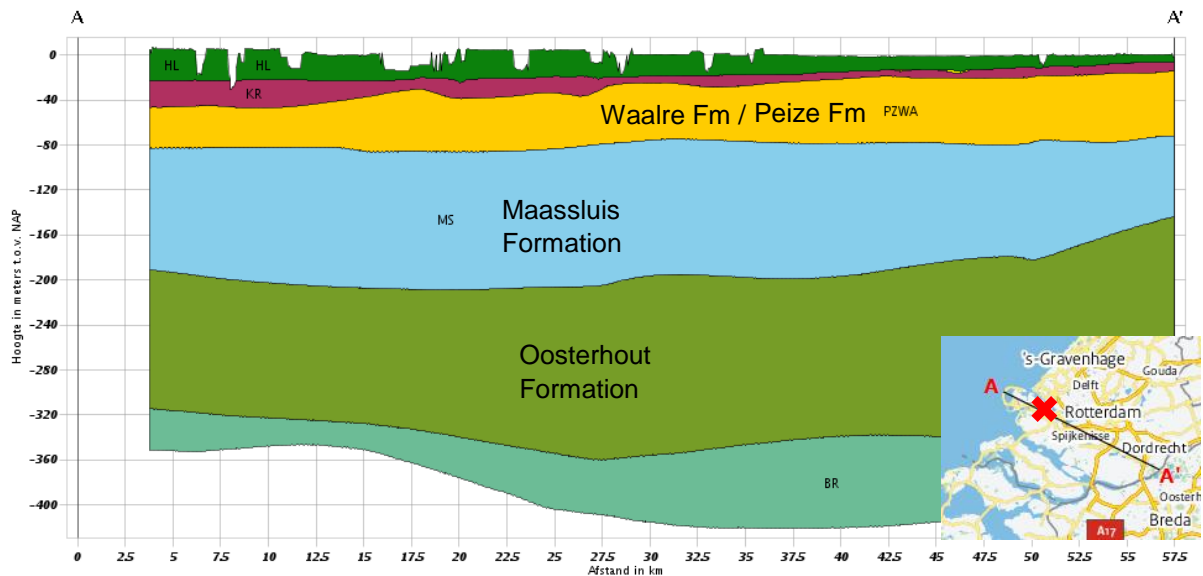


Figure 2.1: Cross-section west of the Roer Valley Graben. The site is located in the middle part of the cross-section.  
Source: Digital Geological Model v2.2.

The Maassluis Formation is overlain by fluvial sands and tidal deposits from the Peize and Waalre Formations. These two formations form a complex system deposited in a prograding deltas context and they interdigitate in the central and western part of the Netherlands. They are, therefore, often considered together as a complex unit in, for example, the REGIS geohydrological model (Vernes et al., 2010). The Waalre Formation corresponds to the fluvial deposition of the Rhine-Meuse system while the Peize Formation corresponds to the fluvial Baltic system, also called Eridanos River system, from the east., It seems that the Waalre Formation, mainly the subunit WA-3, overlays the Maassluis Formation in the surroundings of Brielle, while the Peize Formation is present more to the North. The transition from the Maassluis Formation to the Waalre Formation is also gradual, with a fining-upward trend in grain size and the disappearance of marine shells, although reworked shell fragments can be found in the lower Waalre Formation originating from the underlying Maassluis formation. Above the Waalre-Peize Formation, the Kreftenheye Formation, consisting of fluvial coarse sands and gravels, and the Holocene sediments are successively present. Offshore, the Maassluis Formation grades into the Westkapelle Ground Formation, the IJmuiden Ground Formation and the Winterton Shoal Formation. In order to properly understand the vertical succession of the different layers and the generation of the formation, it is important to have a close look at the geological history and deposit context.

The Tertiary geological setting in the Netherlands is characterized by the presence of the North Sea Basin at the west. It is a large epicontinental sag basin, with a north-south orientation, and developed in response to the gradual lithospheric cooling. Another important element of the regional setting is the major rift system at the southeast that developed during the Eocene and the Oligocene. The Roer Valley Graben, with a NW-SE orientation (visible on Figure 2.2) is part of it. During the Pliocene, the tectonic activity increased and the Roer Valley Graben subsided more and more. A long term tectonic subsidence marks the entire Pleistocene. The North Sea Basin subsidence is accelerated by the development of an important delta, the Eridanos system, that prograded through north-west Europe due to simultaneous uplift of the Fennoscandian Shield. Another delta developed more south, formed by a precursor of the Rhine and alimented by the uplifted Rhenish Massif.

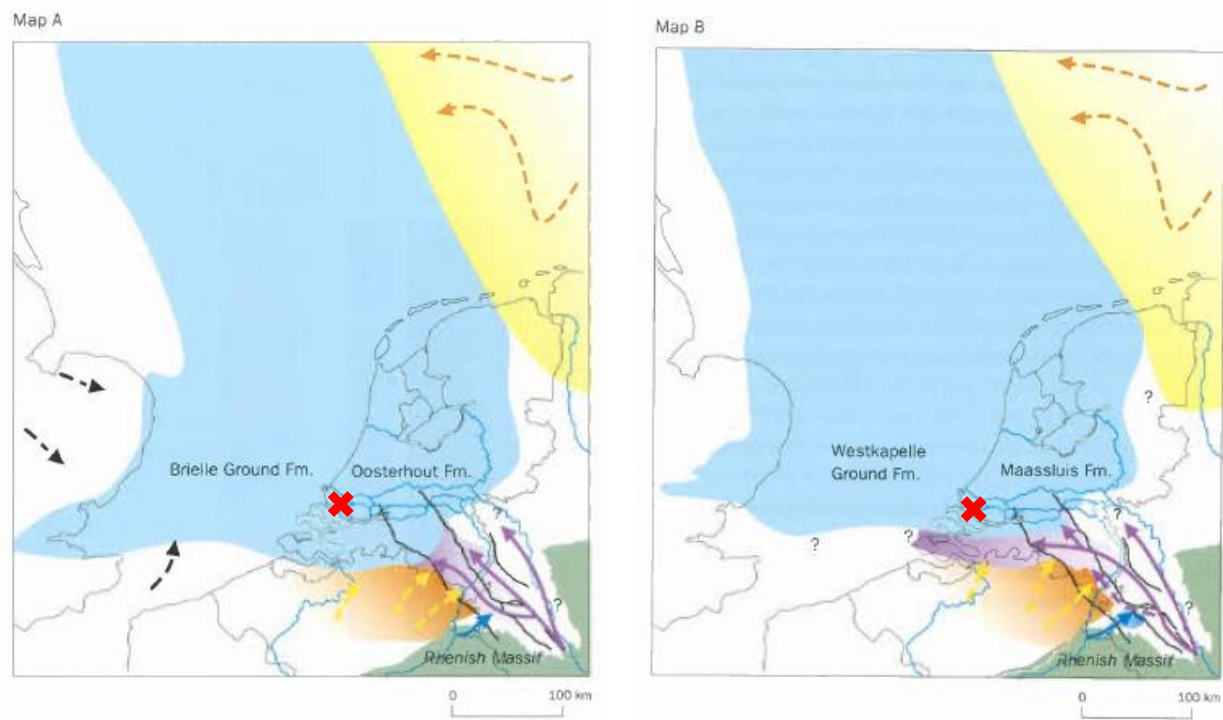
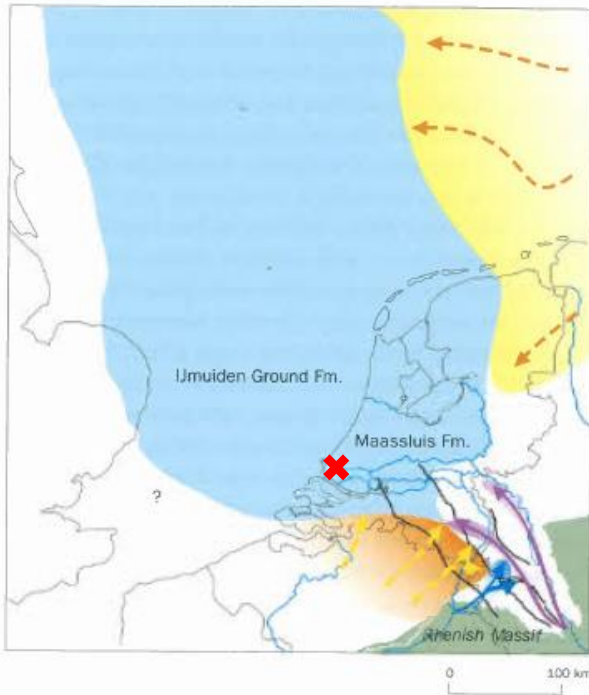
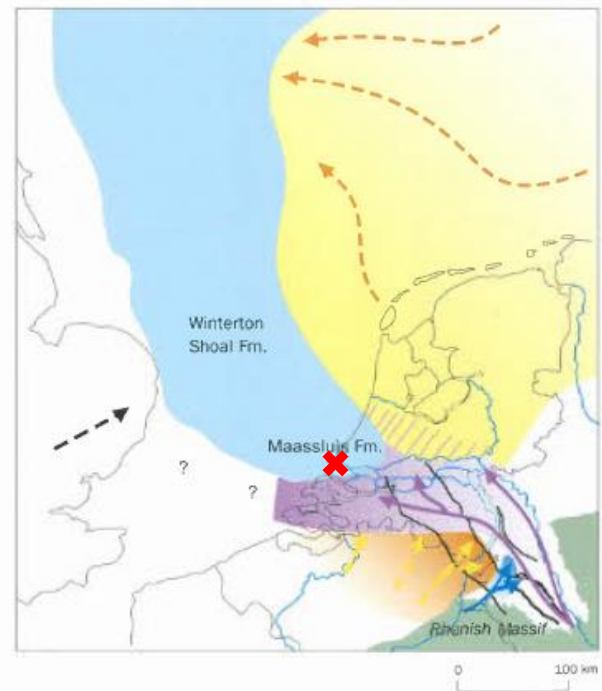


Figure 2.2: (Above and next page) Paleogeographical maps showing the development of the Rhine-Meuse and Eridanos fluvio-deltaic systems in the Southern North Sea Basin during the early Pleistocene. The Roer Valley Graben is indicated with black lines. The site location is indicated by a red cross. Source: Westerhoff, 2009.

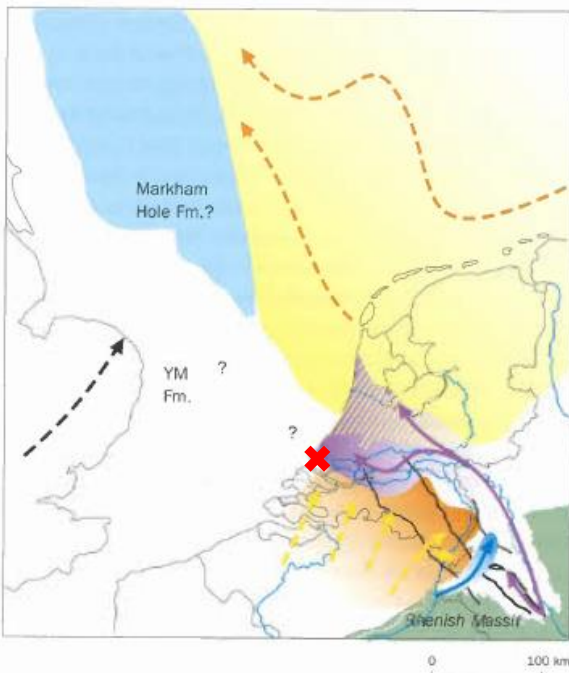
Map C



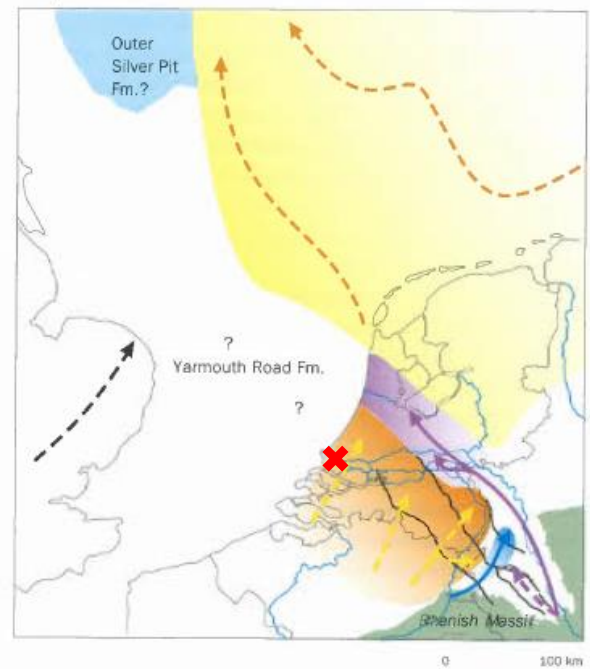
Map D



Map E



Map F



-  Rhine
-  Meuse
-  Belgian rivers
-  Eridanos (Baltic river system)

The development of the Maassluis Formation is then characterized by a near-coastal setting, with tidal and estuarine influence but also with shallow sea features. In the area of Brielle, the main sediment supply came from the Rhine-Meuse fluvial system, from the south-east (Figure 2.2). It is likely to find more proximal deposits, with coarser sand facies and continental influence in this direction. In the seaward direction, i.e. the north-west, the facies will show more continuous fine or clayey sediments with marine influence. The formation is likely deeper in this part since the accommodation space was more important and the sediments are less eroded.

Dalrymple & Choi (2007) described the morphologic and facies trends that are found in fluvial-marine transitions dominated by tidal influence. Those types of facies show an inherent complexity because terrestrial and marine processes interact in this zone. Four main driving factors play a key role: 1) the varying bathymetry and geomorphology of the system, 2) the different types of energy and currents, 3) the frequency, rate and direction of sediment movement, and 4) the salinity of the water. Several sub-environments are found in the transition zone, with varying grain-size distribution, sedimentary structures and organism assemblages (Figure 2.3). The tidal action is responsible for the development of coast-normal, elongated tidal sandy bars that show an erosion base and upward fining successions. These tidal bars contrast with the wave-generated, coast-parallel barriers that are found in an environment dominated by wave action. This will be relevant further in the study. Muddy tidal flats are deposited at the fringe of the estuary, commonly bordered by an erosional channel margin that shows cross-beds stratification. The prodelta, i.e. the seaward part of deltas, is characterized by muddy, finely laminated deposits because the coarsest sediments are deposited closest to the river mouth and the finest ones farthest away.

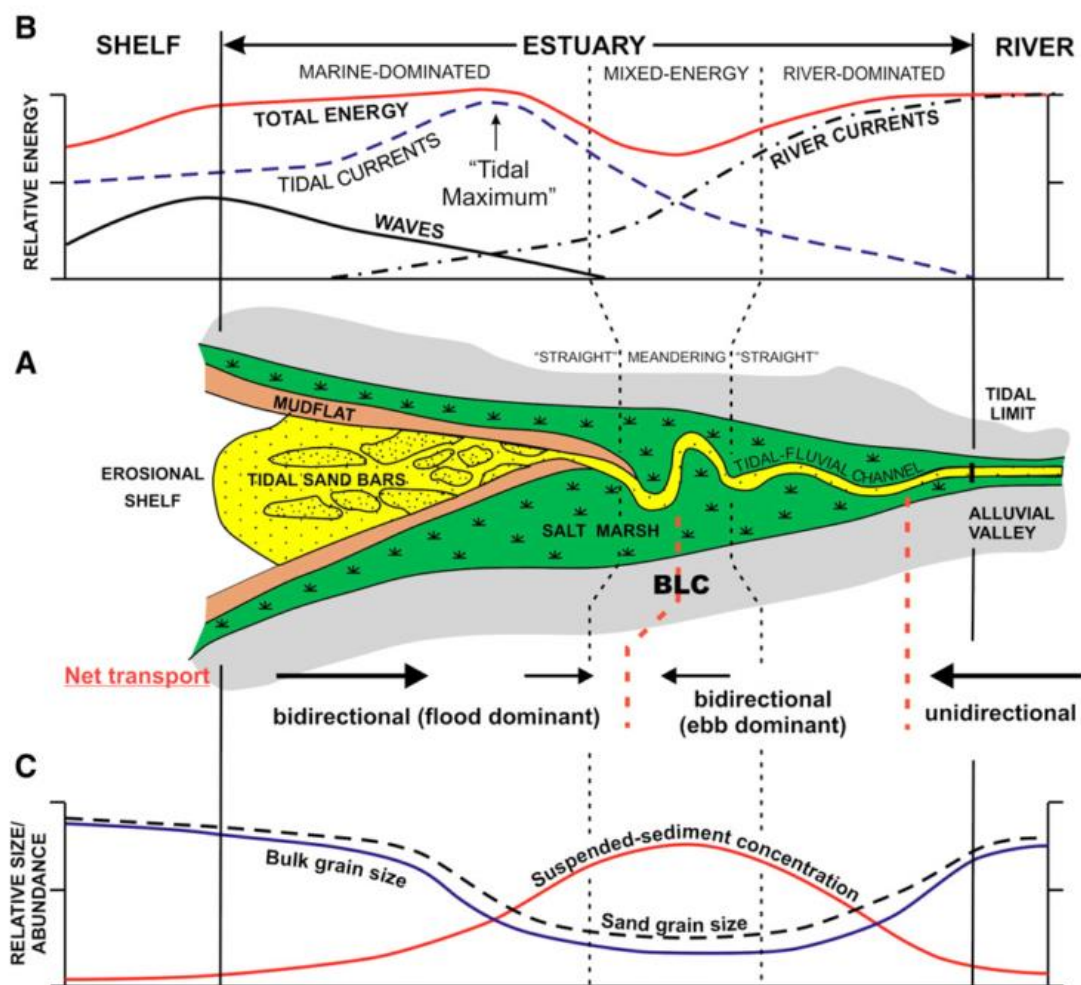


Figure 2.3: A) Schematic map of a tide-dominated estuary. B) Longitudinal variation of the intensity of the three main physical processes and the resulting directions of net sediment transport. C) Longitudinal variations of the grain-size and sediment concentration. Source: Dalrymple and Choi, 2007.

The progradation of the complex delta system is related to the retreat of the coast line in a northwestern direction. The transition between the Maassluis Formation and the Waalre-Peize Formation that corresponds to the fluvial part follows this direction as sediments are deposited. It is in the area of Maassluis and Brielle that the shallow marine context persisted the longest, explaining a more important thickness of the formation in this area, with the top of it at a shallower depth.

The global geometry of the Maassluis Formation therefore results of this deposit environment setting and its evolution. A gradual SE-NW thickening is observed while the younger and shallower deposits took place in the Brielle area. (Figure 2.4) This is visible in the cross-section of the Pleistocene deposits (Figure 2.1).

The lateral and overlying units are marked by a complex interplay of three main river systems: the Rhine, the Meuse and the smaller Belgian rivers. At a broader scale, complexity is increased by the role of the more extensive fluvio-deltaic Eridanos river system. The marine formations represent a more continuous record of marine and deltaic deposits. But the intra-formation scale

shows a high complexity as well, emphasised by the simultaneous presence of different facies, explaining that the Maassluis Formation is described as a complex unit in the REGIS model for example. The complexity of the formation can also be explained by the stacking and the coalescence of sand bars and shifting channel that can be partly eroded. This stacking usually follows the logical of the transgression/regression cycles succession, or the glacials/interglacials cycles. Because of erosion and overlapping of the bars, it is difficult to follow laterally the sequence of these cycles, notably to build cross-sections from boreholes information.

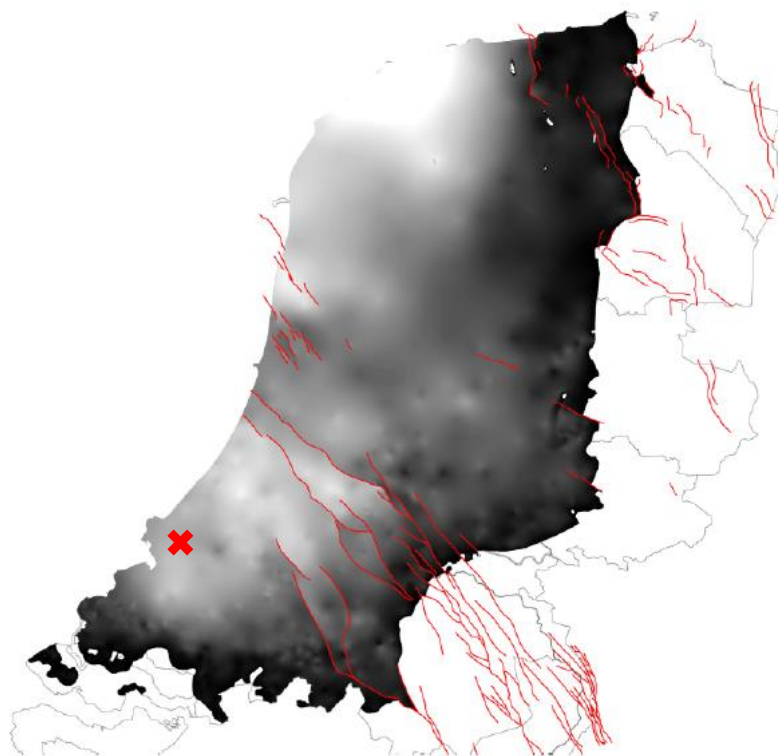


Figure 2.4: Thickness map of the Maassluis Formation. The lighter the colour the thicker the formation is. Along the coastline the thicknesses of 300m are reached while along the eastern margins of the area it reaches several meters. Red lines represent faults which were active in the Maassluis Formation. The site location is indicated with a red cross. Source: Noorbergen, 2013.

## 2.2 Hydrogeology

The following hydrogeological context description is mainly based on the effect study (Buik & Godschalk, 2011) that has been done by the consultant company IF Technology prior to project implementation. For the purpose of the study, two pilot boreholes were drilled at the site in 2011, of 209 m and 102 m deep respectively. From the description of encountered lithology including estimated grain-sizes, a scheme of the aquifer architecture was constructed. Furthermore, a pumping test was carried out in 2011 to determine the hydraulic properties of the aquifer. Together with a study of regional data, this information permits to set the aquifer description and distinguish the following layers (Table 2.1):

- The confining layer, consisting of about 8 meters of clay, peat and sand layers. This layer corresponds to Holocene deposits, a semi-permeable layer highly studied all over the Netherlands ;
  - The first aquifer unit, that is associated with the Kreftenheye Formation, with a thickness of about 40 meters. Consisting of coarse sand mainly, it shows a relative high hydraulic conductivity of about 15 m/d ;
  - The first aquifer is separated from the next aquifer unit by clay and fine sand layers, with a low to medium conductivity of 0,5 m/d, due to two sandier layer of 6 and 3 meters thick respectively ;
  - At 80 meters deep comes the combined second and third aquifer unit that is the aimed aquifer for storage. The mean hydraulic conductivity is about 7 m/d, lessened by local separating layers with a finer lithology ;
- The hydrological basis is found at a depth of about 200 meters, with a clay layer of at least 9 meters thick, the drilling not going deeper.

According to the effect study (Buik & Godschalk, 2011), the water table at the site is on average 0,8 m below the surface and ranges during the year between 0,5 and 1 m below surface. The hydraulic head in the first aquifer is approximately 0,5 m below the surface and it is about 0,3 m above the surface in the combined second and third aquifer. The effect study specifies that the horizontal water flow in both aquifer units is less than 1 meter per year and that this flow goes in southeastern direction. A hydraulic gradient of about  $i = 0,0004$  can then be deduced from this data.

The initial storage aquifer temperature according to the same study is 13°C. This value is derived from Stolk (2000) and calculations in the effect study are made from this value. To be more precise, a well log of temperature measurement can be used to take into account the geothermal gradient. A log is available for a well situated in Rotterdam, at about 20 km of the site (Figure 2.5). It shows an increase of 1°C on 50 meters after 150 m deep, but starting with a higher temperature than noted in the effect study.



Table 2.1: Description and characteristics of the different units present at the site. The height of the rows represents roughly the actual unit thickness. The blue colour is related to the hydraulic conductivity. From Buik & Godschalk, 2011.

relative to NAP)	Thickness (m)	Lithology	Hydrogeology	Hydraulic parameters (transmissivity (m <sup>2</sup> /d) and resistance (days))
+0 to -8	8	Clay, peat and sand	coating	c = 800 days
-8 to -44	36	Moderately coarse sand	First aquifer	kD = 560 m <sup>2</sup> /day
-44 to -63	19	Solid clay and fine sand	First separating layer	c = 1,76 days
-63 to -69	6	Moderately fine sand	Sandier layers	kD = 8 m <sup>2</sup> /day
-69 to -74	5	Solid clay and fine sand	First separating layers	c = 370 days
-74 to -77	3	Moderately fine sand	Sandier layers	kD = 12 m <sup>2</sup> /day
-77 to -80	3	Solid clay and fine sand	First separating layers	c = 370 days
-80 to -168	88	Predominantly fine to medium coarse sand with clay layers	Combined second and third aquifer	kD = 650 m <sup>2</sup> /day
-168 to -180	12	Hard to very hard clay	Local separating layer aquifer	c = 800 days
-180 to -200	20	Predominantly fine to medium coarse sand with clay layers	Combined second and third aquifer	kD = 145 m <sup>2</sup> /dag
> -200	-	clay	hydrological basis	c = ∞

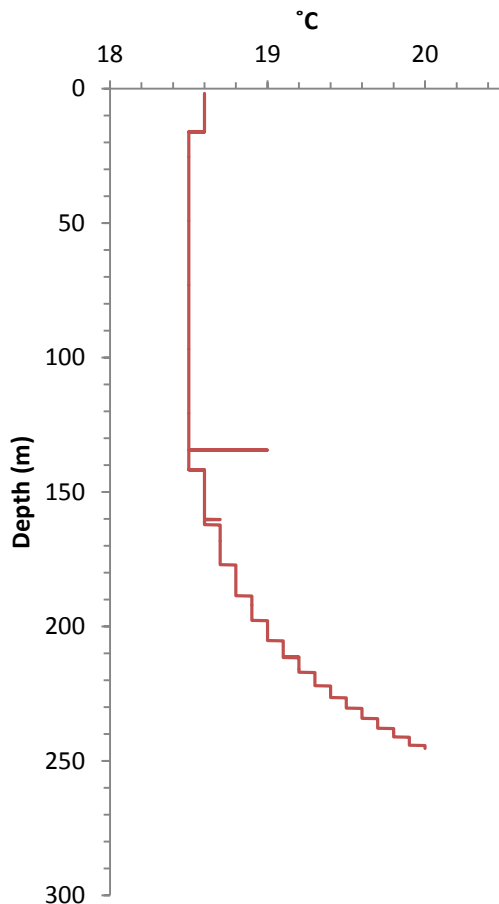


Figure 2.5: Temperature log from a well located 20 km from the site (well coordinates: X: 92461, Y: 437430)

The water in the storage aquifer is saline. The interface between fresh and brackish water, i.e. 150mg/l of chloride, is observed at about 10 m below the surface and the interface between brackish and saline water, i.e. 1000mg/l of chloride, is observed at 30 m below the surface. The calculations in the effect study are based on a chloride content of 6 000 mg/L.

The Strypsche Wetering, which is a “boezemwater”, i.e. a drainage surface water course typical for the polder systems, is present at the west of the site.

### 2.3 ATES system design

The pilot project used in this study is composed of two systems:

- A geothermal installation with wells reaching a water bearing horizon at 2 200 m deep and that runs year-round;
- A high temperature ATES system, between 80 and 200 m deep.

Those two systems are both connected to a central heat exchanger, where the heat is exchanged and distributed over the buildings. The ATES system consists of three groundwater well doublets. A doublet is composed of one hot well and one cold well, located from 100 m from each other. Between a cold well and a hot well, a conveyor line is installed where heat can be exchanged with the central heat system. The terms “cold” and “hot” are used relatively to each other since a cold well can show a higher temperature than natural groundwater in the

surroundings. The configuration of the doublets was designed with the three hot wells in the center and the cold wells located in the external direction.

The running of the installation can be explained following the different seasons (Figure 2.6). During summer, the geothermal plant might produce more heat than the users need. This excess heat is stored in the aquifer through the doublets system. Groundwater is pumped out of the cold well, heated through the exchanger with geothermal heat and re-injected in the hot well at a higher temperature. Along the summer and autumn, heat transport processes occur and temperature decreases at the hot wells.

At the beginning of winter, when the need of heat increases, the pump system is inverted. Groundwater is pumped out of the hot well, releases its heat to the exchanger and is re-injected in the cold well at a lower temperature. This heat, transferred to the central heat system, can be used by the glasshouses in addition to the heat produced by the geothermal plant, which runs continuously. It is important to understand that the water balance remains unchanged since water is always reinjected. Only the thermal balance is changing.

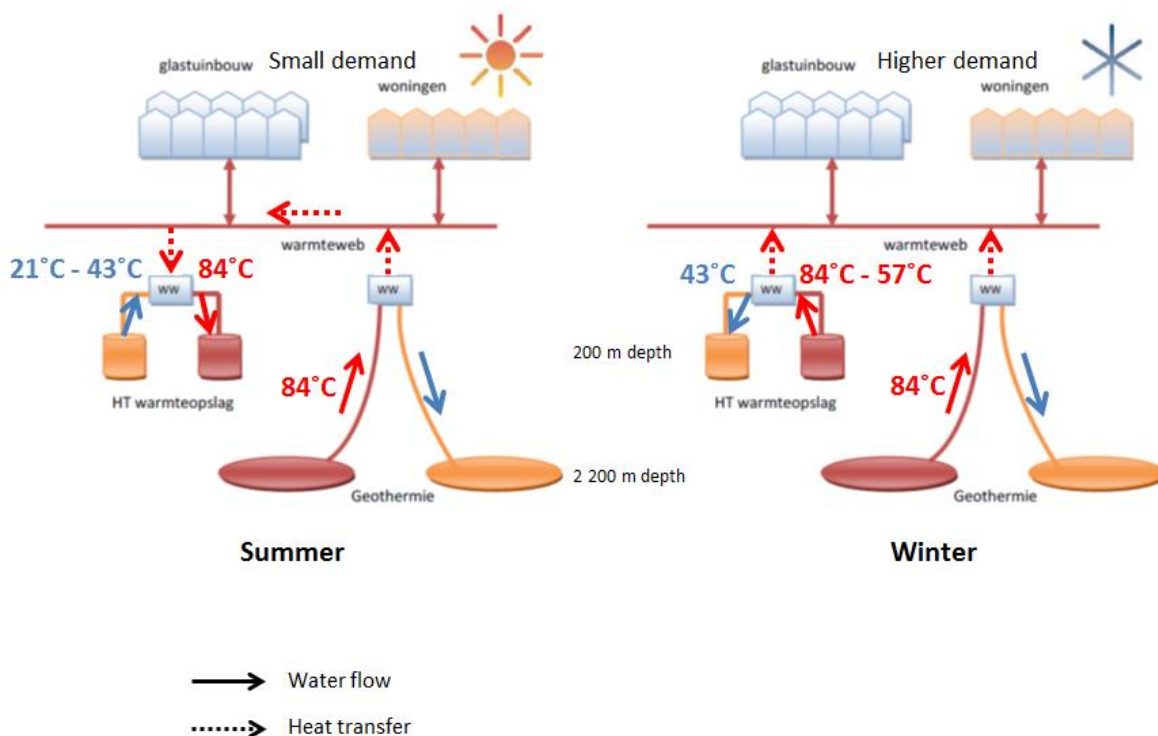


Figure 2.6: Operation condition of the aquifer thermal energy storage system during injection (summer) and withdrawal (winter) periods. The colours of the arrow correspond to the relative temperature difference in the doublet. Modified picture from Buik & Godschalk, 2011.

A modeling exercise permitted the consultant company to deduce that the temperature in the hot wells would reduce from the summer injection temperature 84°C to 57°C before a cycle of storage starts again (Buik & Godschalk, 2011). This loss is central in the understanding of the project efficiency. Another value is suggested by the model. In the first year, groundwater is pumped out at the natural temperature, around 13°C, and heated up to 84°C. But after an entire cycle, the water in the cold wells does not reach back its natural level. According to the calculations, the water would cool down from the winter injection temperature 43°C to 21°C

before being pumped again the next summer (Figure 2.7). Along the lifetime of the installation, the temperature difference between the two wells thus decreases at summer time.

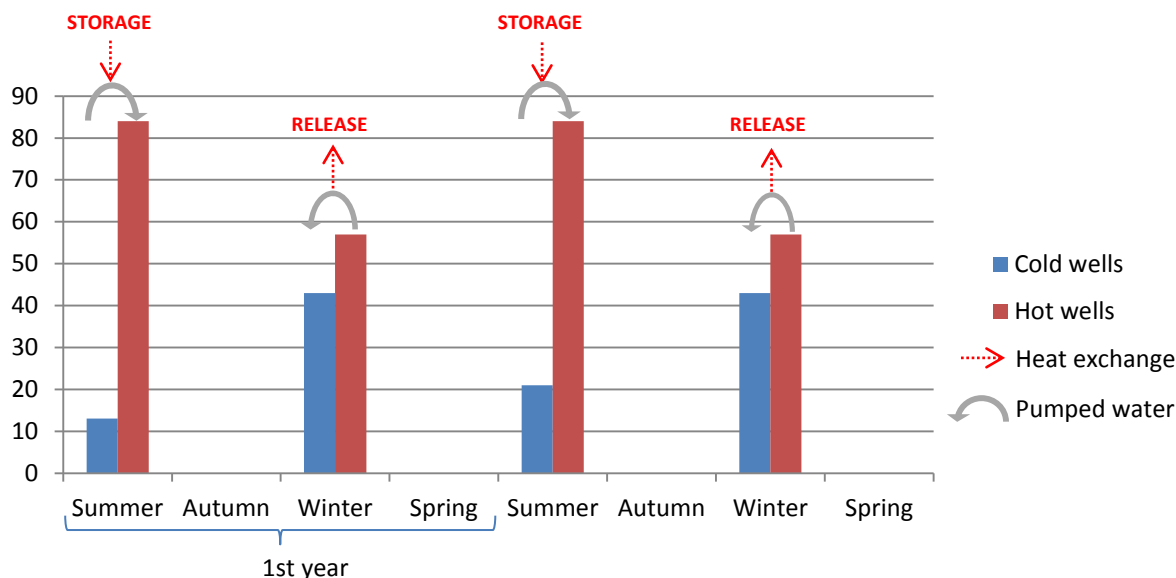


Figure 2.7: Variation of temperature in the hot and cold wells over two years according to the values of the study effect (Buik & Godschalk, 2011)

The consultant company expects after five operating years a thermal influence area that extends to 130 m from the wells in the horizontal direction and between 55 m and 225 m deep in the vertical direction (Buik & Godschalk, 2011). It would thus not reach the first aquifer, which extends until 44 m below surface. The expected exploitation rate is 450 m<sup>3</sup>/h on average, reaching a maximum of 600 m<sup>3</sup>/h. This leads to a yearly rate of 1,45 million m<sup>3</sup>. The model were tested with two exploitation periods of 120 days each, and two rest periods of 60 days each, for 3 years, 5 years and 20 years of exploitation. Concerning the completion of the wells, a minimum of 50 m of filter screen will be placed. The final position of the screen will depend on the encountered aquifer structure at the location of the future wells. They will be placed in the combined second and third aquifer unit, i.e. between 85 m and 200 m below the surface.

This project is considered as a pilot since it derives from the current province groundwater policy on two issues: the energy balance will not be respected between the two wells of a doublet, and the infiltration temperature is above 30°C.

### 3 Aquifer architecture and properties characterization

Hydrogeology is challenging in various aspects: mainly because the studied material is very heterogeneous at various spatial scales. Another major difficulty is that it is not directly accessible. The methods to study aquifers are then indirect and measurements are done on a punctual base. This inaccessibility hinders a correct assessment of the material heterogeneity. Different methods have been developed to recreate this heterogeneity. One of these methods is the stochastic modeling which experiences a growing use. Also, the new abilities of computing permit to model aquifers with a higher resolution. The challenge now is to properly integrate the field data to the model in a geologically realistic manner. For this, a close look is taken at the sedimentary background. This information is then treated statistically to be further incorporated in the model.

The following procedure is followed during the study:

- Analysis of the geology at different scales and from various data (cores, boreholes cuttings, well logs, cross-sections) and understand the repartition of the different textures, facies and geological structures in space (thickness of layers, spacing in the vertical dimension, length of the sedimentary structures, transition between objects)
- Determine the relation between the sedimentary facies and the hydraulic properties (mainly hydraulic conductivity), from gamma-ray and from grain-size distribution
- Simulation of hydraulic conductivity 3D fields with the random field model
- Use of these fields as input in a numerical groundwater and thermal model
- Analysis of the results of the modeling

This chapter presents the first part of this procedure, i.e. analyses of the data and stochastic simulations.

#### 3.1 Methodology and data

##### 3.1.1 Initial data analysis

The architecture of an aquifer is strongly related to its geology. To properly define its hydraulic properties, one must study the geological features from diverse types of data, at different scales and resolutions. The following table resumes the data that were analyzed and their corresponding scale (Table 3.1). The next paragraphs describe the data collection that was made for the study and the analysis of these data.

Table 3.1: Different scales studied along the study

Length (m)	Scale	Data	Resolution (m)
$10^{-1} - 10^0$	Core scale	<ul style="list-style-type: none"> <li>Description and picture</li> <li>Grain-size measurement</li> </ul>	$10^{-1}$
$10^1 - 10^2$ (1D)	Borehole scale	<ul style="list-style-type: none"> <li>Lithology description</li> <li>Grain-size measurements</li> <li>Gamma-ray logs</li> </ul>	$10^0$ $10^0 - 10^1$ $10^{-2} - 10^{-1}$
$10^1 - 10^2$ (2D)	Local scale	<ul style="list-style-type: none"> <li>Comparison of two wells that are close</li> </ul>	
$10^4$	Regional scale	<ul style="list-style-type: none"> <li>Cross-sections</li> <li>Geological deposit model</li> </ul>	

In total, 23 boreholes were listed and used. The following map localizes them (Figure 3.1).

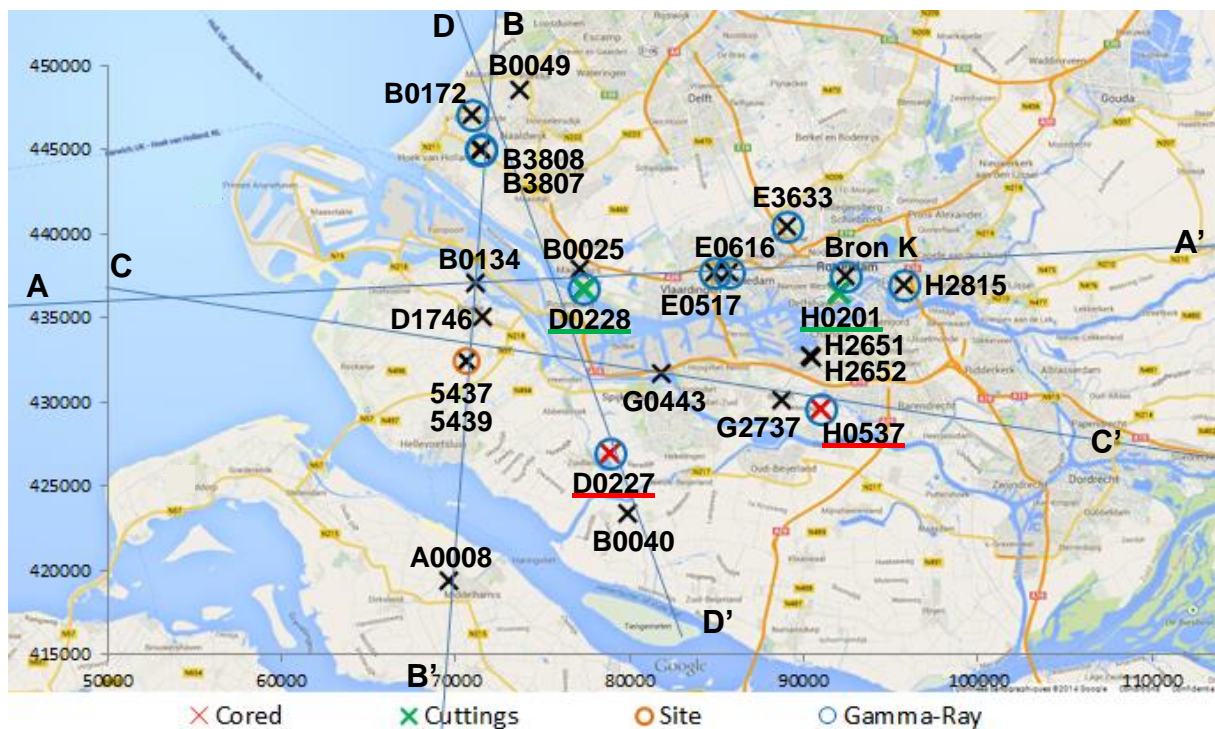


Figure 3.1: Map locating the boreholes used in the study. The cross-sections presented in section 3.2 are also located.

### 3.1.1.1 Core analysis

Sediment core material is one of the few direct ways to study geology and is then a very valuable source of information. It offers the advantage not to alter the structures, in opposition to cuttings for example and to relate units to their original stratigraphic position. Furthermore, it shows a higher resolution than geophysical well logging, highly used in geology. However, it is restricted to one-dimension, which does not permit to observe the horizontal processes as lateral facies changes for example. Caution must be taken to the quality of the core drilling, and to its preservation conditions. Photographs of the undisturbed core are generally taken at the drill rig, which represent precious information for review work. Because it is time-consuming and costly,

core drilling is not done systematically and dedicated to studies with a major interest, usually petroleum geology.

TNO's Geological Survey of the Netherlands (GDN) manages a central core sample storage, which gathers and archives samples from every deep wells made in the country since the introduction of the Dutch Mining Act. This text requires data from wells deeper than 500 m to be made available to the GDN after a confidentiality period of five years. Few cored wells that traverse across the Maassluis Formation were available but only two cores were found with material from the depth of actual interest. Information is resumed in the following table (Table 3.2).

Table 3.2 : Characteristics of the 1 meter cores analysed

Borehole ID	Depth of the well	Available cored interval	Limits of the Maassluis Fm at this location*	Distance from the project site	Pictures available	Core preservation
B37D0227	130 m	98 to 99 m	81 to 200 m	9,9 km	No	Bad
B37H0537	135 m	96 to 97 m	85 to 216 m	20,5 km	Yes	Good

(\*according to the Digital Geological Model built by the GDN)

A major element in core analysis is its qualitative description, based on visual inspection. It includes rock material description, but also, discontinuities, structures, weathering. Total core recovery length is an important indication usually recorded by the driller. It can give information about the rock quality or problems encountered during the drilling. It is important, but not always easy, to distinguish the natural fractures present in the formation from the mechanical breaks that were created during the drilling process and the handling of the core. A discoloration at the fracture can indicate a natural fracture. From the original picture available for the well H0537, three discontinuities can be counted in the 1 meter core and a calculated recovery rate of about 98%. The handling and the storage of the core created a lot of fractures that were not originally present. It is current though that these fractures follow natural weaknesses or changes in the lithology of the rock.

It is common to water the core before description, in order to standardize the description method for elements that shows variation according to the water content (e.g. color or some structural features). The reaction of the sediments to water can also provide information about lithology, as for example clay would not absorb water easily, unlike silt or sandy layers.

The core from the well B37H0537, which presents the best quality, has been described and logged in order to determine the following elements:

- Lithology
- Core recovery
- Color
- Biological elements (shells presence, bioturbation)
- Stratification type (stratified bed, cross-bed, massive bed...)
- Additional observations.

### 3.1.1.2 Grain-size analysis

Directly determining hydraulic conductivity is often too laborious and time-consuming. An indirect way is then needed and it is often done through texture or grain-size distribution determination. Different studies led to establish relations between hydraulic conductivity and grain-size parameters. Grain-size analyses are also commonly used to classify sediments

Grain-size analysis provides information on the dominant lithology of the samples but also on sorting and thus on heterogeneity. It also permits to determine the proportion of a certain range of grain –size (e.g. percentage of clay).

Several samples were collected from four drillings at different locations in order to perform grain-size analysis: 1) from the two cores available at a resolution of 10 cm and 2) from cuttings available for two other wells traversing the Maassluis Formation. The following table resumes the sampling (Table 3.3).

Table 3.3 : Description of the sampling for grain-size analysis

Borehole ID	Nature of the samples	Sampled interval	Vertical resolution	Total number of samples
B37D0228	Cuttings	99m to 215m	2 m	59
B37H0201	Cuttings	98m to 146m	1 m	51
		98m to 235m	5 m	28
B37D0227	Core	98m to 99m	0,10 m	11
B37H0537	Core	96m to 97m	0,10 m	10

The grain-size analyses were performed with the Malvern Mastersizer 2000, a laser particle size analyzer, in combination with an automated wet dispersion accessory Hydro 2000G. This device uses the technique of laser diffraction to measure the size of particles. It measures the intensity of light scattered as a laser beam passes through a dispersed particulate sample. These data are then analyzed to calculate the size of the particles that created the scattering pattern.

There are different ways to prepare the samples before the measurement, depending on the samples nature (presence of shells, organic matter and coarse fraction) and the objectives. Treatment can separate finer grains that tend to aggregate while in-situ measurement is more representative of the real grain-size distribution. In order to compare the effects of the preparation on the results, two different treatments were applied for the first group of thirty samples: one set treated with peroxide, hydrochloric acid and peptized and one without any treatment. The other samples were measured only untreated.

Prior to any treatment, the samples were sieved to remove the elements larger than 2 mm. The two separated fractions were weighed. During this step, the sediments were grinded to roughly disaggregate the clayey elements. This ensures the homogeneity of the samples and allows taking representative subsamples. This has to be done carefully when shells are presents to preserve them since the hydraulic conductivity depends on their in-situ size. For this, samples should be dry.

#### *Treatment protocol*

First of all, 3 to 4 g of each sample is placed in a glass beaker. For this, the samples have to be split properly so each fraction is representative of the whole sample. A sample splitter was used for this purpose. The samples were first treated with concentrated hydrogen peroxide (30%), in order to oxidize the organic material (about 10 ml per sample). Then about 15 ml of hydrochloric acid (32%) were added to dissolve the containing carbonates. After decantation, 0,3 g of sodium



pyrophosphate were introduced in the beakers, to peptize the finest particles. Indeed the clayey grains tend to agglomerate and give larger particle sizes than their actual grain sizes. After each agent addition, the samples are heated to increase the speed and completeness of the reaction and they are subsequently washed with distilled water.

#### *Grain-size measurements*

The samples were then placed in the dispersion unit:

- For the treated samples, concentrated suspension up to 100ml is brought into the unit;
- For the untreated samples, 1 to 2 grams for the most clayey ones and 2 to 3 grams for the sandy ones are directly added in the unit that contains water.

After the sample is added to the dispersion unit, the obscuration level is controlled and adjusted with dispersant addition. For optimal results, the total obscuration of the suspension should be in the range of 5 to 20%. The sample concentration must be sufficiently high to give an acceptable signal to noise ratio in the detector. On the other side, a too high concentration can cause multiple scattering.

A pump (set to 2250 rpm) and a stirrer (set to 850 rpm) are continuously working to ensure the representativeness of the sample all along the measurement. A sonication probe is continuously irradiating ultrasound to disperse agglomerates, at 90% of its possible level. In order to prevent air bubbles in the system that would appear in the results as large particles, degassing is needed between each sample measurement.

The background signal is measured before each sample measurement. Each measurement is done in two stages, the second one using blue light. The measurement gives the fraction of particles in 32 classes from 0,01 to 2000  $\mu\text{m}$  and calculates the particle diameter at which a given percentage of the distribution is below ( $d(0,1)$ ,  $d(0,5)$ ,  $d(0,6)$  and  $d(0,9)$ ). It has to be kept in mind that the results of the laser diffraction are reported on a volume based distribution, and not on a number distribution which would show higher values for smaller grain-sizes.

The grain sizing using laser diffraction presents numerous advantageous, mainly for its rapid implementation and its reproducibility. However, different elements make the results uncertain to a certain extent and have to be considered when it comes to interpret the results. The finest fraction can be underestimated, for example because the lightest particles might be lost into the air when the samples are handled or might be aggregated to each other and thus appear as larger particles. Also, this method presents some limitations for small size, for non-spherical particles and for transparent grains.

#### *Thermogravimetric analysis*

Thermogravimetric analysis (TGA) was conducted on the first group of thirty samples that were both treated and untreated prior to the grain-size analyses. This analysis permits to determine the organic matter content and the carbonate content while measuring the weight loss of the samples by stepwise heating from room temperature to 105, 450, 550, 800 and 1000°C. It is thus possible to correlate those contents to the grain-size analysis results and see the impact of the treatment.

The following table (Table 3.4), derived from a paper of Roskam et al. (2009), presents the different fractions that can be deduced from a TGA.

Table 3.4 : Fractions showing weight loss in TGA. Source: Roskam et al., 2009.

Temperature (°C)	Fraction	Possible side effects
To 105	Moisture	
105-450	Organic matter	Dehydration of clay minerals (up to 1000°C), from 400°C siderite, increase of the weight due to oxidation of pyrite
450-550	Siderite	Organic matter, dolomite, increase of the weight due to oxidation of pyrite
550-800	CaCO <sub>3</sub>	Pyrite, dolomite
800-1000	Gypsum	

From this principle, one can directly deduce the organic matter and carbonate contents using the following equations (van Gaans et al., 2010):

$$OM = TGA_{550} - 0.07Clay$$

$$Carb = TGA_{800} * \frac{M_{CaCO_3}}{M_{CO_2}}$$

Where TGA<sub>j</sub> is the incremental mass loss between temperature j and the previous temperature, M<sub>i</sub> is the molecular mass of compound i. The clay content is derived from the grain-size analysis.

### 3.1.1.3 Cross-sections

Most of the direct data that can be used in geology are derived from boreholes. Thus they provide information in the vertical direction, sometimes with a high resolution, but fail to give indications on the horizontal direction. It is then necessary to interpolate these data to understand what is occurring between the boreholes. It is not the layers that must be correlated, but similar sequences as fining-up sequences or coarsening-up ones.

This can be based on the Walther's Law that states that the facies are stacked vertically in the same way that they vary in the horizontal direction. Indeed, the depositional environments shift laterally as well as they pile up vertically in time. While doing so, it is important to take a close look at the historical context and evolution of the environmental conditions. The sediments record the climate change cycles, sea level changes and tectonic changes. But not all these cycles are registered continually, because of non-deposit periods or location and because of erosion that can "erase" an entire cycle. When it comes to correlate different boreholes this has to be kept in mind. Therefore, a sequence with clay layers above sandy layers might not correspond to the same sequence found in another borehole. This makes the exercise complex and uncertain. The resulting cross-sections have then to be considered cautiously.

The cross-sections are based on two types of data:

- The gamma-ray logs, which indicate natural emission of gamma rays by the formation all along the borehole. It has been shown that this parameter is closely related to clay content in the layer since clay includes radioactive elements as uranium or thorium. Those logs are commonly used for well-to-well correlation. The signal can be flawed by glauconite-bearing sands.

- The lithological logs, built from lithology descriptions made during the drilling. A common classification has to be used in order to use them simultaneously. It is important to keep in mind that they are based on subjective geological observations and descriptions (generally there is no measured data for grain-size values) so the quality of those type of data can be variable. In addition, their quality is highly dependent on the drilling methods. Some methods do not always permit to relate sediments to their proper depth position. It can then be useful to adjust the real depth position based on Gamma-Ray logs when both are available.

Seismic surveys would provide an interesting support to this work. However, vertical resolution is not always sufficient to distinguish sub-units in a formation. This method was not further examined given the time limits and the availability of the data. Also, other types of data, as biostratigraphical information or heavy-minerals logs, are generally used to build more precise cross-sections.

#### 3.1.1.4 Close wells

The horizontal borehole density is not enough to grasp the horizontal compound of the aquifer heterogeneity. Indeed, their resolution depends on the distance between the boreholes, which varies between 3 and 10 km. At this scale, it is possible to look at the geological basin geometry and polarity. However, the studied processes of heat flow occur at a shorter scale and the influenced area extends to a few hundreds of meters. It is difficult to obtain a high density of data on such a small area. It is possible though to study wells that are close enough but in a different area and consider them as analogue for the area studied. For this, they must not be too far from the site studied and at a similar position in the basin scale, i.e. deposited under similar conditions.

Three pairs of wells have been found that satisfy those criteria. See Figure 3.1 for the location of these wells. Details are presented in the following table. These wells are, therefore, examined closer and compared to each other.

Table 3.5 : Characteristics of the three pairs of wells studied that are close from each other

ID	Depth (m)	X	Y	Distance from each other	Distance from the site	Available data	
						Gamma-Ray	Lithology description
5437	209	70661	432413	4,8 m	At the site	No	Yes
5439	102	70661	432413			No	Yes
B37B3807	190	71485	444911	78 m	12,5 km	Yes	No
B37B3808	190	71487	444989			Yes	No
B37H2652	229	90400	432660	141 m	19,8 km	No	Yes
B37H2651	228	90540	432640			No	Yes

### 3.1.2 Hydraulic conductivity estimation

Hydraulic conductivity is a major parameter in water flow and transport understanding and plays an important role in most of the groundwater management issues, e.g. remediation of contaminated groundwater or drinking water production. Unfortunately, it is particularly complex and time consuming to measure it directly in the field. Most commonly, pumping tests are used to measure hydraulic conductivity. Besides being long to perform, those tests usually results into a large-scale average value that does not reflect the real heterogeneity and anisotropy of the aquifer.

Numerous investigators have then established empirical relations to estimate hydraulic conductivity from borehole data, which provide more accurate and local stratigraphic information. These relations are widely commented and tested in the literature (Krumbein et al., 1943; Shepherd, 1989; Segal et al., 2009...). Since grain-size analyses are quicker and easier to perform, a lot of these relations are based on grain-size distribution. In this study, the Kozeny-Carmen relation is used (Bear, 1972):

$$K = \left(\frac{\rho g}{\mu}\right) \left(\frac{n^3}{(1-n)^2}\right) \left(\frac{D50^2}{180}\right)$$

where K is the hydraulic conductivity,  $\rho$  the water density,  $\mu$  its viscosity, n the porosity and D50 the median grain-size diameter. The term that concerns water is set to  $70071,4 \text{ cm}^{-1} \cdot \text{s}^{-1}$ .

The hydraulic conductivity along the aquifer could then be calculated for two different boreholes:

- At the site, from the estimated grain-sizes at the pumping test borehole (well n°5437). The mean grain-size is visually determined for the sandy layers during the drilling. For the clay layers, no grain-size is indicated in the lithological description. Alternatively, the grain-sizes were deduced by analogy with well B37D0228 for which grain-size analyses were performed for clay as well. The drilling also contains sandy layers containing more than 30% of shells fragments. Also no grain-size is indicated for these layers, a mean grain-size was estimated from literature values (Stuurman, 1995).
- At well B37D0228, 8km from the site, from the grain-size measurements that were performed.

The porosity was adjusted to calibrate the results with the hydraulic conductivities that were measured with the pumping test at the site. This gave an average porosity about equal to 27%, which is consistent with the common values.

### 3.1.3 Stochastic simulation

Geostatistics aims to describe the spatial variation of a given property that is observed in different locations. It is based on the estimation of the probability distribution of this property. It derived from the need of interpolation in the mining geology field in the late 1960s. The main application used to be the mapping of an attribute from local measured data, using the kriging methods. The research field then evolved toward conditional simulation to build stochastic "images" based on the spatial distribution of a variable (Deutsch & Journel, 1992). It is now applied to a great number of fields as hydrology, petroleum geology and environmental sciences and it is an active research topic, for example with multivariate geostatistics or sequential indicator simulation (Dell'Arciprete et al., 2014, Kessler et al., 2013).

For this study, conditional simulation is used. It consists in generating different realizations of the spatial distribution of the studied attribute, here hydraulic conductivity. Those realizations are equally probable and all reflect the imposed statistical properties. These realizations are then all used as model input and the analysis of the different model outputs can then give an appreciation of location-specific uncertainty, through the calculation of the results variance (fig.). Another interest in using simulation instead of kriging methods is that it prevents the smoothing effect that the latter involves. Kriging is interesting to show a global trend but fails to represent the real variation of the attribute considered.

This choice means that hydraulic conductivity is treated as a continuous variable. Another approach possible would have been to take into account hydrogeological facies and then use an indicator simulation method, as in Stafleu (2011) or Bierkens (1994).

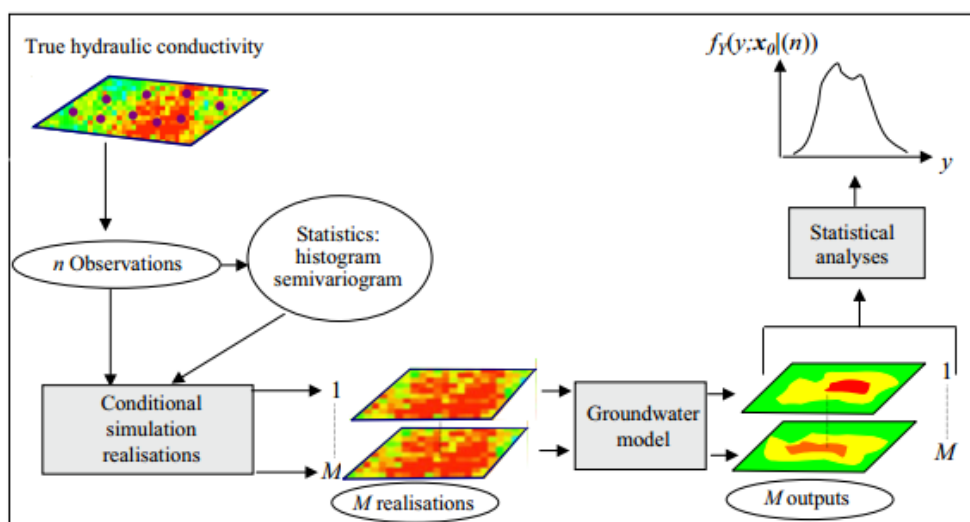


Figure 3.2. Schematic representation of Monte Carlo simulation applied for uncertainty analysis in hydraulic conductivity in groundwater modelling. (From Earth Surface Hydrology)

Different methods exist for simulating realizations. One of the most common algorithms for this in stochastic modeling is the Sequential Gaussian simulation. It is based on the mean of the variable, and the semi-variogram of the space function related to it. Each node of the given grid is visited in a random order with a different path for each realization, and is simulated according to neighboring data. This process loops until all nodes are simulated.

The following procedure was performed during the study:

- Variograms are constructed as a tool to quantify spatial correlation;
- Ranges are determined according to the variograms;
- Different hydraulic conductivity realizations are generated.

Each step is described in the next paragraphs.

#### Variograms construction

A good way to understand and quantify the spatial structure of a property is to construct its variogram (Figure 3.3). The variogram is a measure of variability. It is defined as the variance of an ensemble of values separated by a lag distance  $h$ , i.e. the average squared difference of values separated by  $h$ :

$$\gamma(h) = \frac{1}{2} \text{Var}\{Z(u+h) - Z(u)\} = \frac{1}{2n} \sum \{Z(u+h) - Z(u)\}^2$$

Here,  $Z(u)$  is the value of the studied attribute at the location  $u$  and  $n$  is the set of all pairs that have a distance  $h$ . The semivariogram  $\gamma(h)$  is the half of the variogram  $2\gamma(h)$  but it is often referred as variogram in the literature, as will be the case in this report. The variogram is calculated for all locations  $u$  in the study area and for different lags  $h$ .  $\gamma(h)$  is then plotted against these lags. As it can be expected, the longer the lag is, the more different the values are likely to be, thus the highest the variogram is.

To interpret the variogram, few parameters can be determined, either visually or by fitting a variogram model:

- The sill is the plateau that is reached by the variogram when there is no more correlation between the distance and the value; it corresponds to the variance of the entire field.
- The range is the distance where the sill is reached, that means there is no spatial relationship between the considered point and point farther away this distance.
- The nugget is the value of the variogram at the origin (i.e. the intersection of the variogram and the y-axis), which can differ from zero. It can be interpreted as a measuring error or a geological microstructure that is not properly assessed in the sampling interval.

This is true when the assumption is made that the ensemble of the value (i.e. the random function) is stationary. This means that the mean and the variance are the same at any location and that there is no trend observed. A variogram that increases beyond the sill variance can correspond to a geologic trend, for example fining or coarsening upward. A cyclicity can be observed in the variogram, in particular when attributes are considered in a vertical direction. This may be linked to periodicity in the stratification. It can give information about the average thickness of the bedding (Deutsch, 2003). Another important indication the variogram analysis can give concerns the geometric anisotropy. This is evaluated by comparing the vertical and horizontal sill and range. For example, the presence of a lenticular formation will show a larger range in the direction of lens elongation (Chiles and Delfiner). However, there is often a scarcity of data in the horizontal direction, which makes this comparison difficult.

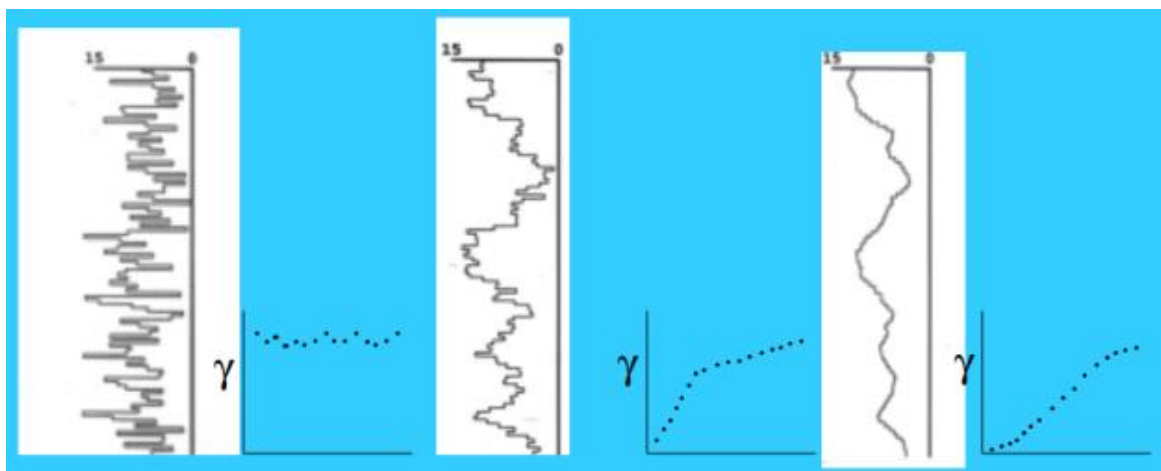


Figure 3.3. Different types of variograms with corresponding distribution of a given parameter along the vertical dimension. (from [www.staios.com](http://www.staios.com))

Different variograms were built from the collected data, but only vertical variograms. Indeed the well density is not high enough to give horizontal variograms of good quality. The variograms were then fitted visually with theoretical models to obtain the different parameters. The main objective here is to get an order of magnitude of the vertical range that represents the geological heterogeneity due to the layering. This range will then be used in the next step. Analysis and comparison of the variograms build from the close wells mentioned earlier were particularly focused.

The exponential model corresponds the best to the empirical variograms. One thing though as to be kept in mind: the effective range, used in the stochastic simulation, is actually the third of the actual range, since the variogram reaches the sill asymptotically (Chiles and Delfiner). This corresponds then to 95% of the sill. Also, when the variogram model is being fitted, the first part of the function must be particularly focused.

#### *Hydraulic conductivity field generation*

In order to generate the stochastic simulation, the geostatistical software GSLIB, developed at Stanford, was used. From the first edition released in 1992, GSLIB is freely accessible and has been constantly enhanced. It is widely used in stochastic hydrogeology. Most specifically, the program 'sgsim' was used.

The simulation is conditional, which means that the realizations honor initial data values at their locations. The initial data used are the hydraulic conductivities calculated from the grain-size analysis (via the Kozeny-Carmen relation) present in the drilling description at the site. The data file indicates the vertical position, i.e. the depth below the ground, and the normal transformed logarithm of the calculated hydraulic conductivities. It concerns only the aquifer part, i.e. between 80 m deep and 200 m deep.

The realizations are simulated for a grid with similar horizontal dimensions: 50 rows and 50 columns of 10 meters width. The grid has the same number of layers than the simpler model, 22 layers, but with a regular discretization and covers the aquifer thickness, between 80 m and 200 m deep. The 'sgsim' program uses the simple kriging to determine the field parameters. The type of variogram structure must be specified. The exponential model was chosen. Three ranges must be specified as well: the maximum horizontal range, the minimum horizontal range and the vertical range. In order to simulate the elongated facies of the tidal bars, the two fixed horizontal ranges were set different, with a ratio 10/7. Two different scenarios for horizontal range are used since it could not be determined with experimental variograms: 1000 m and 100m, in order to test different level of heterogeneity. A brief sensitive analysis was performed with the program to properly understand the effect of the different parameters to set, mostly the nugget effect and the different direction ranges. The nugget effect were set at 0,15, giving a result visually satisfying but consistent with the experimental variograms.

The multiple-grid concept was used in the simulation. This permits to take into account the long-range structure of the layering, by first simulating a coarse-grid and then use it as conditioning for a second finer grid simulation.

A last step is necessary before implementing the realizations in the model: rearrange the grid so it can be read by the hydrogeological model program, and separate each layer in one matrix. This was done using the program MatLab. During this step, the values are back-transformed and

an exponential function is applied to undo the log transformation so the final values are hydraulic conductivities in meters per day.

## 3.2 Results

After presenting the results from the thermo-gravimetric analysis permitting to explain grain-size measurements results, the results of the collected data analyses is presented with increasing scale, leading to input parameters for the modeling part.

### 3.2.1 Results of the TGA and comparison of the different grain-size measurements

The results of the grain-size analysis of the set that was both treated and untreated before measurement must be compared, in the light of the organic and carbon content determined by TGA, in order to understand the effect of the treatment on the samples. Table 3.6 presents the following data:

- The difference in  $d(0,5)$  measured by the sizer between the untreated and treated sample, calculated as following:  $\frac{d_{untreated}-d_{treated}}{(d_{untreated}+d_{treated})/2}$ . This value is picked because it is used to calculate the hydraulic conductivity in the next steps. If the treatment impacts strongly this value, it will have an effect on the whole study.
- The clay content. That is the percentage of grains that are less than  $8\ \mu\text{m}$ . The samples that are classified as clay according to the triangle texture classification (more than 8% of clay content) are highlighted in yellow. The showed values correspond to the untreated set.
- The coefficient of uniformity, calculated by the ratio between  $d(0,6)$  and  $d(0,1)$ . A low coefficient means that the sample is uniform, i.e. all grains are about the same size, whereas a higher coefficient means that the grain-size distribution is wider. The values above 20 are highlighted. The showed values correspond to the untreated set.
- The carbonate content and the organic content deduced from the TGA analysis. The values above 5,5% for carbonate and above 0,5% for organic matter are highlighted.



Table 3.6. Results of the grain-size and thermo-gravimetric analysis

	Difference in d(0.5) between the two set (%)	Clay content (%)	Uniformity d(0.6)/d(0.1)	Carbonate (wt-%)	Organic matter (wt- %)
D90-91	2,2	6,39	13	3,6	0,29
D101-102	0,9	0,93	2	3,7	0,09
D105-106	15,2	7,00	23	5,9	0,28
D109-110	43,7	22,36	20	16,8	0,83
D113-114	105,7	21,03	56	13,7	0,67
D118-119	-21,1	34,45	9	9,9	1,11
D121-122	7,7	7,50	15	5,5	0,32
D125-126	0,8	3,11	2	5,4	0,15
D129-130	1,0	1,02	2	2,8	0,08
D133-134	1,3	3,82	9	3,9	0,27
D137-138	15,5	11,76	55	9,7	0,57
D141-142	32,1	15,96	46	6,9	0,56
D145-146	13,5	5,90	14	5,2	0,30
D149-150	0,9	1,08	2	2,8	0,09
D153-154	162,5	29,58	64	10,2	0,95
D157-158	-0,5	1,23	2	4,3	0,10
D161-162	16,0	12,33	50	9,0	0,63
D165-166	-0,1	0,00	2	2,5	0,10
D169-170	1,2	3,54	2	4,9	0,03
D173-174	0,9	2,24	2	2,5	0,10
D177-178	11,9	14,91	46	8,3	0,49
D181-182	19,8	16,04	48	6,3	0,99
D185-186	-8,6	1,69	2	19,5	0,11
D189-190	133,4	28,13	56	5,0	1,02
D193-194	134,8	26,79	43	14,5	0,78
D197-198	26,3	18,19	45	13,3	0,87
D201-202	1,0	0,92	2	3,9	0,13
D205-206	62,9	23,53	53	13,7	1,16
D209-210	39,4	29,15	16	15,9	1,00
D213-214	52,0	26,75	21	14,0	1,19
<b>Correlation coefficient with the difference in d(0,5)</b>		<b>0,81</b>	<b>0,72</b>	<b>0,52</b>	<b>0,72</b>

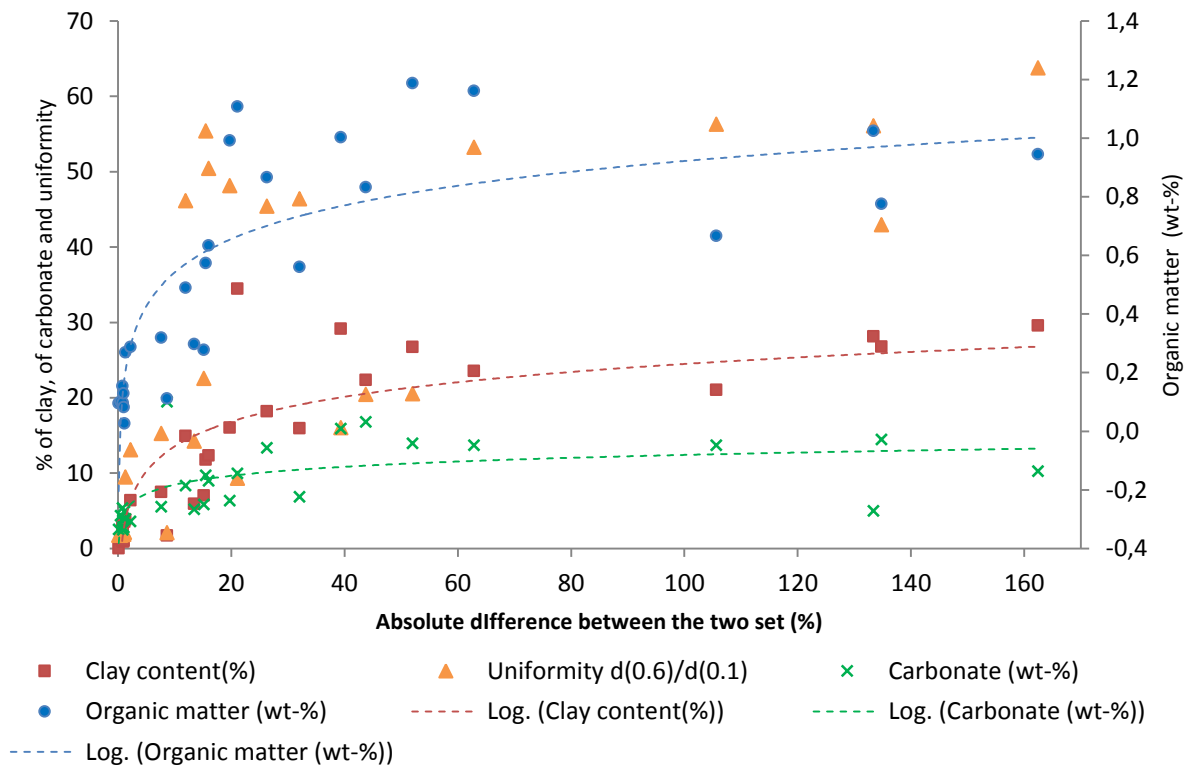


Figure 3.4: Correlation between difference in  $d(0.5)$  between treated and untreated samples and other parameters

Comparing the data permits to see that mainly the clay samples are biased by the treatment (Figure 3.4) and the ones with a wider distribution, to a lesser extent though. The TGA revealed that the higher content in carbonate and organic matter are found in the clayey samples.

The following figure shows an example of how a clay sample (D113-114m) behaves after the treatment (Figure 3.5). An important finer fraction is lost. The increase in the coarser fraction is to be interpreted carefully: it is only an effect of the loss of the fine fraction since the results are a percentage and then relative. This was observed in the other samples as well.

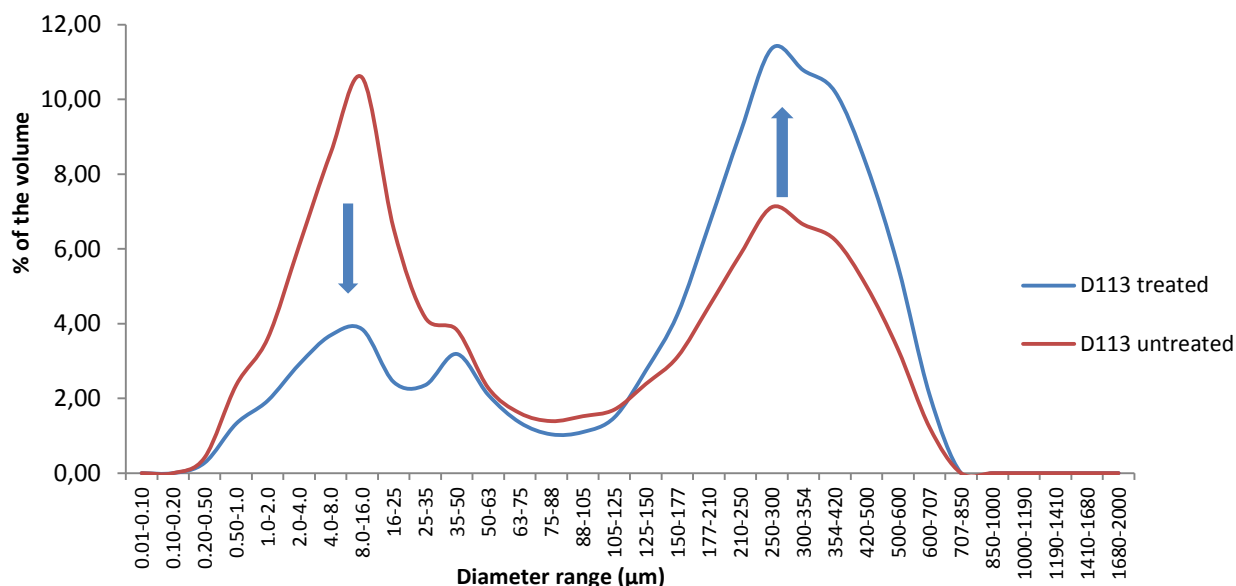


Figure 3.5. Grain-size distribution for the sample D113 from the borehole B37D0228, both treated and untreated. The arrows show the effect of the treatment.

This loss in the finer fraction is likely due to the removal of organic matter by the hydrogen peroxide and of carbonate by the hydrochloric acid, which are present mainly in the clayey samples. This fine fraction may correspond to small grained chalk. Therefore, the intended effect of separating the agglomerated clay did not occur; indeed the treated samples would have showed a higher content in finer particles. Also, the dissolution of the biggest carbonate shells present in the measured sample (but still lower than 2 mm) did not significantly impact the resulting distribution in the upper part of the range. Therefore, it can be expected that the untreated samples measurements gives results that are more representative of the real field distribution.

The results of the data analysis are then presented for the different studied scales: at the core scale, at the borehole scale, at the local scale and at the regional scale.

### 3.2.2 At the core scale

The detailed logging and the original photographs of the core H0537 and the original cores descriptions of H0537 and D0227 are presented in the annexes. The following paragraphs present the results of the two one meter cores analysis.

The cores are representatives of two different facies. According to the original core description files, the core D0227 is representative of a shell-containing sand layer while the core H0537 belongs to a thin clayey horizon that is identified in the Digital Geological Model of the Geological Survey of the Netherlands (Mulder et al., 2003).

The poor quality of the core D0227 does not permit to describe the structures properly. However, the presence of shells permits to affirm that this section belongs to the Maassluis Formation. The quality of the core H0537 is better and this core could be properly described. Though this layer does not contain shells, the adjacent ones do according to the original description. The dominant presence of really fine sand, silt and clay layer can indicate a marine environment with the

influence of waves. The mica flakes visible in the core also show that the eroded sediments did not experience a long transport or high energy conditions that would have destroyed them.

The core scale presents a high heterogeneity on the two cores. Over one meter, different beds are distinguished, with different structures and that react differently to the sprayed water for example. The thickness of these layers is about 10 centimeters. The results of the grain-size analysis performed on the cores samples also show heterogeneity visible at a really short scale, mainly for the core D0227. The following figures (Figure 3.6) present the grain-size distribution of the core samples and show the lithology classes according to the NEN 5104 (Institute of Normalization in the Netherlands).

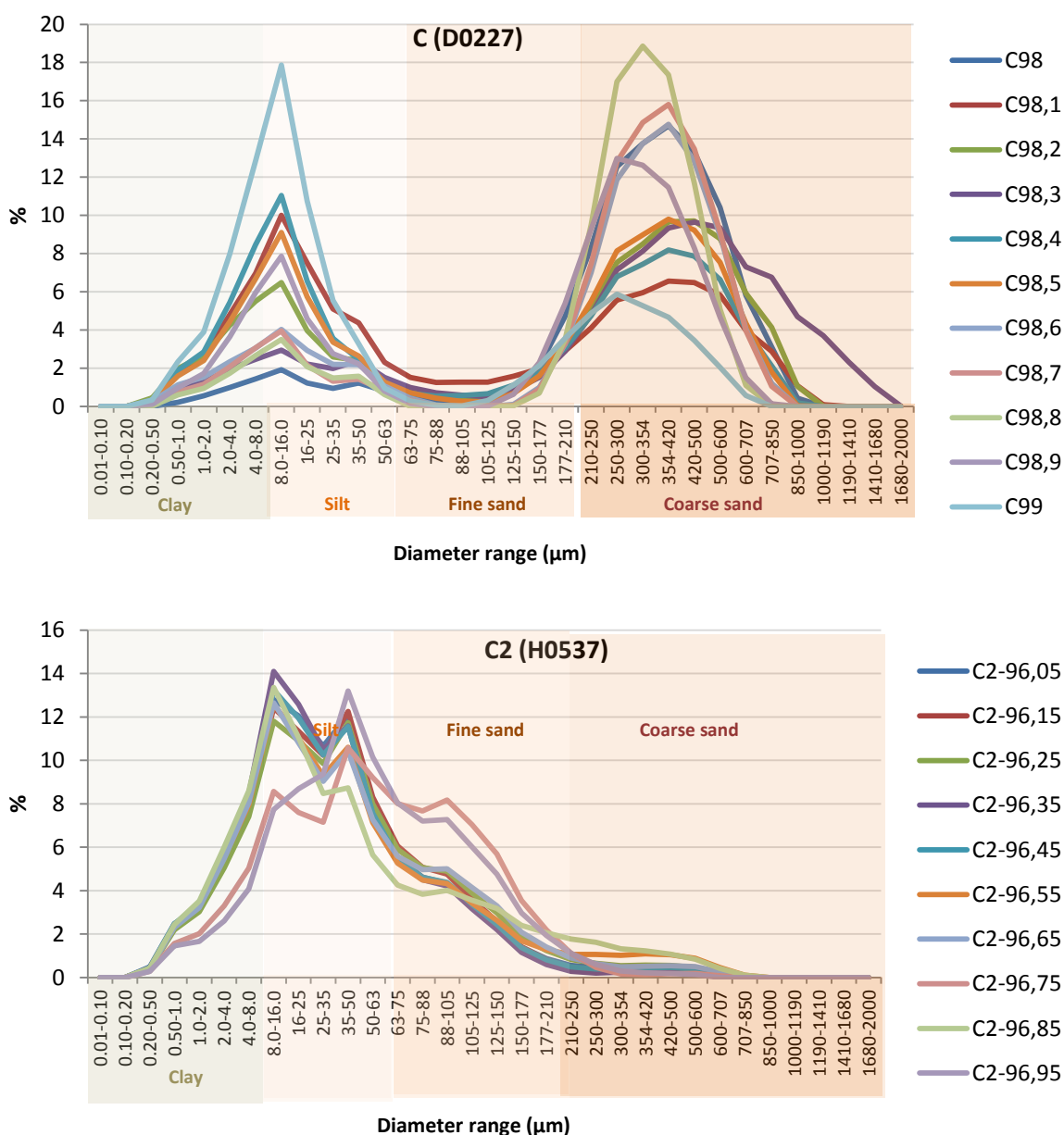


Figure 3.6. Grain size-distribution of the 1 meter cores samples from cores D0227 and H0537

The following figures present the percentage of the main lithology fraction along the core, also deduced from the grain-size analysis (Figure 3.7).

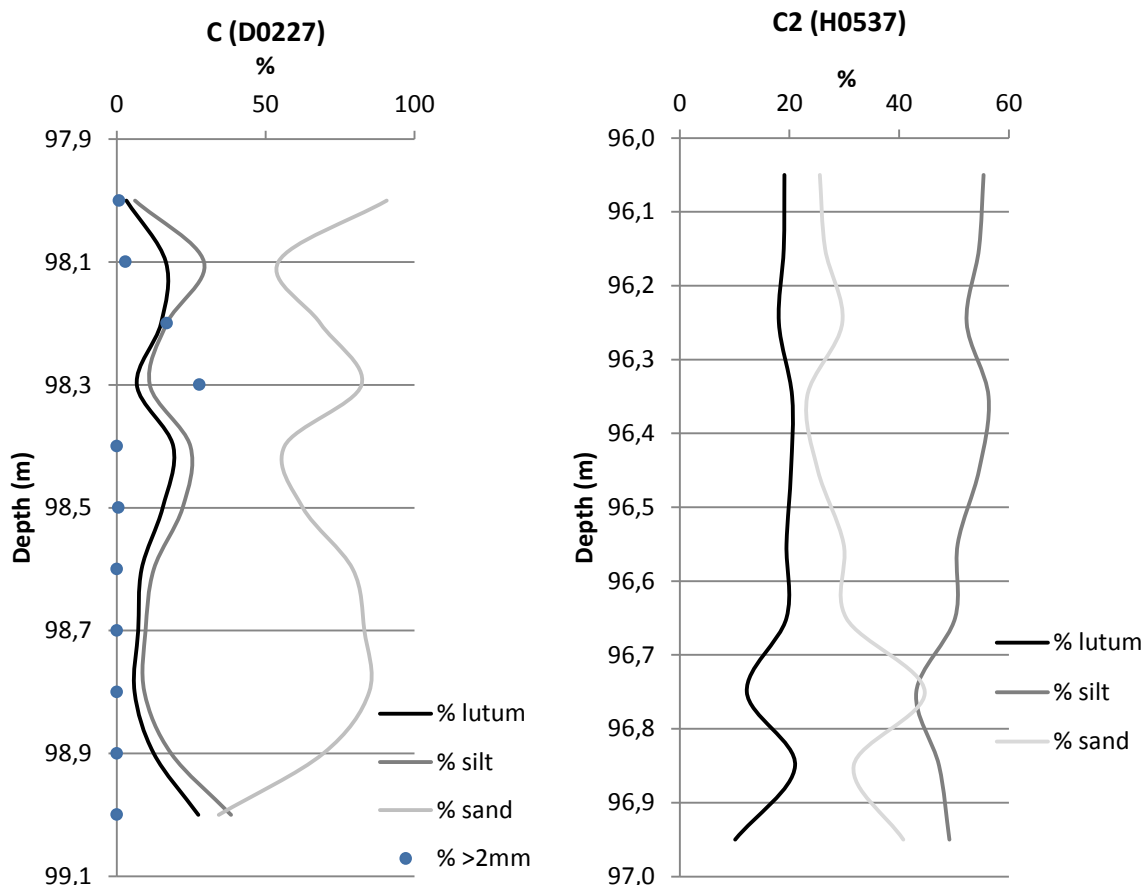


Figure 3.7. Percentage of clay, silt and sand along the core length, according to the grain-size analysis for cores D0227 and H0537, the blue dots correspond to the fraction above 2 mm that was removed from the samples prior to the measurements, it gives an approximation of the shells contents. "Lutum" means "clay".

If the triangle texture classification, used by the Geological Survey of the Netherlands, is applied, core D0227 reveals six different textures while the core H0537 show the same texture along the core.

Finally, hydraulic conductivity can be calculated with the Komeny-Carmen relation from the median grain-size. The standard deviation of its logarithms can be later compared at different scale. Results are summarized in the following table (Table 3.7).

Table 3.7. Calculated hydraulic conductivities for cores D0227 and H0537

Wells ID	Min K value (m/d)	Max K value (m/d)	Mean K (m/d)	Standard deviation of log (K)
D0227	0,046	18,2	9,4	0,75
H0537	0,093	0,38	0,17	0,21

The core D0227 shows a higher heterogeneity than the other core. This is mainly due to the presence of the shells layers, which has a strong effect on the different parameters.

### 3.2.3 At the borehole scale

The grain-size analysis performed on cutting samples from well D0228, along the Maassluis formation, shows a wide variety of distributions (Figure 3.8). The application of the texture classification gives ten different textures for these samples (Figure 3.9).

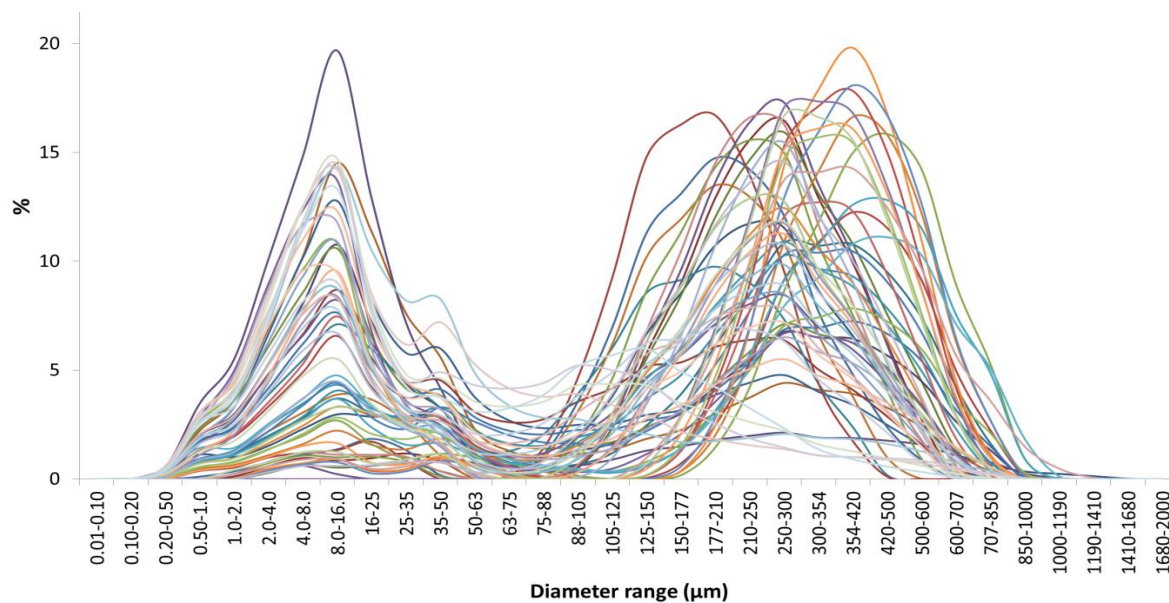


Figure 3.8. Grain-size distribution of the 59 samples from well D0228 along the Maassluis Formation

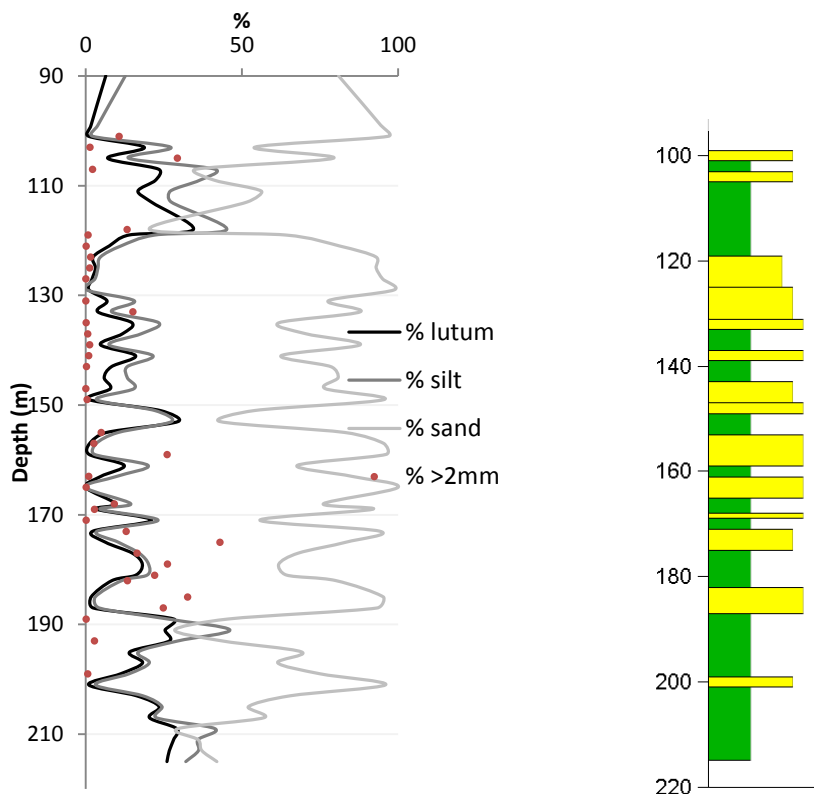


Figure 3.9. A) Percentage of clay, silt and sand along the Maassluis Formation, according to the grain-size analysis, for well D0228, the red dots correspond to the fraction above 2 mm that was removed from the samples prior to the measurements, it gives an approximation of the shells contents. "Lutum" means "clay". B) Lithological log of well D0228. Clay is represented in green (5 different clayey textures) and the different sand textures in yellow.

As done at the core scale, hydraulic conductivity was calculated from the median grain-size. The following table (Table 3.8) shows these results for the cuttings samples that were studied along the entire thickness of the Maassluis Formation (well D0228) as well as for the mean grain-sizes indicated in the drilling description at the project site (well 5437).

Table 3.8. Calculated hydraulic conductivities for wells 5437 and D0228

Wells ID	Min K value (m/d)	Max K value (m/d)	Mean K (m/d)	Standard deviation of log (K)
5437	0,01	15,2	6,3	0,86
D0228	0,02	19,7	6,1	0,79

The standard deviations show a slightly higher heterogeneity at this scale than at the core scale. Indeed, the one meter cores were specific for one facies while that the whole formation comprises different facies.

The variograms were constructed for the gamma-ray values for the section corresponding to the Maassluis Formation from 11 wells. See Figure 3.1 to locate these wells. The characteristics of the variograms are summarized in the following table (Table 3.9).

Table 3.9. Characteristics of the variograms constructed. The range column gives the range determined by fitting an exponential model, the trend column indicated whether or not a trend is visible in the variogram, the lag distance of the first peak is representative of the average thickness of the bedding (according to Deutsch, 2003), the actual range column corresponds to the lag distance where the global variance is reached.

ID	Length (m)	Resolution of the gamma-ray log (m)	Modelled range (m)	Trend	Lag distance of the first peak (m)	Global variance	Actual range (m)
B37B0172	58	0,02	8,5	Y	3	303,5	8
B37D0227	49	0,05	7,2	N	1,3	57,9	5
B37H0537	50	0,05	3,4	Y	3	161,8	19
B37E0616	120	0,1	5	N	6	213,3	13
B37H2815	77	0,05	3,8	N	6,2	26,5	8,5
B37E3633	132	0,05	3,8	Y	3	89,3	24
BronK	132	0,1	7,5	N	5	108,8	9
B37D0028	116	0,1	4	Y	2	43,6	13

If all the variograms are considered at the same time (Figure 3.10), a general variogram that would be representative for the entire formation can be modeled and then used for the field generation. The parameters used for the exponential model are indicated in the figure. The variograms values have been normal transformed to be compared. Variograms built from parameters derived from the grain-sizes analysis (clay percentage, d(0,5), d(0,1), lithology classes), not shown here, gave the same order of magnitude for the range.

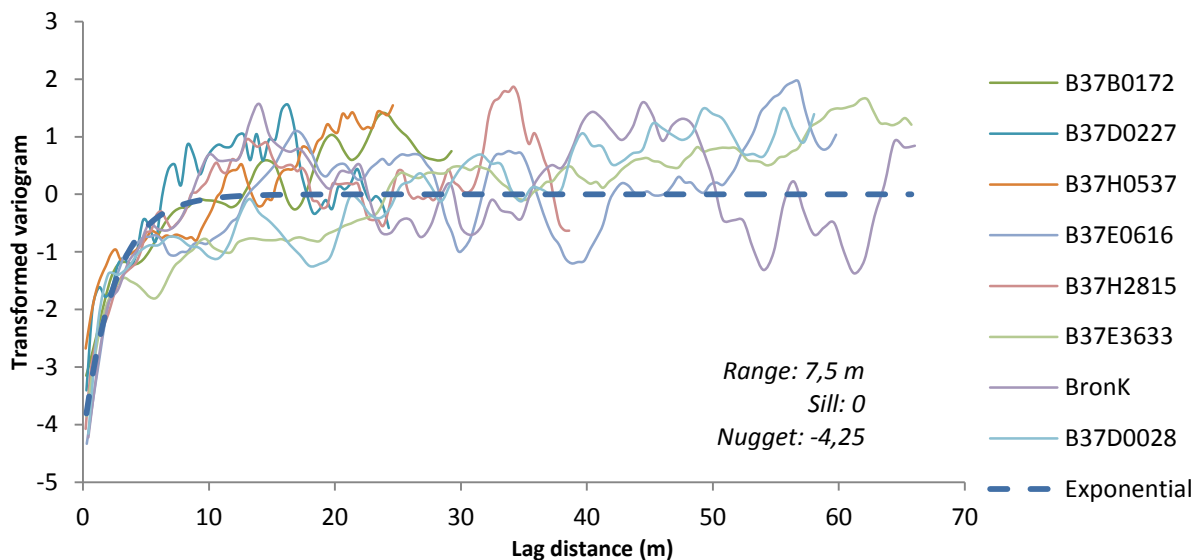


Figure 3.10. Variograms of 8 wells and exponential model variogram that fits the best. Values were normal transformed to be compared.

However, when the variograms are studied in detail, two spatial structures can be distinguished: a first structure with a range below 5 meters, around 3,5 meters, with generally the presence of the nugget effect, and a second wider structure, with a range around 8 or higher without a high nugget effect. This is for example visible on the variogram of the well B37B0172 (Figure 3.11).



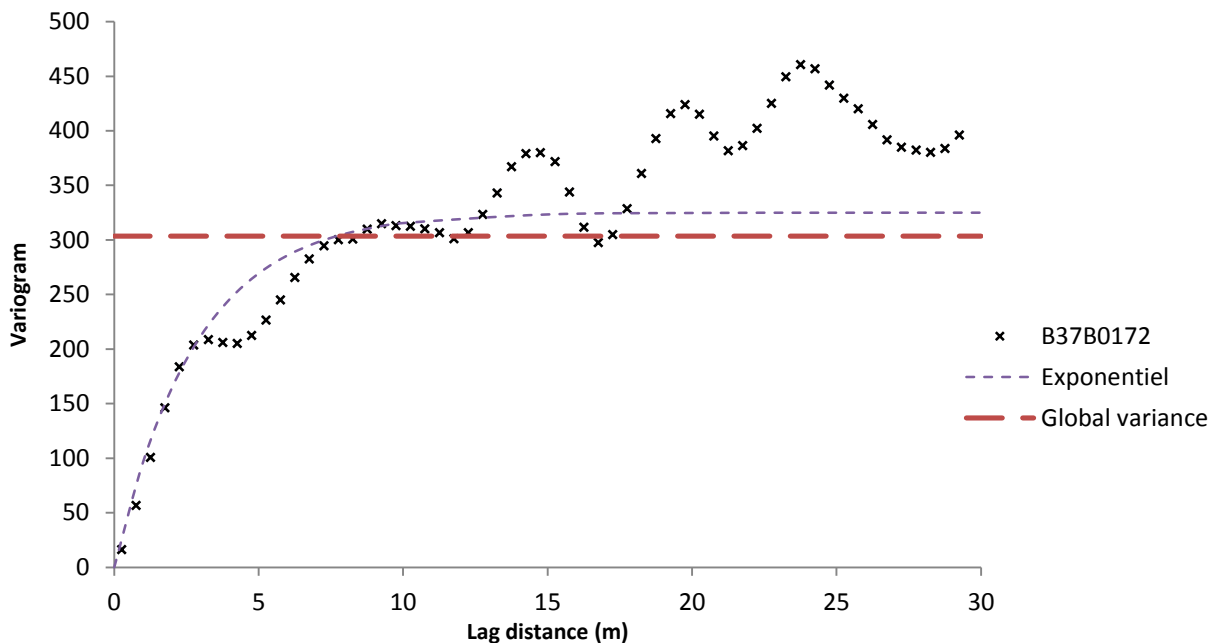


Figure 3.11. Variogram of the well B37B0172, showing the different spatial structures. A trend is visible in this variogram, as well as cyclicity. The red dashed line shows the variance of the gamma-ray values.

These two structures may correspond to the difference between clay layers and sandy layers for the wider structure and to the beddings present in these layers for the second. This finer structure is dependent on the gamma-ray log resolution that is less precise than for example the detailed core description.

### 3.2.4 At the local scale: close wells

So far, only the vertical heterogeneity was closely studied. A second dimension can be added when studying wells that are relatively close: the horizontal heterogeneity. The variogram of the gamma-ray values was built for the two wells B3807 and B3808 that lie 78 m from each other (Figure 3.12).

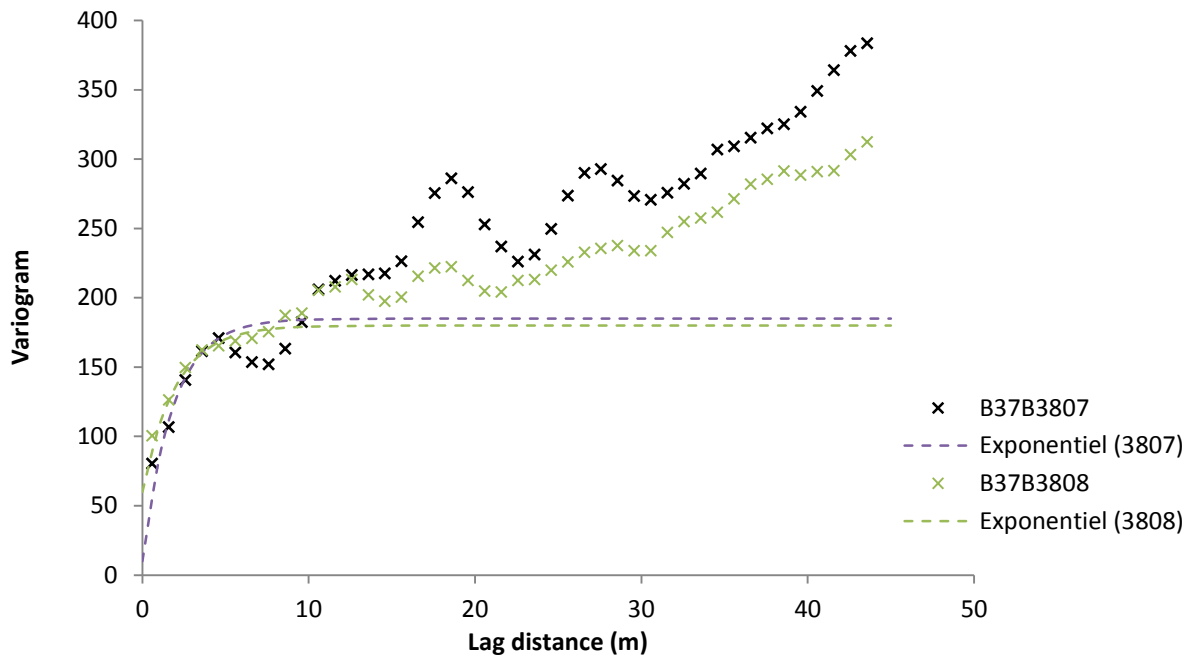


Figure 3.12 . Comparison of the variograms of the pair of wells B3807 and B3808

They show a similar structure, especially concerning the shortest lags. The well B37B3807 appears with a more pronounced trend.

The gamma-ray values can be compared visually too (Figure 3.13). They are indeed similar all along the formation and do not show much difference. For example, the clayey layers around 85 m deep and 120 m deep are found in both logs. For the two other pairs, gamma-ray logs were not available but only lithology description (Figure 3.14). Comparing the lithologies of H2651 and H2652, drilled 140m ahead, it is visible that the sediment nature is already varying at such a distance. The wells at the site, with distance of 5 meters only, show a much closer lithology, but still not exactly similar, for example at 60 meters deep.

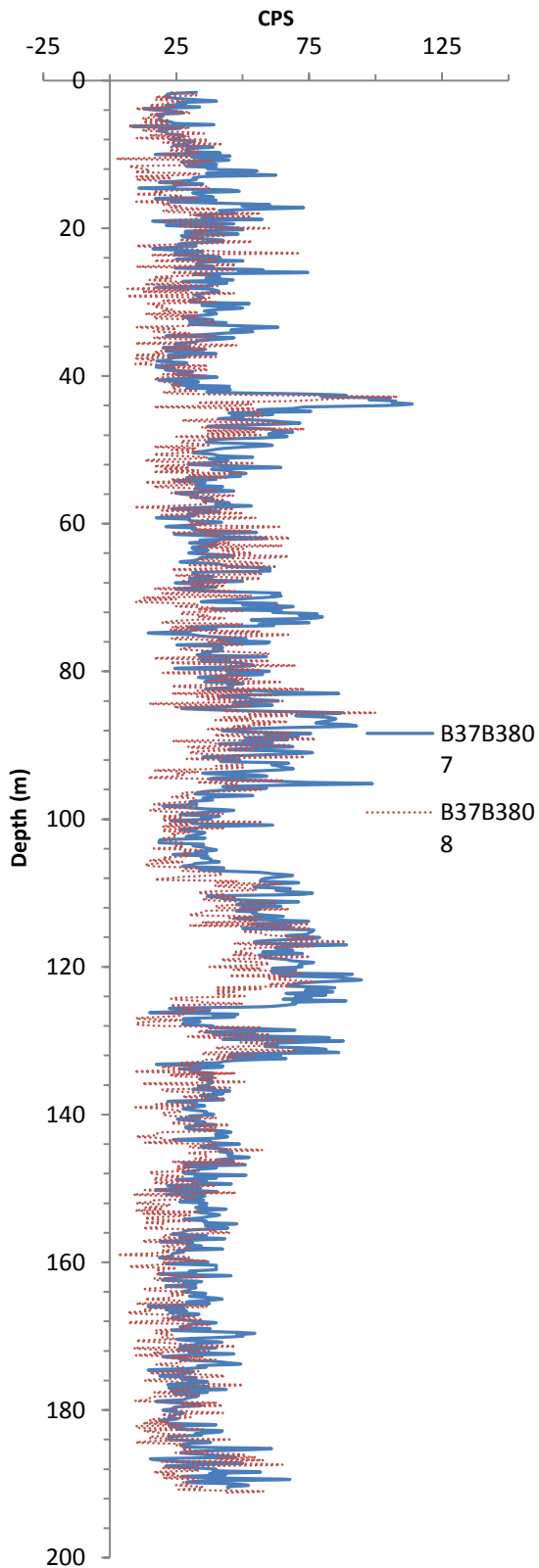


Figure 3.13 . Comparison of the gamma-ray logs of the pair of well B3807 and B3808

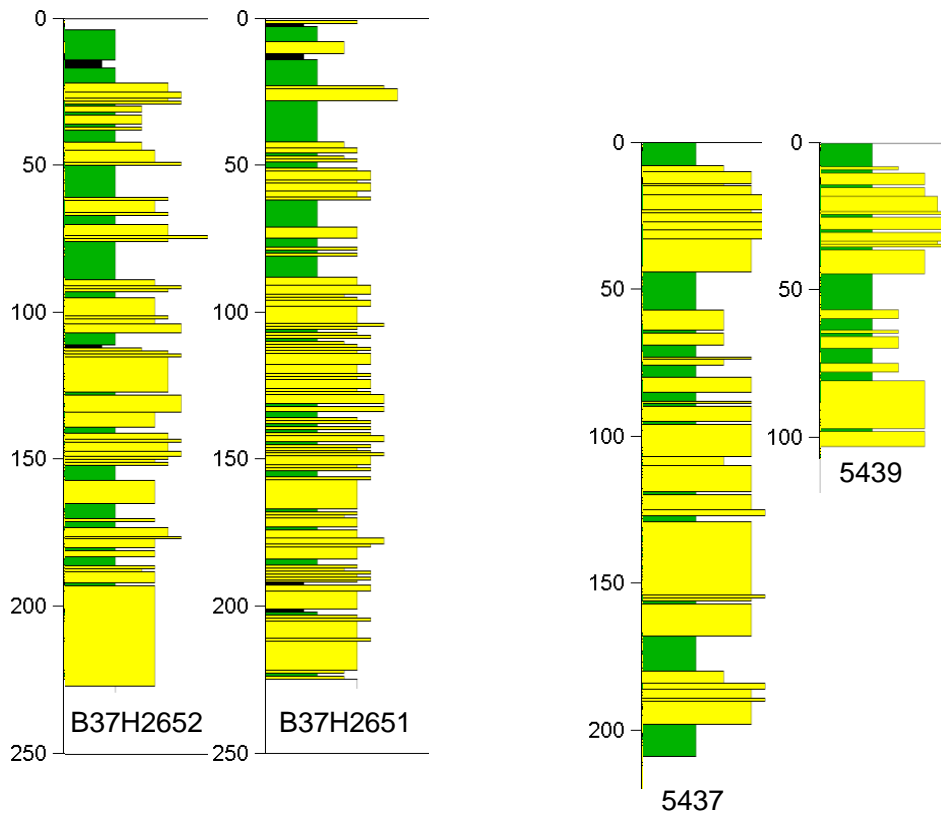


Figure 3.14 . Comparison of the lithological logs of the pairs of a) H2651 and H2652 and b) 5437 and 5439.

### 3.2.5 At the regional scale

The building of lithological cross-sections (Figure 3.15, Figure 3.16, Figure 3.17 and Figure 3.18) permits to zoom out and study the formation as a whole. It is interesting to see whether or not the confining layers present in the aquifer at the project site, can be followed throughout the formation.

The cross-sections B-B' and C-C' both show a common clay basis to the Maassluis formation that corresponds to the hydrogeological basis found in the drilling at the site. However, this layer is not visible in the other two cross-sections. Also, the cross-sections do not reveal the polarity of the basin and the expected predominance of clay in a northwestern direction is not visible. The building of cross-sections demonstrates the complexity of the basin and that the picture of a “layered cake” with continuous layers is wrong at the kilometer scale. The horizontal correlation will thus be smaller than the common distance of few kilometers between the drillings.

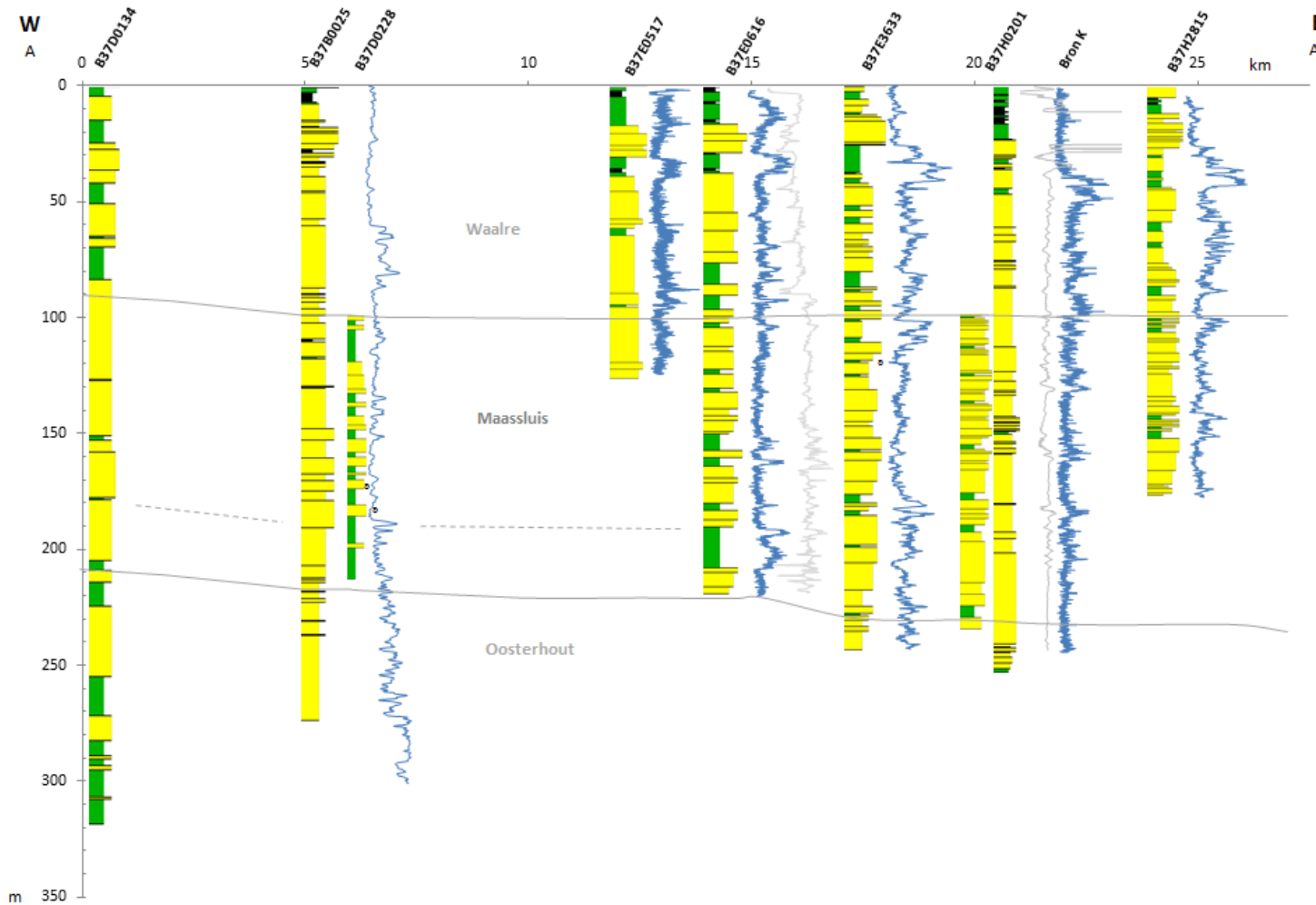


Figure 3.15. Lithological cross-section A-A' including gamma-ray logs in blue and spontaneous potential in grey. The Maassluis Formation boundaries, indicated in grey, are determined from the DGM. Clay layers are distinguished from sand layers by a different colour. Sand layers themselves are individualized by the width of the layers according to their coarseness. The symbol  $\varnothing$  indicates the presence of shell-rich layers (sand containing more than 30% of shells above 2 mm). See Figure 3.1 for the location

What is the hydrological efficiency of high-temperature aquifer thermal energy storage when combined with a geothermal plant?

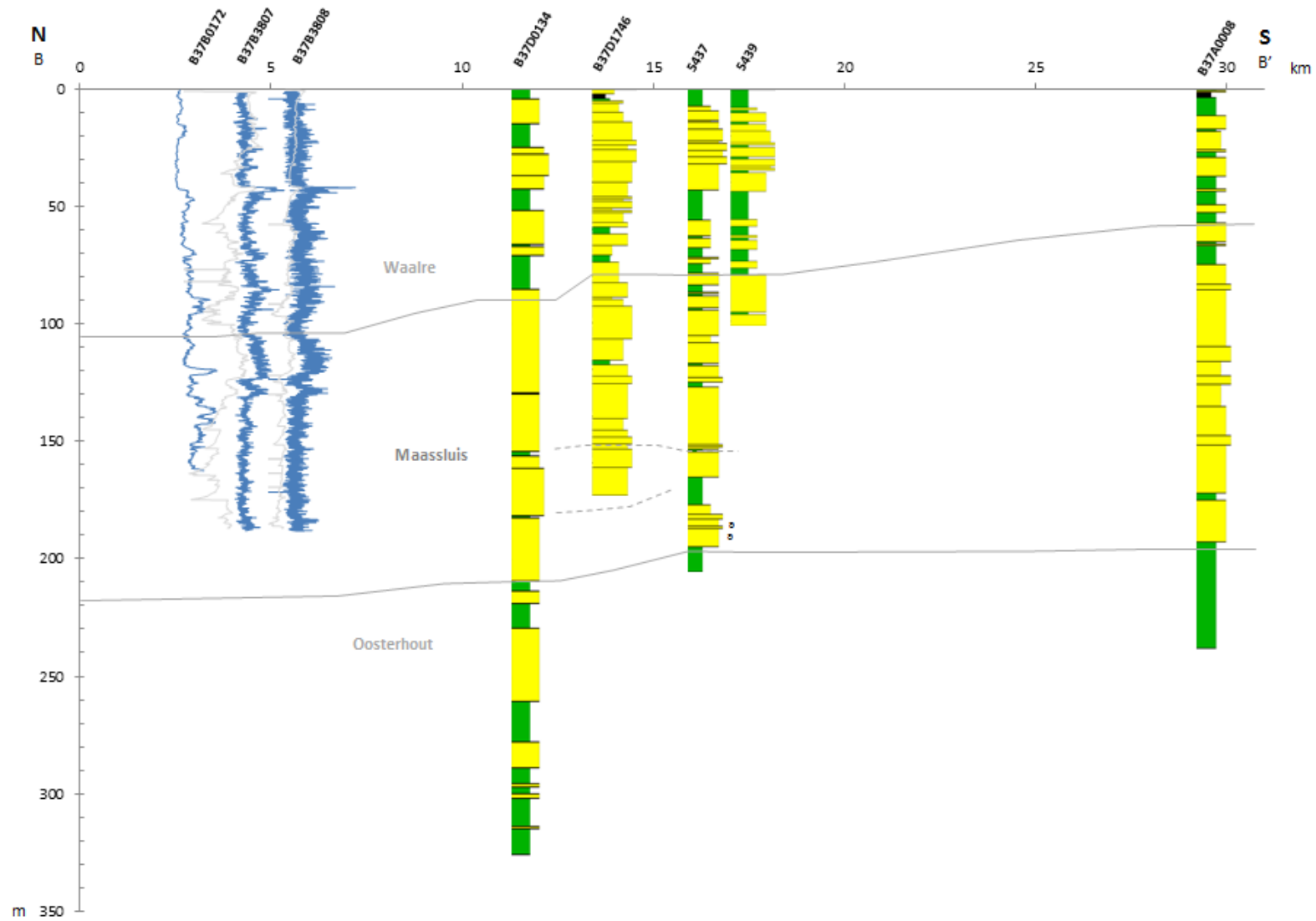


Figure 3.16. Lithological cross-section B-B' including gamma-ray and spontaneous potential logs. See figure 3.15 for legend and Figure 3.1 for the location.

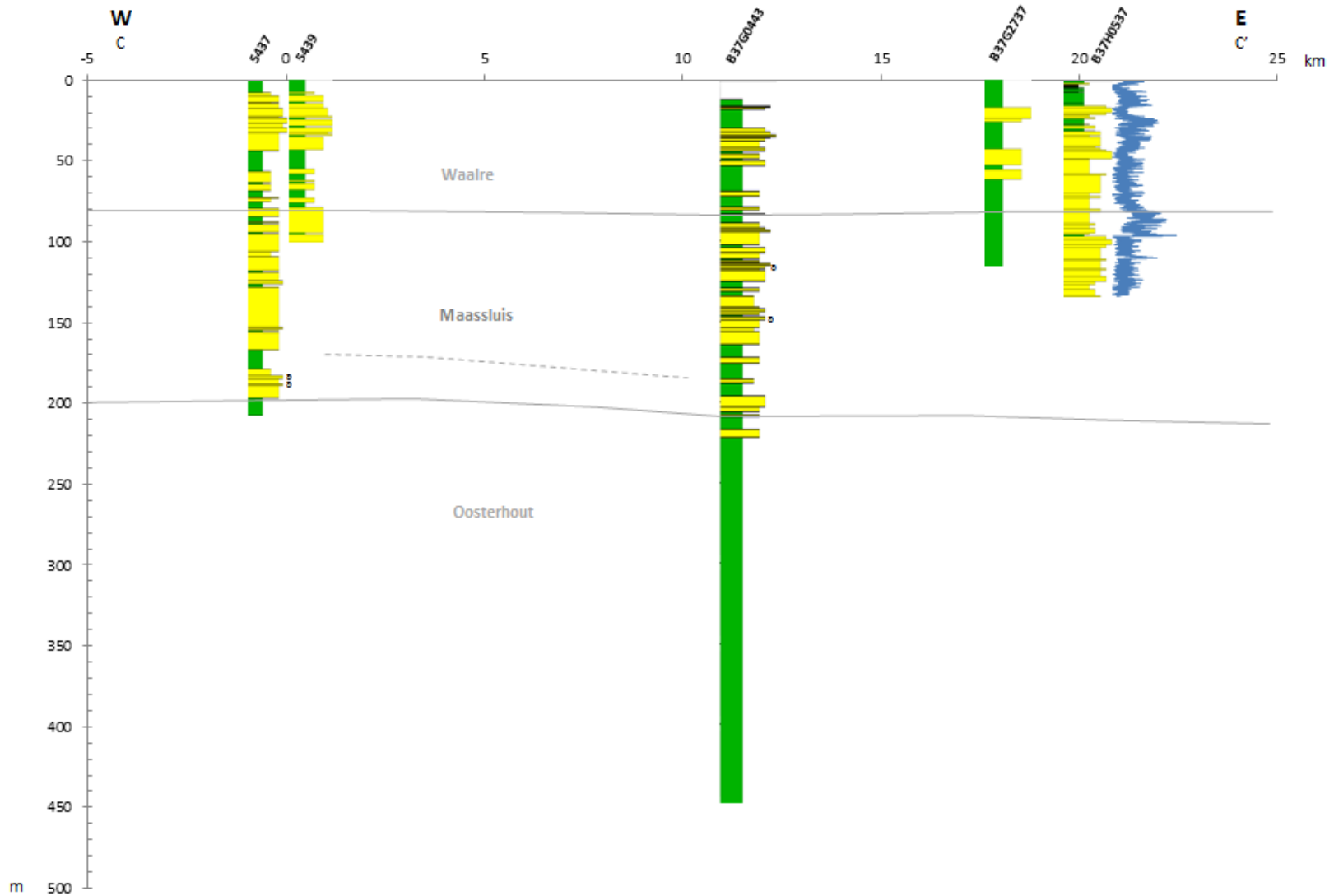


Figure 3.17 . Lithological cross-section C-C' including gamma-ray logs. See figure 3.15 for legend and Figure 3.1 for the location.

What is the hydrological efficiency of high-temperature aquifer thermal energy storage when combined with a geothermal plant?

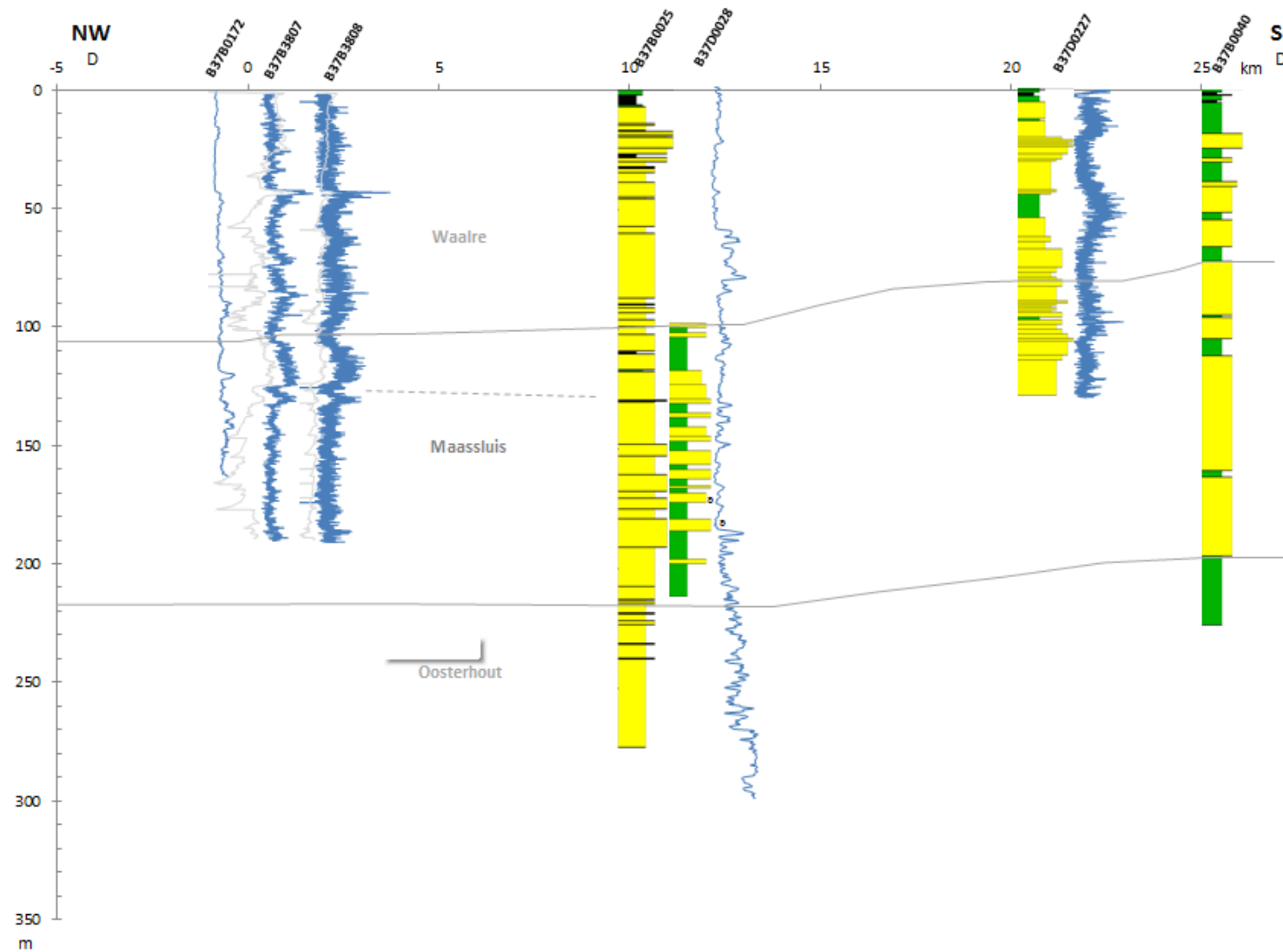


Figure 3.18. Lithological cross-section D-D' including gamma-ray logs. See figure 3.15 for legend and Figure 3.1 for the location.



### 3.2.6 Summary

Analysis of the collected data revealed the heterogeneity of the formation at different scales. A main spatial structure emerges from the variogram analysis, with a range between 7 and 10 meters. A secondary finer structure was also observed, with more uncertainties though, depending on the resolution of the data. Only the first structure will be reproduced in the stochastic simulation. The quick sensitive analysis performed with the 'sgsim' program showed that a range of 7 and 10 meters give approximately the same results so a range of 10 meters will be used for the final realizations. The analysis did not permit to obtain a horizontal correlation range since there are too many uncertainties in between the boreholes. Therefore, two different horizontal ranges will be tested for the simulation: 1000 meters and 100 meters, implying an increasing horizontal heterogeneity.



## 4 Model exercise

The previous chapter presented the investigation done to properly grasp the aquifer architecture and characteristics. All this work will now be used to build the transport model and to assign the proper values for each parameter. In the first part of this chapter, the modeling methodology is described, together with the different scenarios that are tested. Then a second part presents the results of the modeling exercise.

### 4.1 Model construction

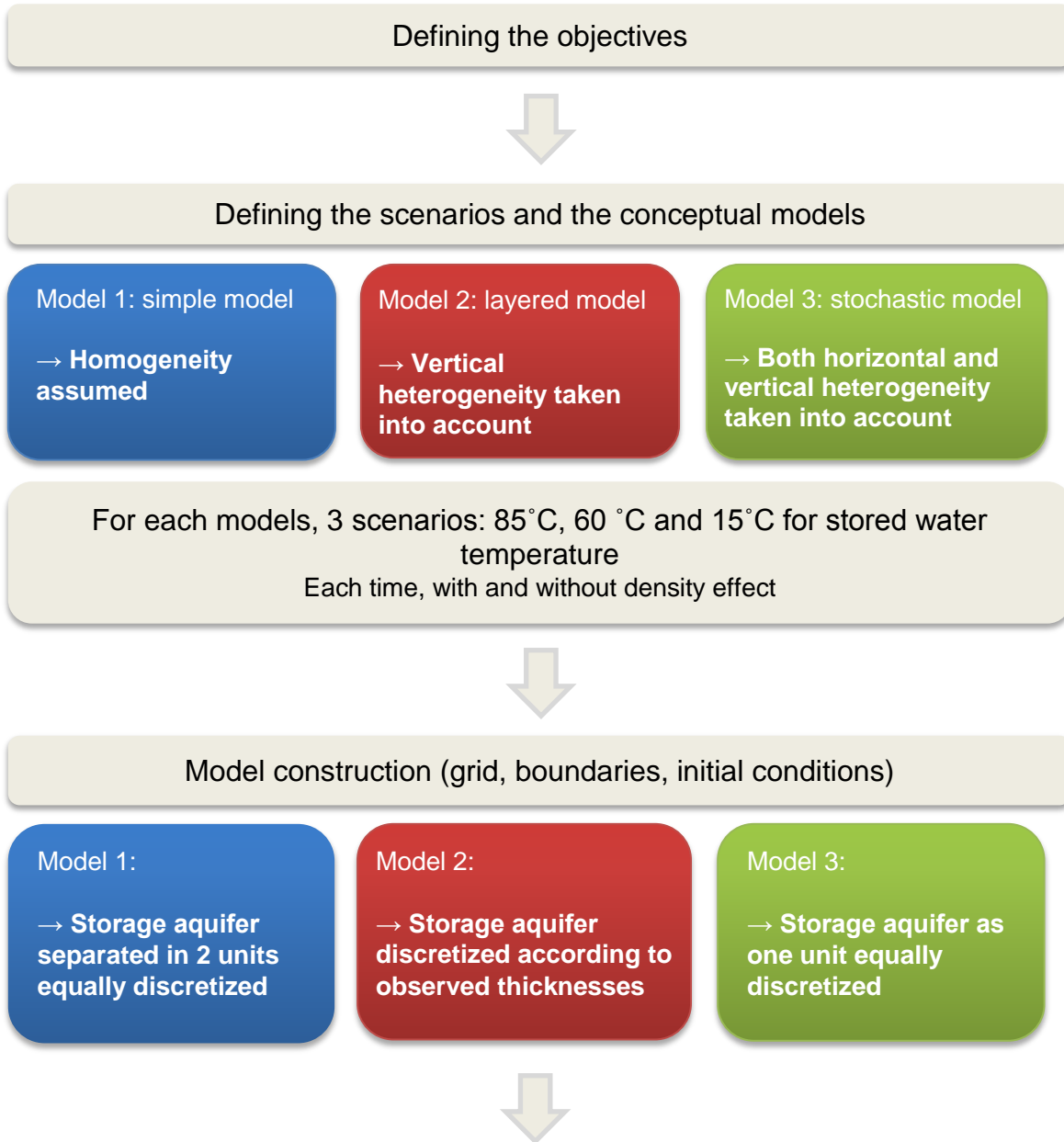
To investigate the effect of heterogeneity on the efficiency of the ATES system, three different types of models were developed, with an increasing complexity and closer to reality:

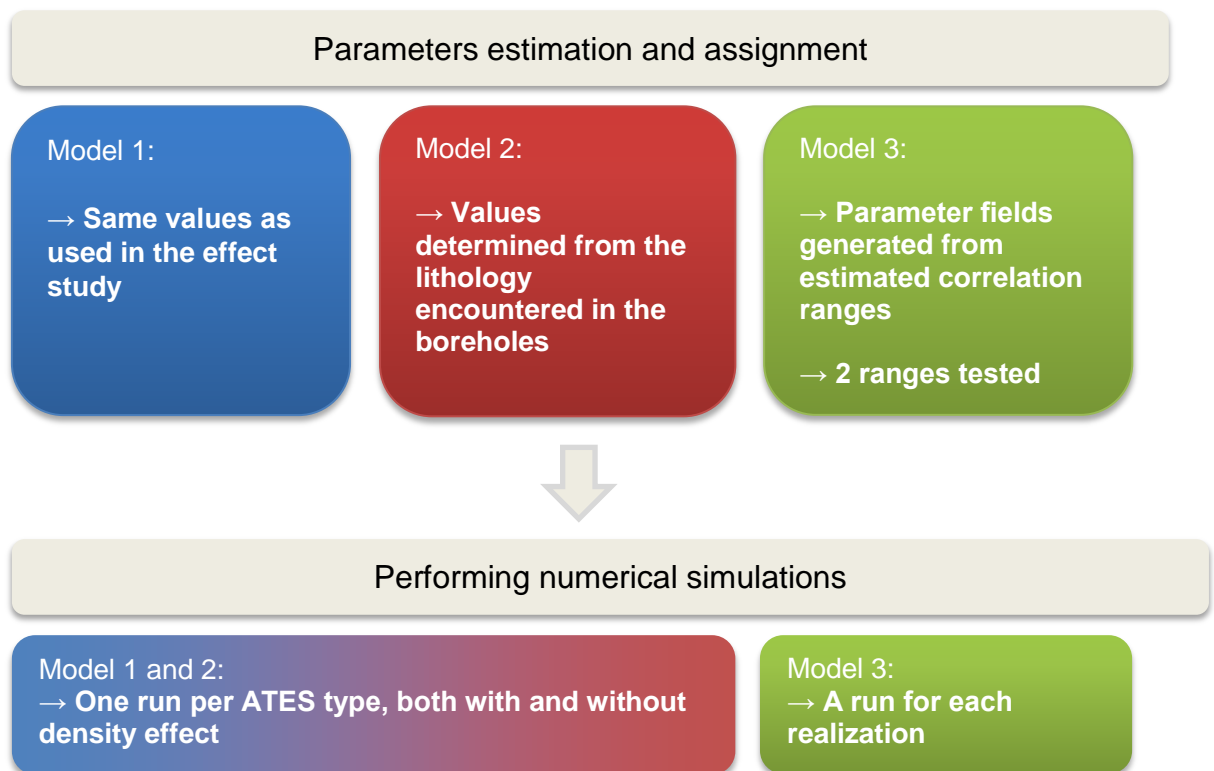
- 1) Similar to what was done for the effect study. In this, the aquifer is considered as homogeneous, with averaged parameters.
- 2) The heterogeneity is represented by geologic layering. Here, only the vertical dimension is complexified since the layers have constant parameter in the horizontal direction. The vertical discretization is then based on the lithology description that was made during the pumping test drilling.
- 3) The hydraulic conductivity fields are generated with stochastic simulation and thus take fully in account the heterogeneity both vertically and horizontally while it honors the field data. Two levels of heterogeneity are considered, with two different horizontal correlation ranges: 1000 m and 100 m. The vertical range stays constant in both versions at 10 m. Five different realizations are run.

Another objective of the modeling is to compare the different ATES designs, their efficiency and how heterogeneity affects them. For this, variable storage temperatures are tested:

- 84°C as designed in the pilot project, with a reinjection temperature of 43°C after heat extraction during winters.
- 60°C to represent medium-temperature storage, with a reinjection temperature of 30°C. This value was adjusted so the temperature in the hot wells does not reach it after extraction.
- 15°C for low-temperature storage, with a reinjection temperature of 6°C, similar to the storage temperature as commonly applied for ATES in the Netherlands (Sommer et al., 2013).

The following chart summarizes the steps of the modeling exercise:





#### 4.1.1 Simulation domain and boundary conditions

Modflow, MT3DMS and SEAWAT (references: Modflow: Harbaugh, A. W., 2000; MT3DMS: Zheng, C., and P. P. Wang, 1999; SEAWAT: Langevin et al., 2008) were used to model groundwater and heat flow. The 3D model domain covers an area of 500 m by 500 m with cells dimension of 10 m by 10 m. The total depth is 250 m and was discretized by a total of 26 layers. The layer thicknesses in the aquifer part are regular in the models 1 and 3 but follow the geological layer thicknesses in the second model, varying between 1 and 25 meters thick. The first layer is defined as unconfined and the others are confined. Observation points were input in one hot well and one cold well. The groundwater flow direction is aligned to the y-axis that would correspond in the reality to the south-east/north-west direction.

The three following figures show a scheme of the three different model domains (Figure 4.1, Figure 4.2 and Figure 4.3).

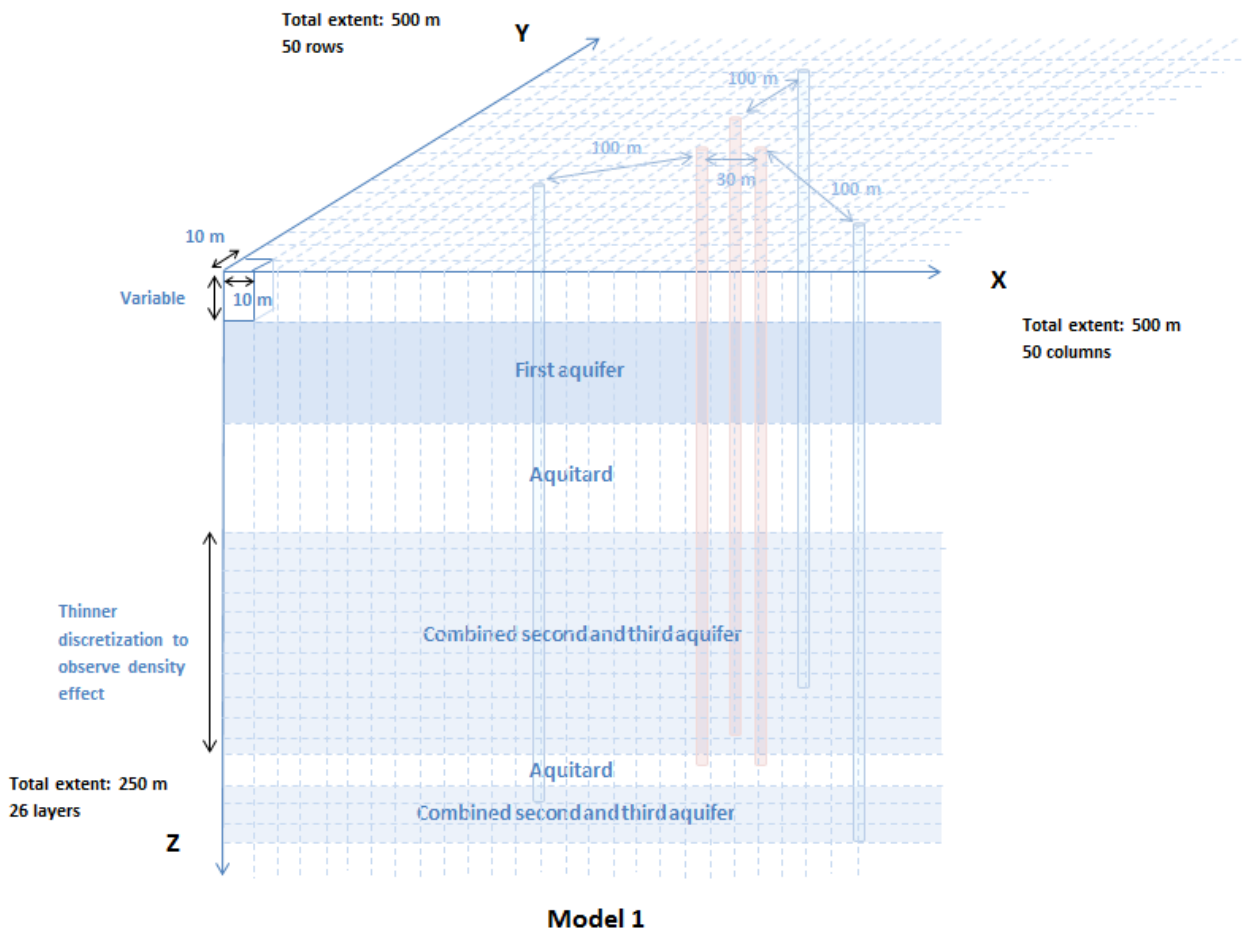


Figure 4.1. Schematized domain of model 1. Not to scale.

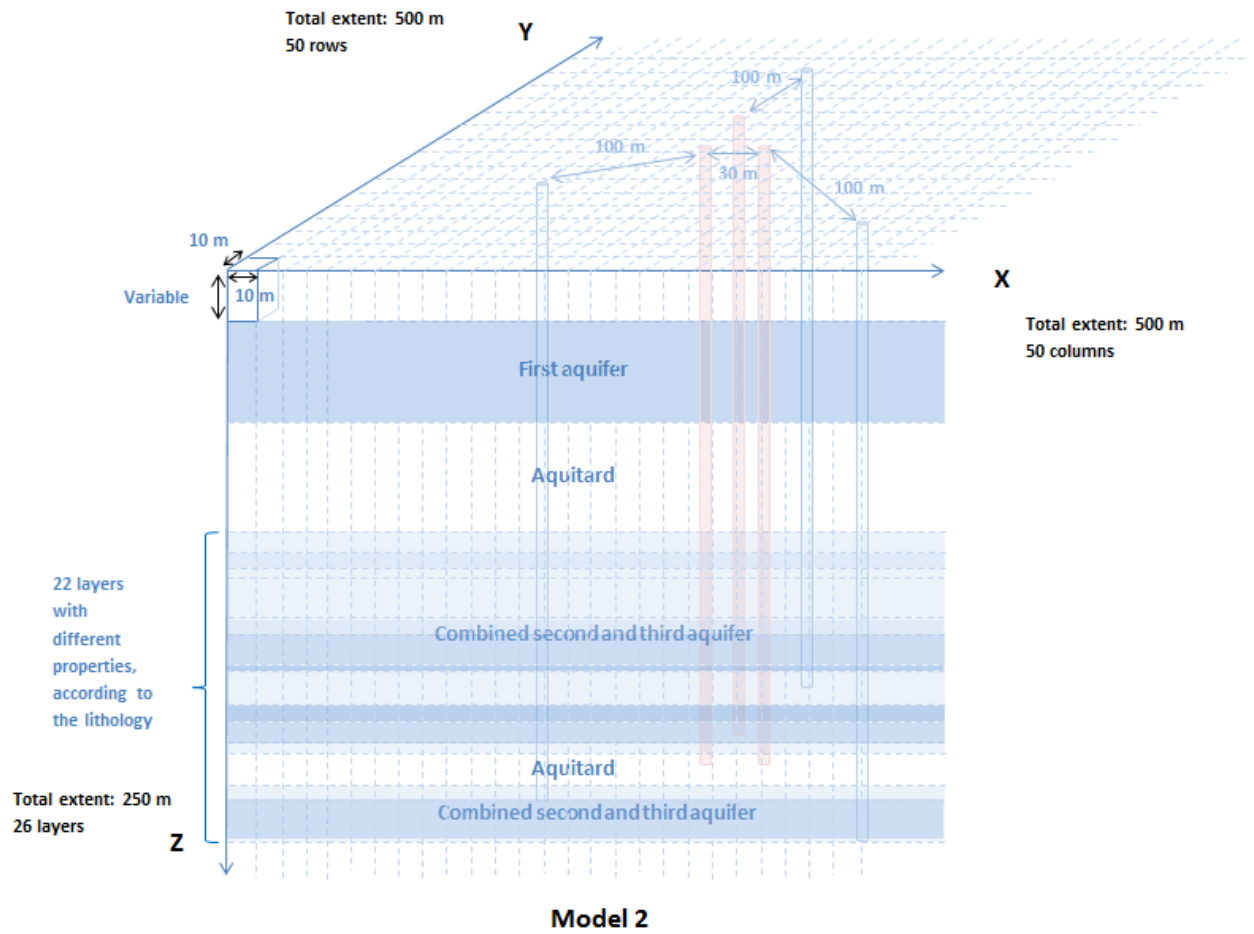


Figure 4.2. Schematized domain of model 2. Not to scale

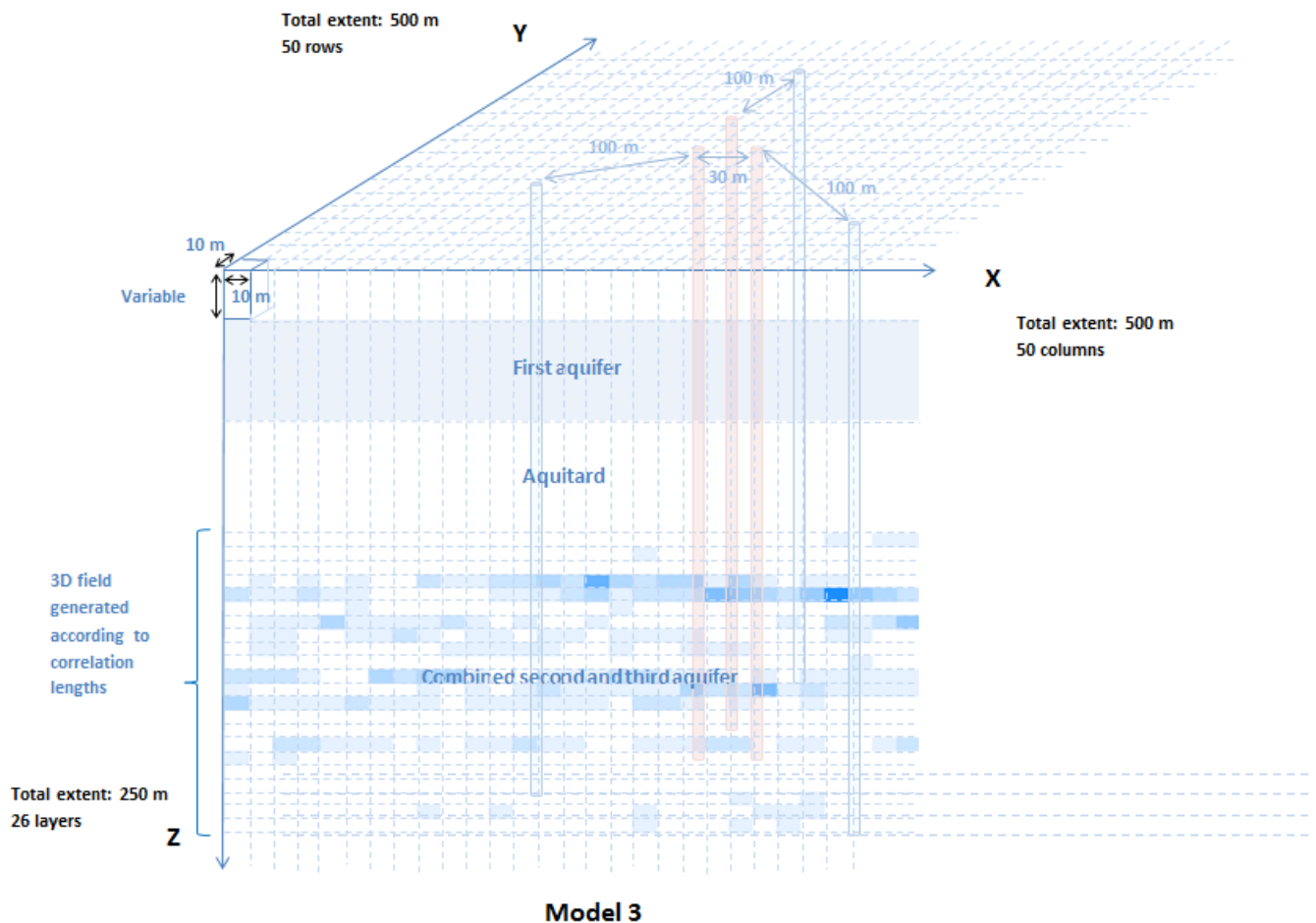


Figure 4.3. Schematized domain of model 1. Not to scale

The west and east boundaries are specified as constant hydraulic head, set as -0.4 and -0.6 meters in the first two layers and 0.4 and 0.2 m in the 2<sup>nd</sup> and 3<sup>rd</sup> aquifers and the aquitards, to honour the hydraulic gradient and water table described in chapter 1. It is worth wondering whether this difference of 0.8 m in hydraulic heads between the first aquifer (layer 2) and the storage aquifer (layer 4 to 25) creates an upward flow that would influence the flow in the storage aquifer itself. Yet, a low vertical hydraulic conductivity (0.014 m/d) is set for the layer inbetween (layer 3) (see section 4.1.2) that limits this influence. One can calculate an approximate upward flow through one column in the layer 3 using Darcy's law, giving a value of 0.03 m<sup>3</sup>/d, which is small relative to the pumping rate.

The north and south boundaries have no flux conditions. These boundaries conditions are invariant in time. No recharge is taken into account. The initial hydraulic heads were derived from a preliminary steady-state simulation. Regarding the temperature conditions, the initial temperature is set as 13°C in the first layers and then follows the thermal gradient derived from a temperature log (Figure 2.5). The constant head cells are assumed as constant temperature, too. The model runs in a transient state, for a period of five years. The total simulation time is discretized in twenty stress periods corresponding to the seasons: 120 days during injection in summer and during withdrawal in winter and 60 days for the two rest periods. A total of 1800 time steps is reached.



### 4.1.2 Flow parameters

The main parameter that varies between the three models is the hydraulic conductivity (K). Indeed, numerous studies revealed that flow parameters are more variable than thermal ones and play a more important role in groundwater process. Chevalier (1997) outlined that thermal parameters are in general better known than hydrogeologic ones. Also some studies, as Ferguson (2007) has demonstrated that variations in thermal conductivity have minimal effect on model results.

The values for the two first models are summarized in the following table (Table 4.1). The comparison column represents the weighted-average, by thicknesses, of the second model values for the layers corresponding to the model 1.

Table 4.1. Hydraulic conductivity values used in model 1 and 2

Layer i	Model 1		Model 2		Comparison for horizontal K	
	Horizontal K (m/d)	Vertical K (m/d)	Horizontal K (m/d)	Vertical K (m/d)	Horizontal K (m/d)	Vertical K (m/d)
1	0,01	0,01	0,01	0,01	=	=
2	15,1	3,8	15,1	3,8	=	=
3	0,57	0,014	0,57	0,014	=	=
4	7,3	1,5	6,80	1,5	6,8	1,4
5			0,08	0,0125		
6			5,48	1,5		
7			0,03	0,0125		
8			7,41	1,5		
9			4,97	1,5		
10			6,46	1,5		
11			2,80	0,0125		
12			6,86	1,5		
13			12,72	1,5		
14			0,08	0,0125		
15			7,46	1,5		
16			11,18	1,5		
17			9,74	1,5		
18	0,80	0,0125				
19	7,76	1,5				
20	0,0125	0,0125	0,0125	0,0125	=	=
21	7,3	1,5	4,03	1,5	7,6	1,8
22			15,22	3,8		
23			7,16	1,5		
24			15,22	3,8		
25			6,86	1,5		
26	0,01	0,01	0,01	0,01	=	=

The hydraulic conductivity value of the layers that contains more than 30% of shells fragments (n°22 and 24) can be expected to be much higher according to the literature (Stuurman, 1995), but the values were calibrated to correspond to the effect study model.

For the model 3, the hydraulic conductivity field were generated by stochastic simulation with the values of model 2 as conditional data. Five different realizations were produced, all honouring this conditional data (see section 3.1.3). The following figure shows an example of the generated field for a correlation range equal to 1000 m (Figure 4.4).

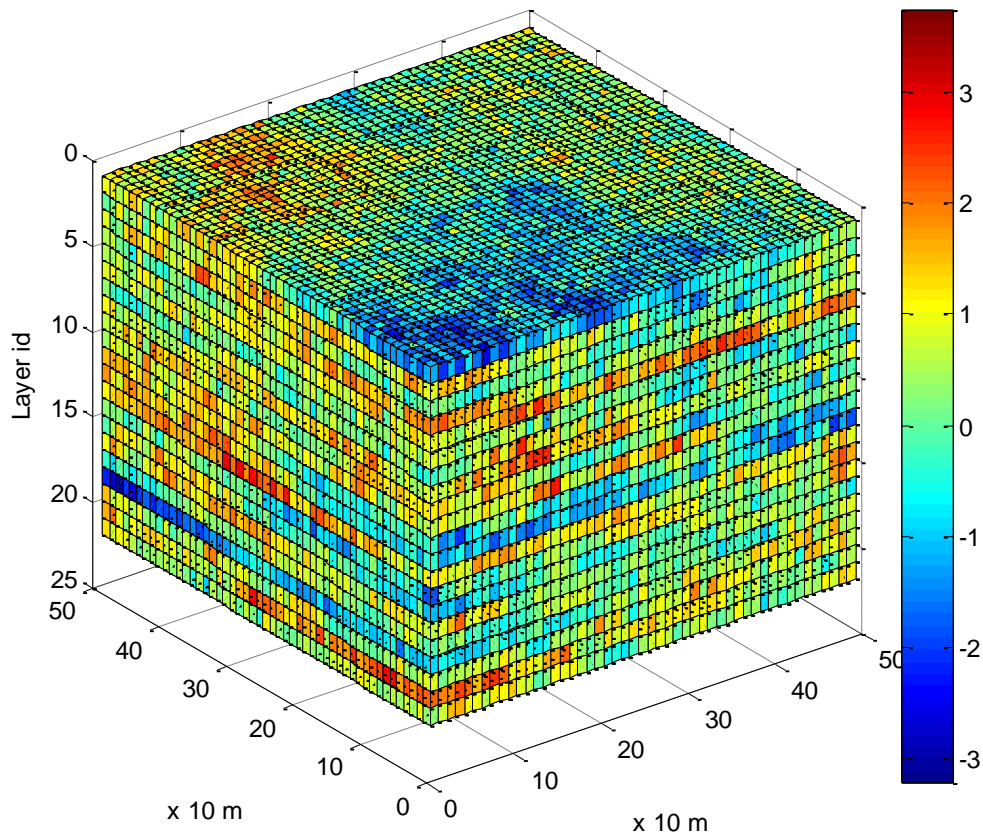


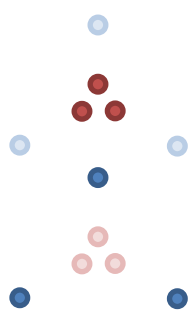
Figure 4.4. Example of one stochastic realization, with a maximum horizontal correlation range of 1000 m. The logarithm of hydraulic conductivities in meter per days.



Vertical hydraulic conductivities are used by the model code to calculate vertical leakage. In the model 3, since the value change for each cell, the vertical K is set as 1/10 of the horizontal K.

Specific storage was considered equal for the aquifer layers ( $10^{-4} \text{ m}^{-1}$ ) and for the confining layers ( $10^{-3} \text{ m}^{-1}$ ), according to the literature (Batu, 1998). Porosity and specific yield for the unconfined layer are fixed at 0,25.

The operation conditions for injection and withdrawal rates in the pumping wells, described in Table 4.2, stem from the pilot project design. Wells was defined in all the aquifer layers of the combined second and third aquifer.

Table 4.2. Operation conditions of the ATEs system along a year



	Summer = injection (120 days)	Autumn = rest (60 days)	Winter = withdrawal (120 days)	Spring = rest (60 days)
	Injection at 84°C in the central hot wells 		Pumping in the central hot wells 	
	Pumping in the external cold wells		Injection at 43°C in the external cold wells	

In the three models, a total flow rate of 6042 m<sup>3</sup>/d is extracted during the injection and withdrawal periods, for a total extracted or injected volume of 725 000 m<sup>3</sup> per period. This rate is divided by three to determine the rate at one well. Then this rate is distributed along the aquifer layers, proportionally to the transmissivity of the layer in model 1 and 2 and equally distributed in the model 3.

### 4.1.3 Thermal parameters

The process of heat flow can be considered as analogous to the solute transport processes. Then the MT3DMS code, initially created for solute transport, can be used with temperature as solute species (Hecht-Mendez et al., 2010; Thorne et al., 2006). The code implies to specify a diffusion coefficient  $D$  that describes the diffusive flux of the solute and a distribution coefficient  $K_d$  that is used to simulate sorption and chemical reactions.

Two main processes govern heat flow: conduction, depending on the thermal conductivity  $k_T$  and convection that depends on heat capacity  $c$ . Heat conduction has been proved similar as Fickian diffusion (Thorne, 2006), which means that transport occurs in response to a gradient of temperature:

$$\varphi = -k_T \cdot \frac{dT}{dx}$$

where  $\varphi$  is the thermal flux in the  $x$  direction, and  $dT$  the temperature difference over a distance  $dx$ . The diffusion coefficient needed for transport simulation can then be related to thermal conductivity:

$$D_T = \frac{k_T}{n \cdot \rho \cdot c_w}$$

where  $D_T$  is the thermal diffusion coefficient,  $n$  the porosity,  $\rho$  the water density and  $c_w$  the specific heat capacity of the water. The aquifer thermal conductivity depends on both the solid conductivity and fluid conductivity, which can be weighted by volume.

To determine the distribution coefficient for temperature, the following equation can be used:

$$K_{d\_temp} = \frac{c_s}{\rho \cdot c_w}$$

A linear sorption isotherm is selected to represent the thermal exchange between the water and the solid, thus the exchange is not function of temperature. The following values were used to determine the thermal parameters, according to the effect study or the literature (Table 4.3).

Table 4.3. Thermal parameters used in the model

Porosity	n	0,25	(-)
Water density	$\rho$	999,7	Kg/m <sup>3</sup>
Thermal conductivity <sup>(1)</sup>	$k_T$	1,7	W/m/K
		2,4	W/m/K
		2	W/m/K
Fluid heat capacity <sup>(2)</sup>	$C_w$	4192,1	J/kg/K
Solid heat capacity (sandstone and clay) <sup>(3)</sup>	$C_s$	920	J/kg/K
<b>Molecular diffusion coefficient</b>	$D_T$	<b>0,14</b>	m <sup>2</sup> /d
		<b>0,20</b>	
		<b>0,16</b>	
<b>Thermal distribution factor</b>	$K_{d\_temp}$	<b>2,195E-04</b>	m <sup>3</sup> /kg
<b>Longitudinal dispersivity <sup>(4)</sup></b>	$\alpha_L$	<b>0,5</b>	<b>m</b>

<sup>(1)</sup> determined from the effect study, varies between aquifer and confining layers

<sup>(2)</sup> from Sommer et al. (2013)

<sup>(3)</sup> from Langevin (2008)

<sup>(4)</sup> from Bridger and Allen (2010)

The SEAWAT program permits to take into account the density effect (Langevin et al., 2008). It actually runs a coupled version of MODFLOW and MT3DMS. Fluid density is calculated as a function of the simulated fluid temperature and the effect of density variation on groundwater flow can then be simulated. The ratio between density variation and temperature variation is set as -0,375. The models were run both without and with the variable density flow to be able to compare them and to study the density effect.

#### 4.1.4 Output treatment

Different output can be studied: hydraulic heads, drawdowns and temperatures.

The main variable to look at the efficiency of the ATEs system is the thermal recovery, defined as the ratio between thermal energy that is extracted from the surface and what was injected (Sommer et al., 2013):

$$TR = \frac{\int_{extraction} c_w \cdot Q \cdot (T - T_{nat}) \cdot dt}{\int_{storage} c_w \cdot Q \cdot (T - T_{nat}) \cdot dt}$$

Another variable that is used to analyse the results is the energy balance ratio (EBR) (Sommer et al., 2003). It is calculated as following:

$$EBR = \frac{E_{cold}^{extracted} - E_{warm}^{extracted}}{E_{cold}^{extracted} + E_{warm}^{extracted}}$$

The amount of cold energy that is extracted from the aquifer storage is expressed by:

$$E_{cold}^{extracted} = \int_{cold\ extraction} c_w \cdot Q \cdot abs(T_{extr} - T_{inj}) \cdot dt$$

The same calculation permits to calculate the amount of warm energy extracted. The energy balance ratio is not expected to be close to zero since it is high temperature storage site, meaning that there is an obvious heating of the subsurface.

## 4.2 Model results

The results from the modeling exercise are presented in the next sections. After having presented the results of the reference case and a brief comparison with the effect study results, the effects of heterogeneity are presented by comparing the different models simulations. Then the results of the density effect are showed, followed by the influence of the storage temperature and the eventual impact of thermal storage on the first aquifer unit.

### 4.2.1 Reference case and comparison with the effect study results

The reference case corresponds to the first model, with the same assumptions than what was previously done for the effect study, i.e. a homogeneous aquifer comprising two separated permeable layers. The injection temperature of this reference case is 84°C as designed in the pilot project and the density effect is taken into account. The comparison with the effect study results are presented simply as an indicator. It has to be stated that no particular focus was made to calibrate the model on them.

#### *Thermal plume extent*

Figures 4.5 and 4.6 show the thermal plume observed after 5 years of exploitation (at the end of a recovery period after the winter season), with cross-sectional and plan views respectively. The cross-section (the trace of the section is represented on the plan view by a dotted line) goes through a hot well and a cold well. The background flow is perpendicular to the section plan so its influence on the thermal plume extent is not visible here. The hydraulic conductivity used in the model is showed by a color scale, the most intense blue being the most conductive. The plan views shows the aquifer between 130 and 140,5 meters deep (i.e. the 14<sup>th</sup> layer) at the end of a recovery period after injection (t=1620 days) and after withdrawal (t=1800 days) respectively.

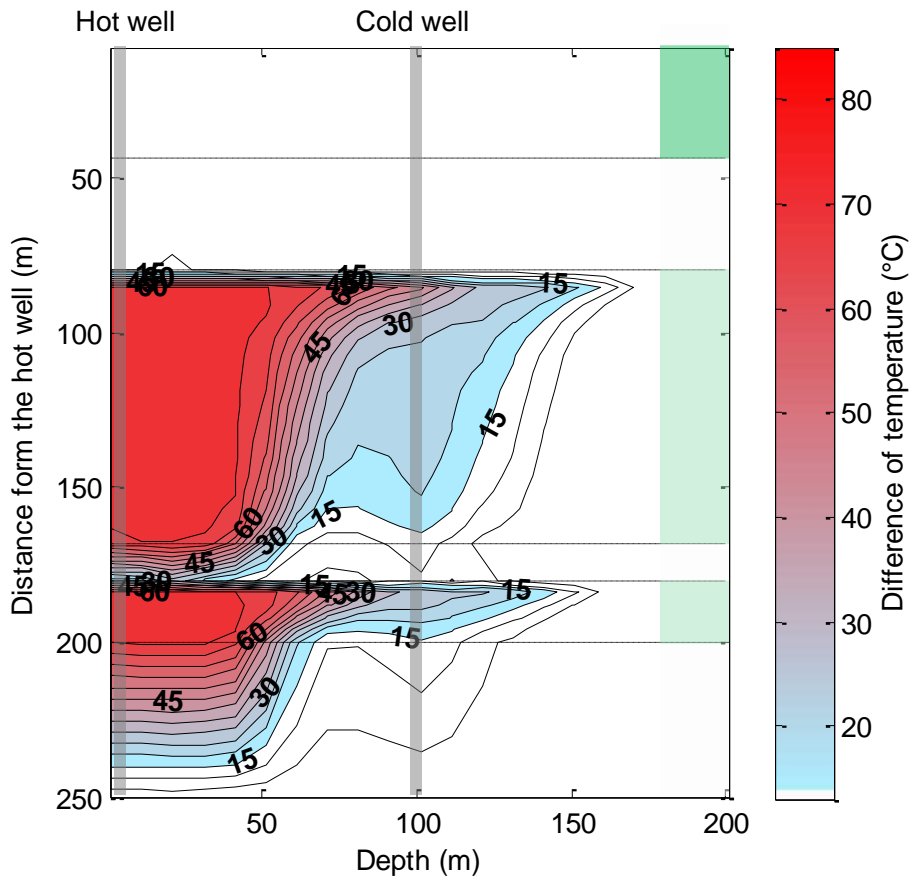


Figure 4.5. Cross-section of the resulting temperature difference with initial temperature in model 1, at t=1800 days. The green scale represents hydraulic conductivity.

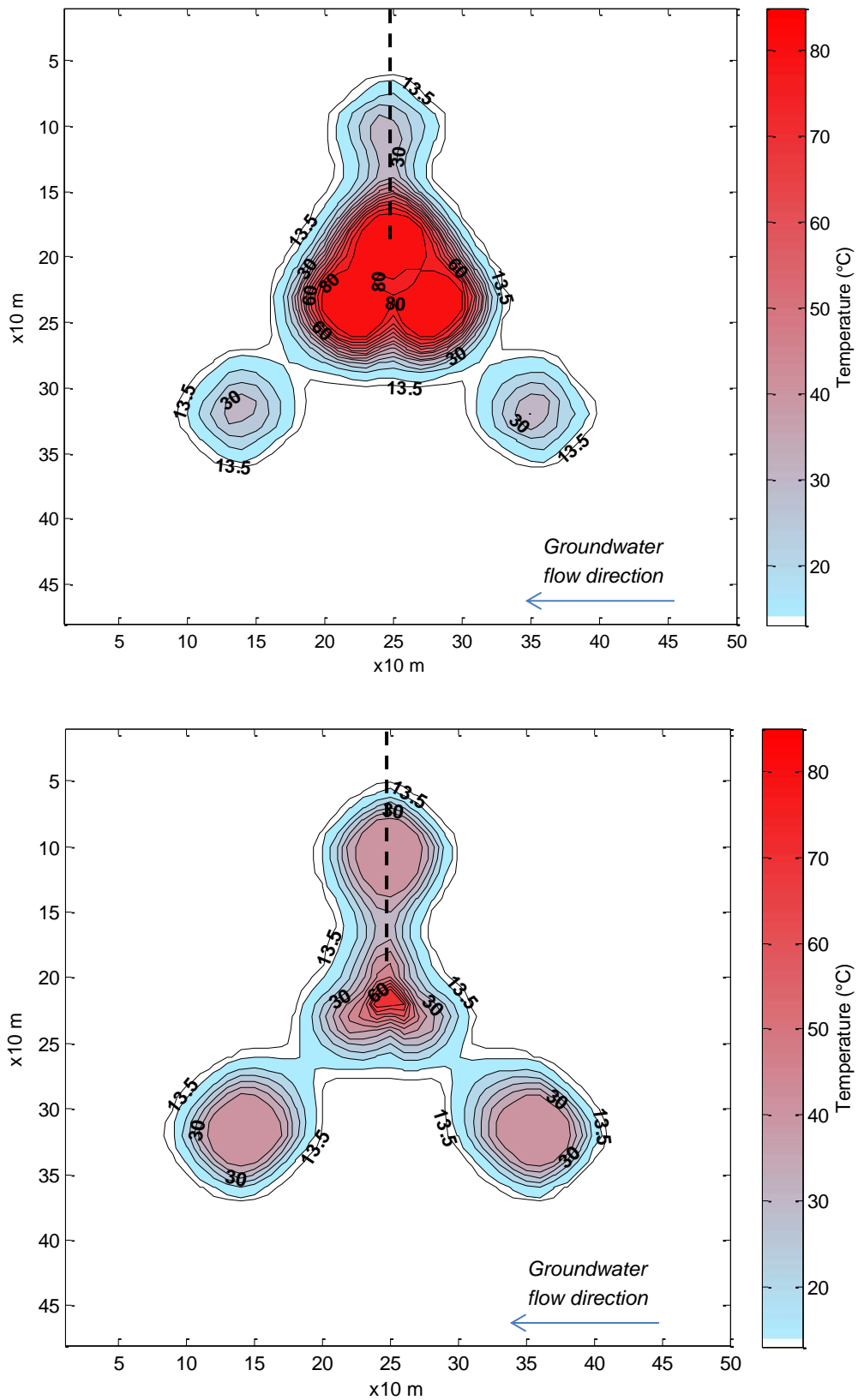


Figure 4.6. Plan views showing resulting temperature of model 1 at  $t=1620$  and  $t=1800$ , using the same scale, at a depth between 130 and 145 m. The dashed line shows the location of the cross-section (figure 4.4).

What is the hydrological efficiency of high-temperature aquifer thermal energy storage when combined with a geothermal plant?

The thermal plume expands to a maximum of about 160 m away from the hot wells in the top of the aquifer layers. This is similar to the results of the effect study model, shown in Figure 4.7. There is interference between the cold and the hot wells after the storage period, but only in the top of the aquifer. This interference does not seem to affect negatively the cold well since the temperature does not exceed 45°C at the location. The heating of the hydrological basis appears more extensive than it should because of a much coarser discretization in this unit. Indeed, one single value is interpolated over a thickness of 50 meters.

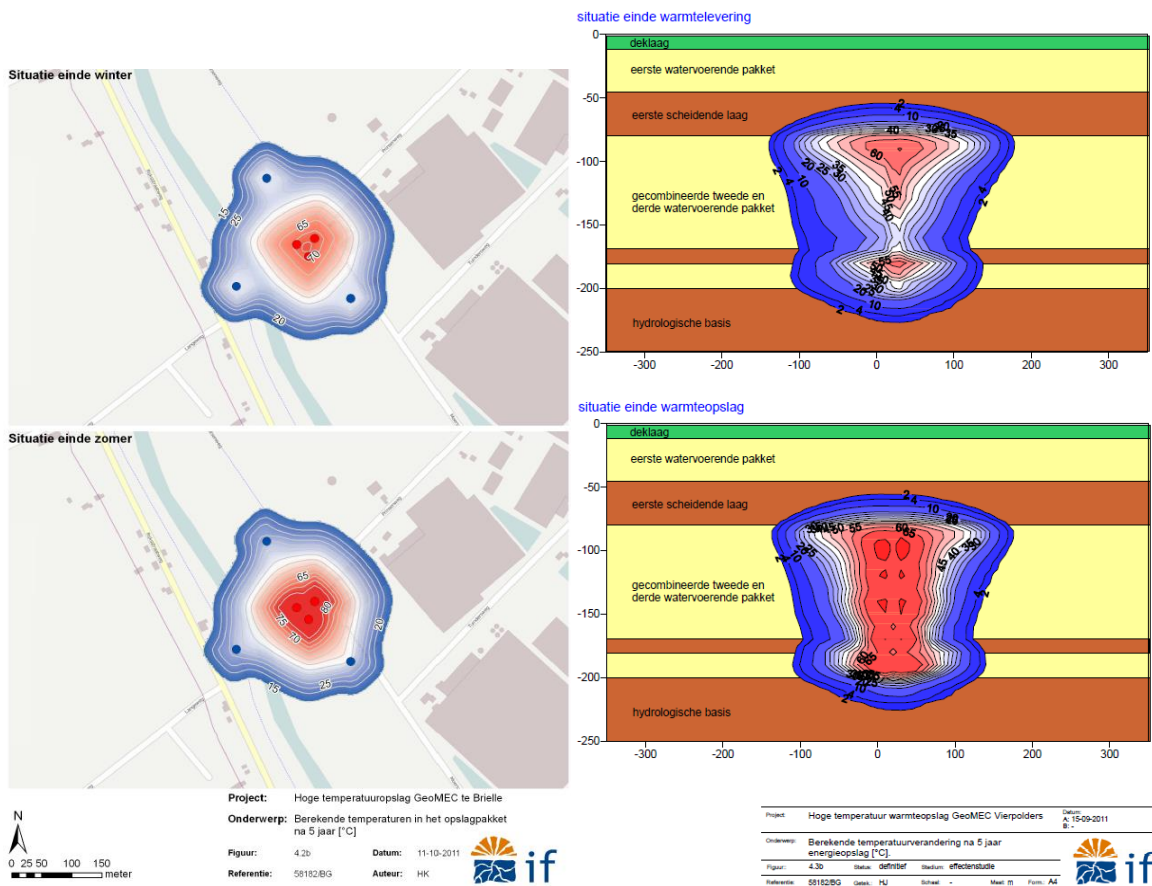


Figure 4.7. Temperature influence (difference with initial temperature) results from the effect study (Buik & Godschalk, 2011). Top figures show the plume at the end of the winter season and bottom ones at the end of summer, after 5 years of exploitation.

Temperature variation during the cycle

The temperature variation in a hot well and a cold well through the five years of exploitation are showed in Figure 4.8. The wells correspond to the one shown in the cross-section, i.e. the most northerly ones. As an indication, the different exploitation periods are plotted for the first year. In the effect study it was mentioned that a temperature of at least 57°C is required to supply heat. This is represented in the graph by a dotted line.



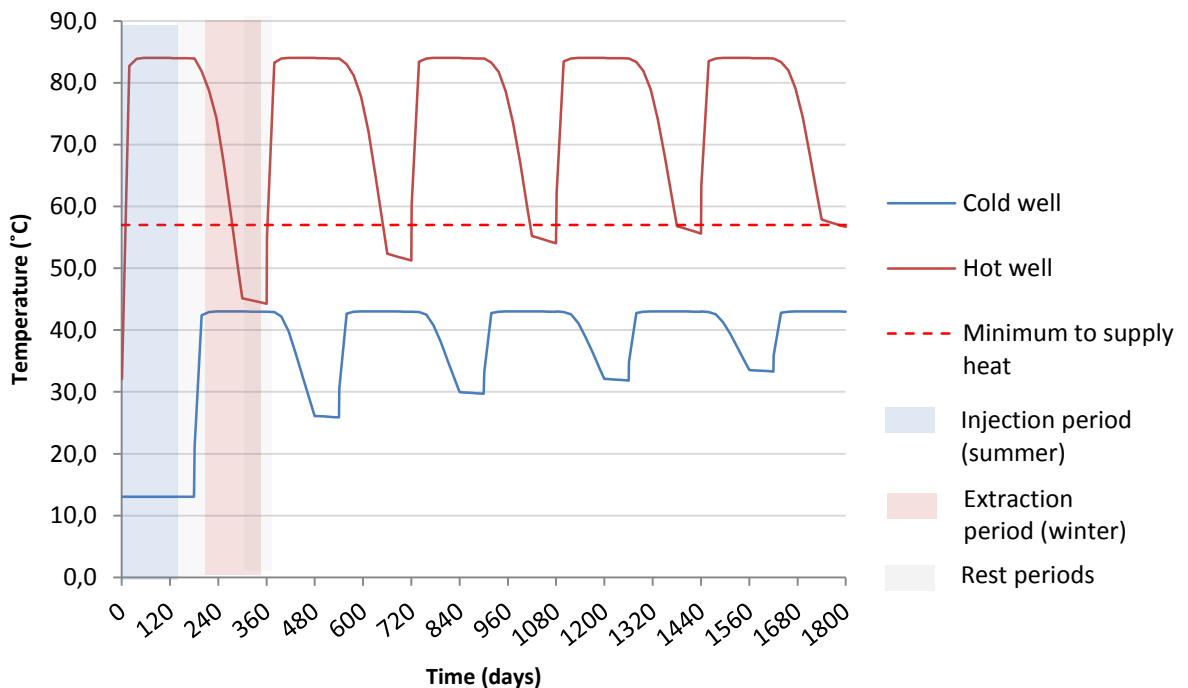


Figure 4.8. Temperature variation in a hot and a cold well through the five years of exploitation.

It is visible (Figure 4.8) that the storage aquifer warms up at the wells location. The temperature decreases very little during the recovery periods, only few degrees. The storage conditions are thus favorable with respect to background flow and thermal conduction. Temperature decreases mainly during pumping periods. After a first year of injection/withdrawal, the temperature in the hot well reaches a minimum of 44,3°C. After five years, the temperature in the hot well varies between 84°C and 56,7°C. The effect study specifies an interval between 84°C and 57°C (Figure 4.9) which is then consistent with these results, though the period is not stated in the study. According to the first model, the system is not capable to provide heat during the entire cold season in the first three years. Concerning the cold well, temperature varies between 43°C and 25,9°C during storage in the second year, and between 43°C and 33,3°C in the fifth year. Here, the values differ slightly from values in the effect study that indicates an interval of 43°C to 21°C.

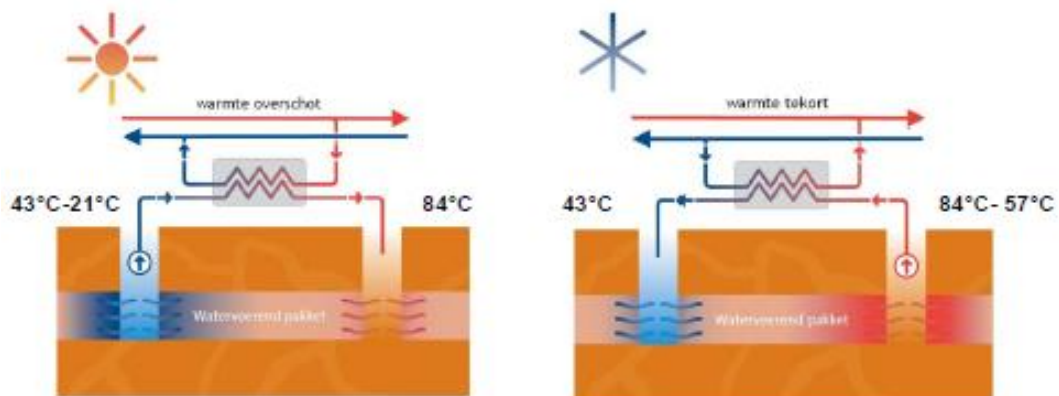


Figure 4.9. Operation conditions according to the effect study ((Buik & Godschalk, 2011)

*Hydraulic influence*

The figures 4.10 and 4.11 show the drawdown in the storage aquifer (between 130 and 140,5 meters deep) after 5 years of exploitation, both at the end of a recovery period after injection ( $t = 1620$  days) and after withdrawal ( $t = 1800$  days). The hydraulic influence area does not expand beyond the model boundaries while the effect study (Figure 4.12) shows an extent much larger. However, the latter likely show the drawdown immediately after injection and withdrawal (before recovery). Also, the difference can be due to different boundaries conditions and their distance to the wells.

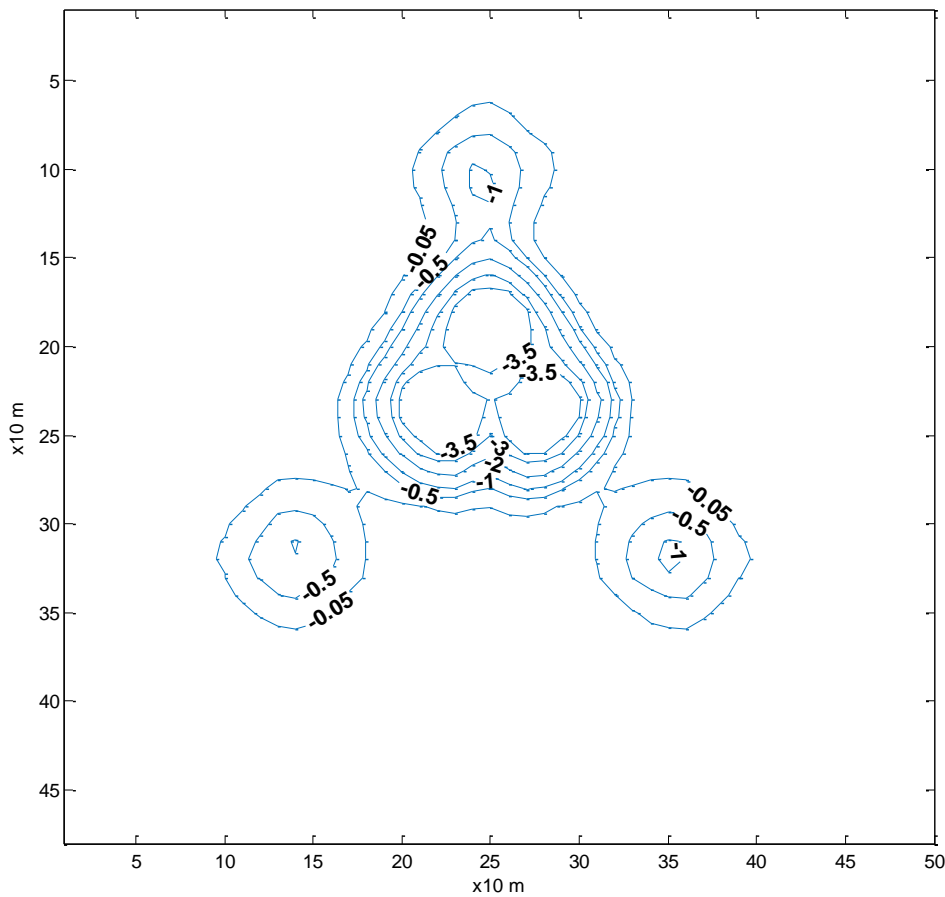


Figure 4.10. Drawdown in meters in the storage aquifer at a depth between 130 m and 140.5 m after an injection period after 5 years of exploitation ( $t = 1620$ ).

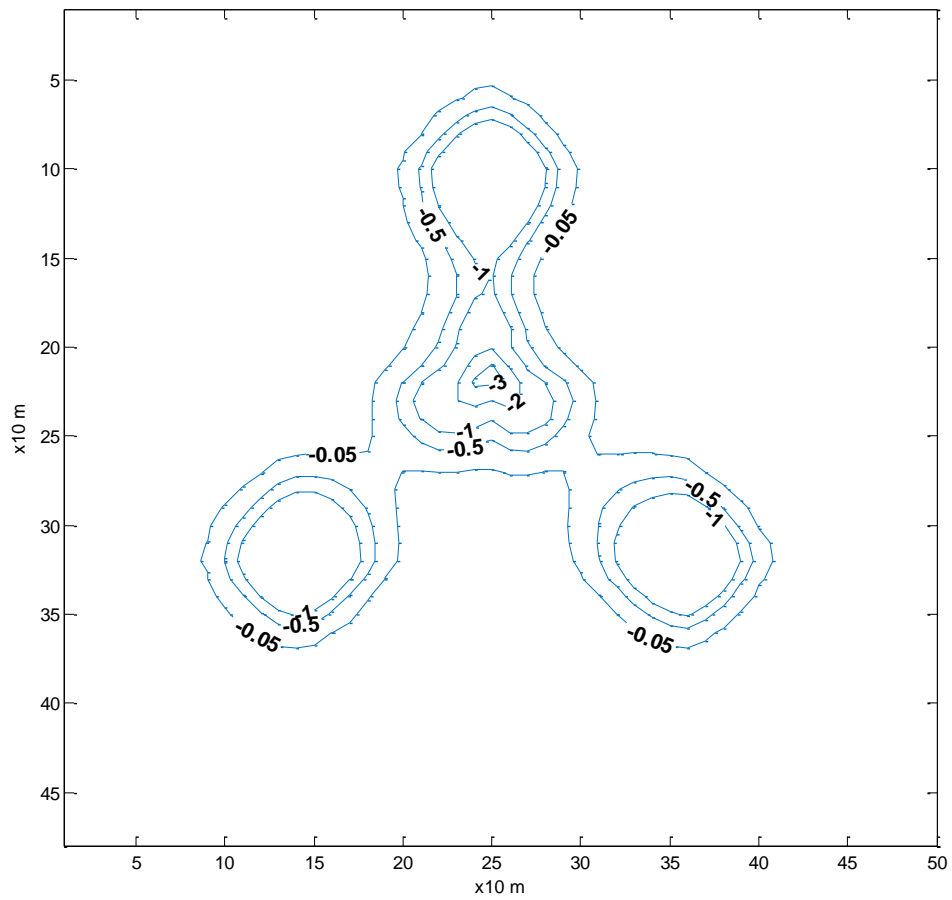


Figure 4.11 Drawdown in meters in the storage aquifer at a depth between 130 m and 140.5 m after an extraction period after 5 years of exploitation ( $t = 1800$ ).

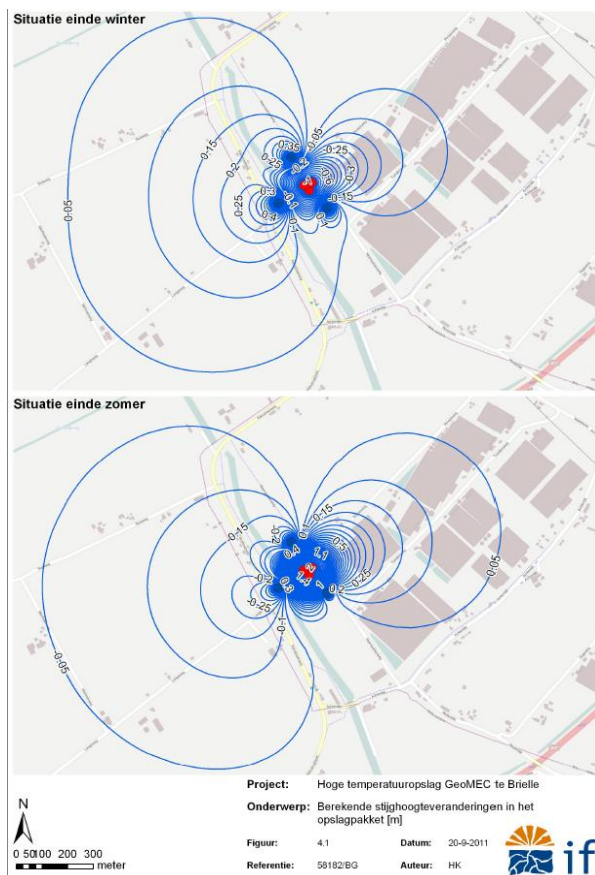


Figure 4.12. Hydraulic influence in the storage aquifer at the end of winter (top figure) and at the end of summer (bottom figure) according to the effect study (Buik & Godschalk, 2011)

## 4.2.2 Impact of the heterogeneity

### 4.2.2.1 Thermal plume

The Figure 4.13 shows the thermal plume for the three types of model. Concerning the third model type, the realization that is closest to the mean of the five realizations is represented, and this holds for the two tested correlation length ( $a_{3a} = 1000$  m and  $a_{3b} = 100$  m). The cross-sections correspond to the end of the recovery period after five years of exploitation ( $t = 1800$  days) and show the most northerly wells. Two lines at 50 m and 150 m are represented to make the comparison easier. The scale of hydraulic heterogeneity is indicated at the right side of the cross-sections with a green color scale, the most intense green being the most conductive.

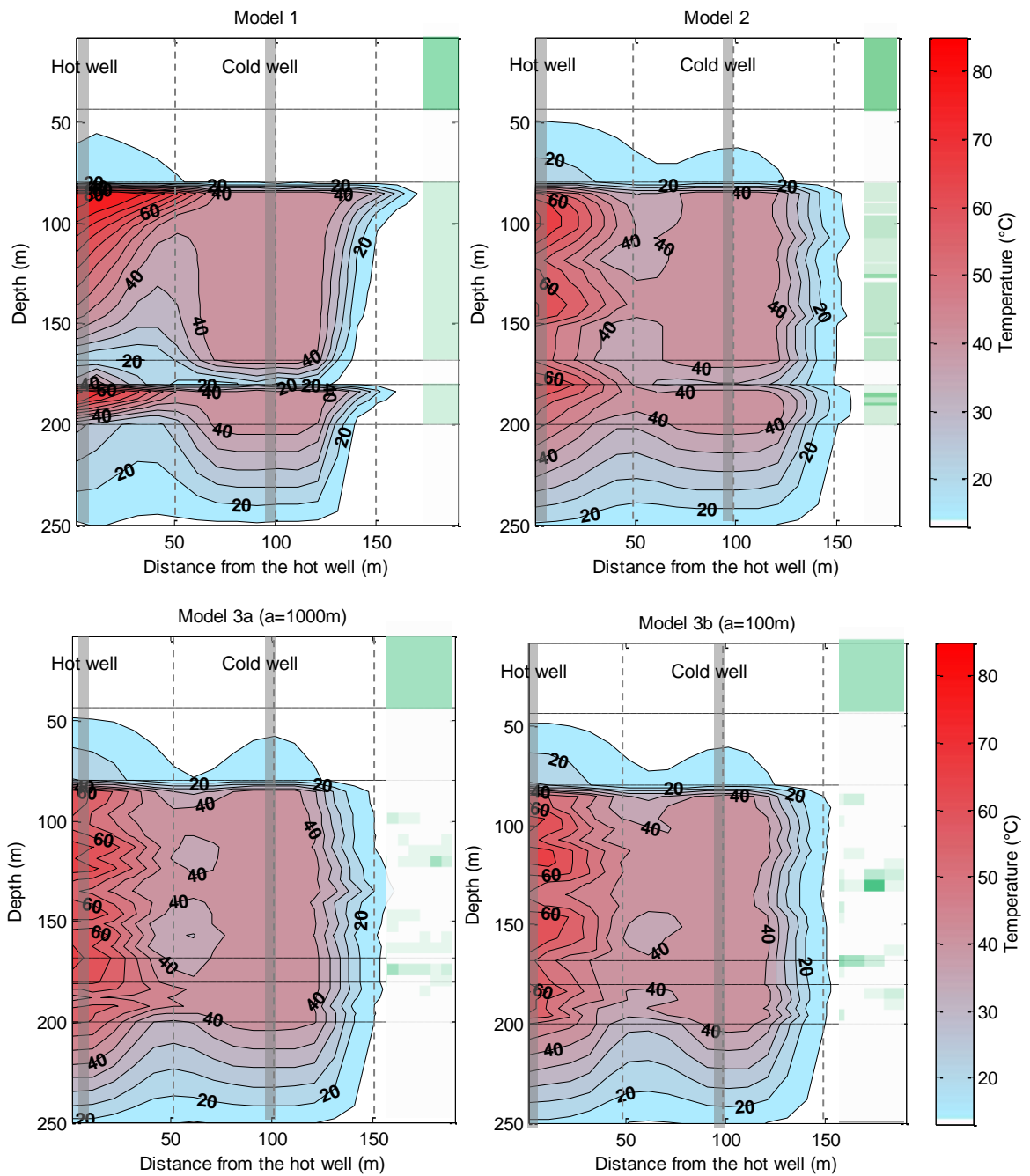


Figure 4.13. Extent of thermal plume for the four different types of model after 5 years of exploitation ( $t = 1800d$ ).  
The green scale indicates the hydraulic conductivity.

The differences among the four thermal plumes extent are relatively small. Some dissimilarities can be noted though:

- The extent of the global thermal front is slightly smaller in the most heterogeneous model (n° 3b). The 15°C isotherm barely reaches a distance of 150m from the hot well.
- The density effect seems to be diminished in the three heterogeneous model (n° 2, 3a and 3b) compared to the homogeneous model, which leads to a more equal temperature distribution along the wells and a lower maximum temperature. The following table

presents the maximum temperature for the four cross-sections at the hot well (Table 4.4).

Table 4.4. Maximum temperature along the hot well in the four types of model

Model	1st	2nd	3 <sup>rd</sup> a	3 <sup>rd</sup> b
Maximum temperature (°C)	81,2	71,0	67,9	66,6

The density effect is discussed in the following paragraphs.

- The thermal influence in the layer above the aquifer seems to be underestimated by the homogeneous model (n°1). The impact on the first aquifer unit is assessed in the following paragraphs.

#### *Uncertainty in heterogeneity*

The Figure 4.14 shows the thermal plume extent for the five different realizations with a maximum horizontal correlation range of 1000 m (model 3a). The same is shown for model 3b (range = 100m) in Figure 4.15. It is possible to see some differences between the five realizations in both cases, for example with interference between the wells to varying degrees.

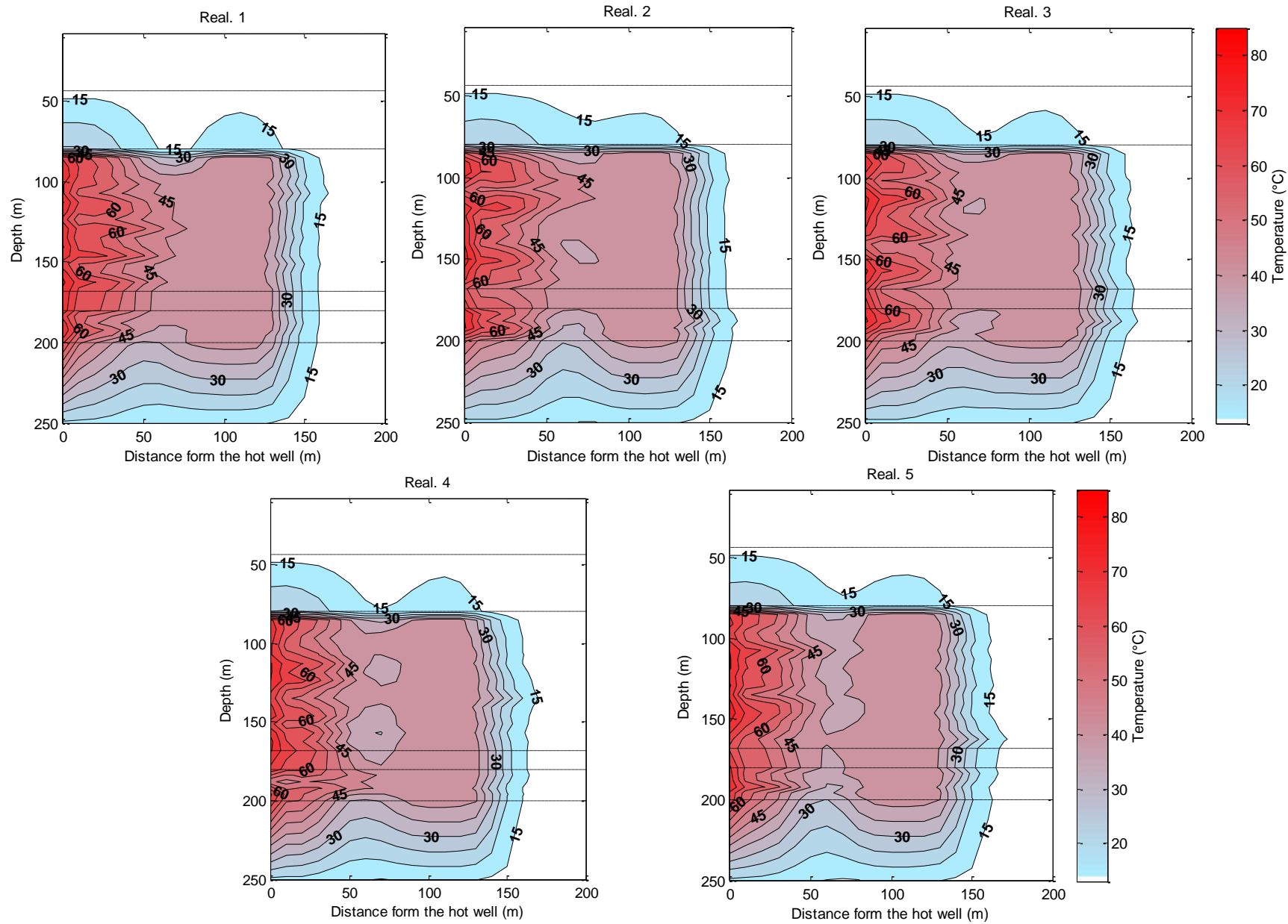


Figure 4.14. Cross-sections of the resulting temperatures for the five different realizations with a horizontal correlation range of 1000 m (model 3a)

What is the hydrological efficiency of high-temperature aquifer thermal energy storage when combined with a geothermal plant?

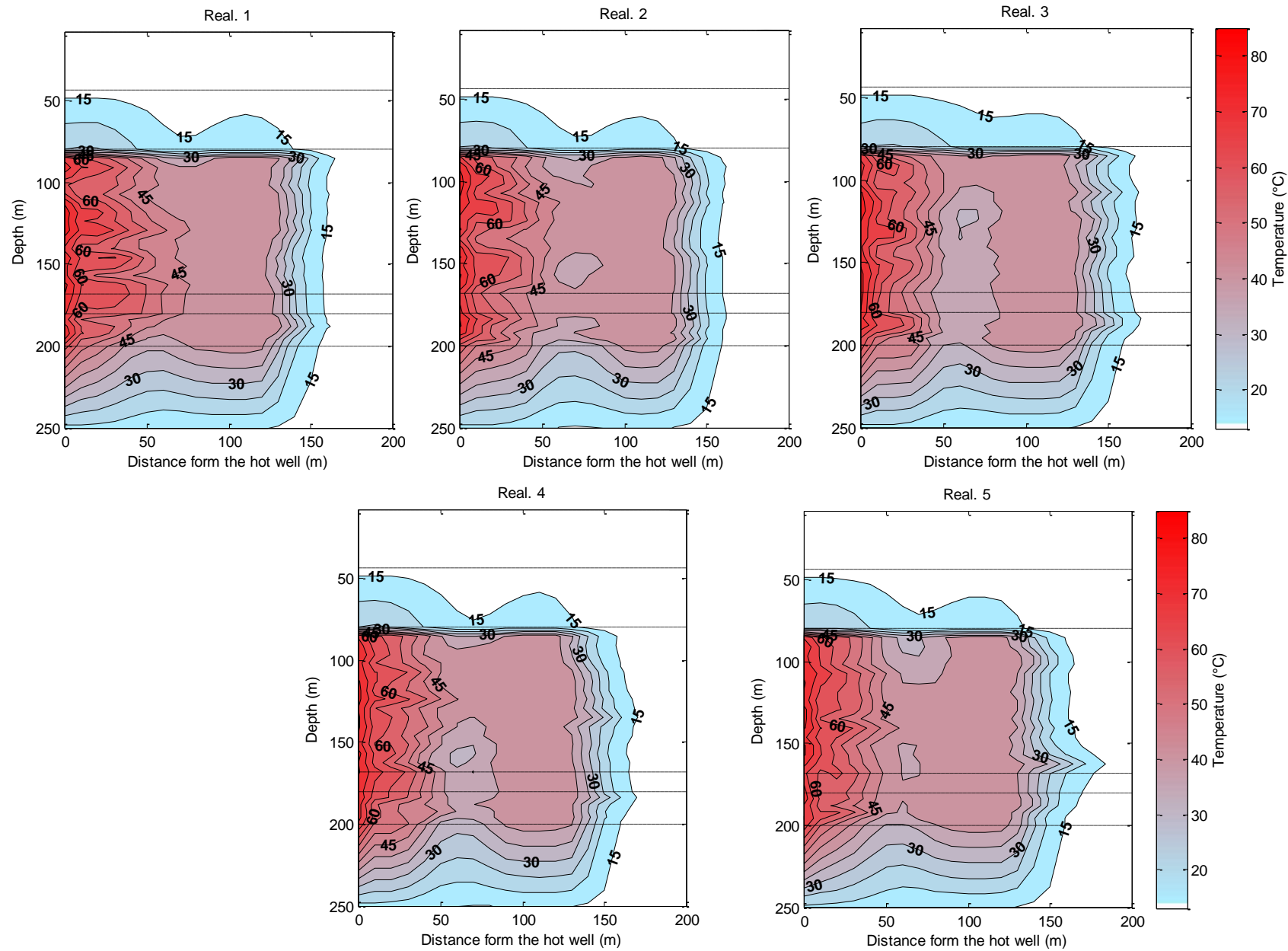


Figure 4.15. Cross-sections of the resulting temperatures for the five different realizations with a horizontal correlation range of 100 m (model 3b)



The study of thermal recovery and energy balance ratio provides a more accurate picture of the impact of heterogeneity.

4.2.2.2 Thermal recovery and energy balance ratio

The thermal recoveries of the hot and cold wells are shown for the different models in figures 4.14 and 4.15 respectively, calculated for five years of exploitation with injection temperature of 84°C. Considering the third model, the dashed grey lines show the minimum and maximum among the five realizations while the colored line is the mean of the five realizations.

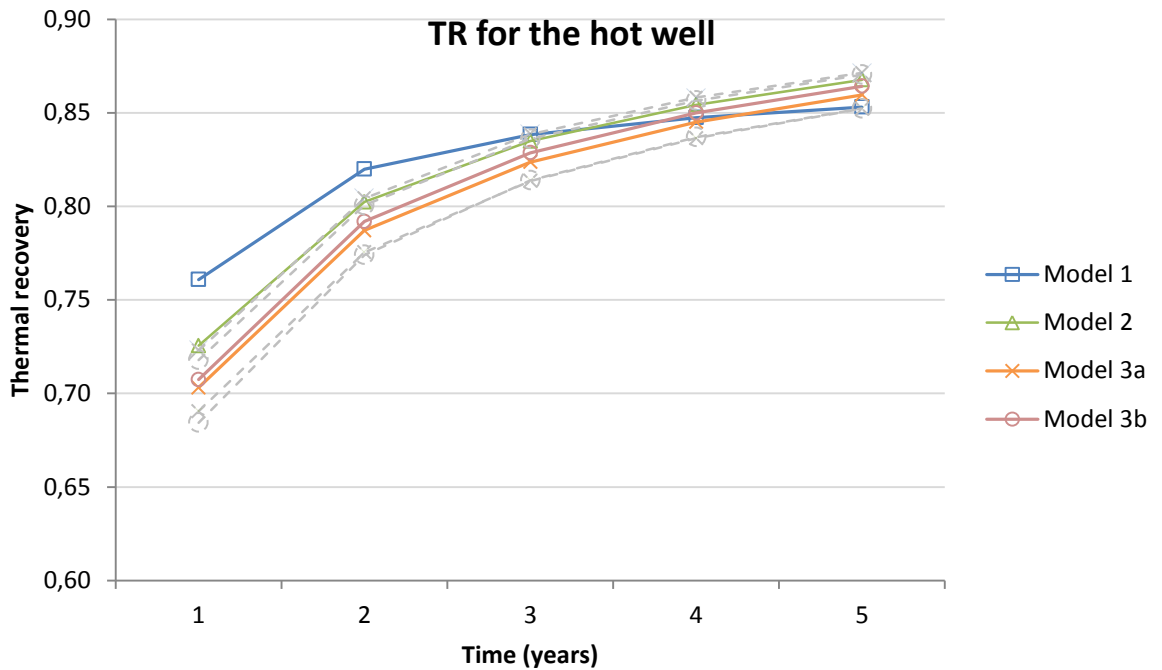


Figure 4.16. Thermal recovery for the hot well the different types of model with injection temperature 84C

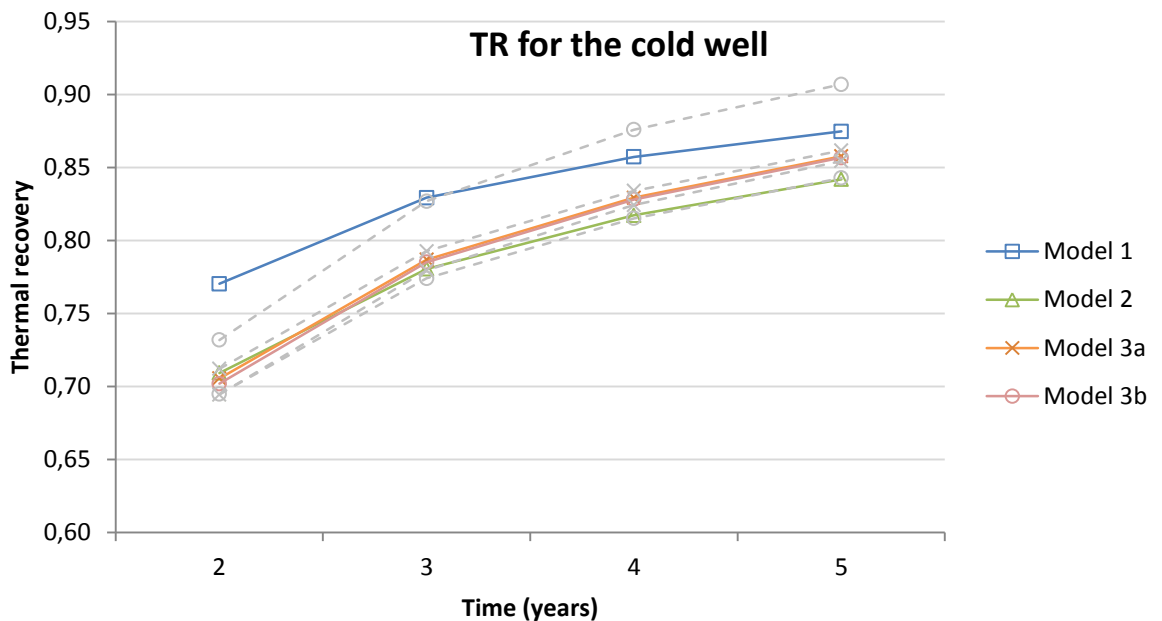


Figure 4.17 . Thermal recovery for the cold well the different types of model with injection temperature 84C

Here again, the thermal recovery does not vary much among the different models, with a maximum difference of 8% and more generally around 5%.

In both the cold and the hot wells, the first model is characterized by a slower increase of the recovery along the five years of exploitation. In the hot well, model 1 initially overestimates recovery and gradually the models converge to same outcome, around 86%.

The layered model (n°2) gives a slightly better efficiency of the hot well of about 1,5% than when both vertical and horizontal heterogeneity is considered.

Concerning the third model, a different horizontal correlation range does not seem to impact the efficiency of the storage, showing a difference of only 0,5% of thermal recovery in the hot well between the model 3a and 3b. The difference between the five realizations is globally around 3%.

The following figure shows the energy balance ratio (EBR) for the three models, after five years of exploitation (Figure 4.18). An EBR close to zero would mean that there is no net heating or cooling of the aquifer. Given the storage temperature, it is obviously expected to observe a relatively high EBR, meaning the aquifer warms up. The EBR is decreasing in the course of years because the aquifer warms up more slowly once already warmed. The results show that the more heterogeneous the model is, the higher the EBR, mostly at the beginning of the exploitation.

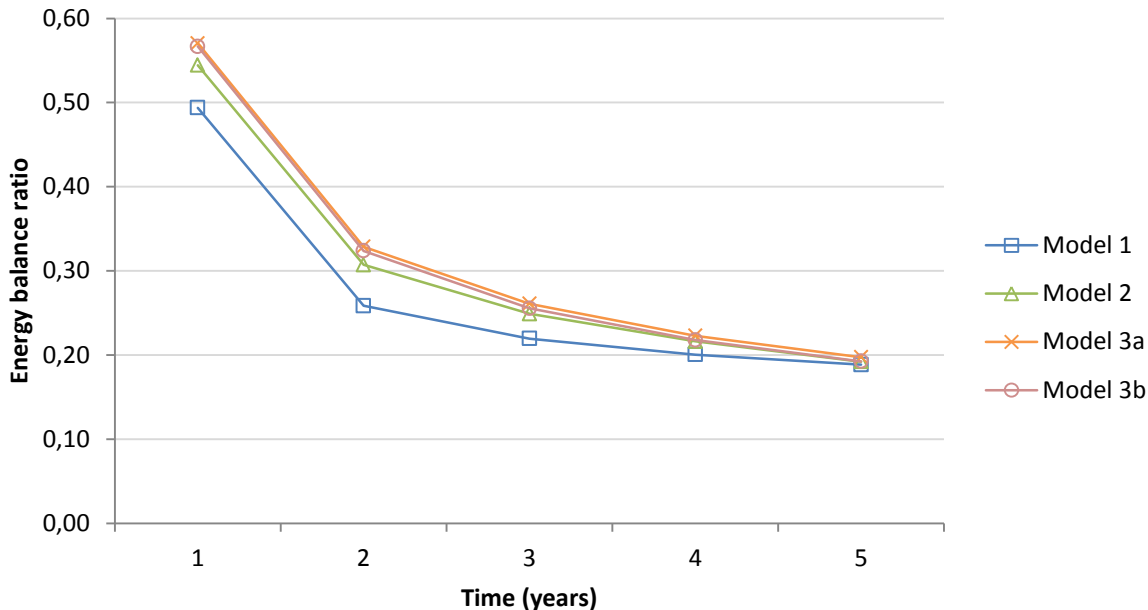
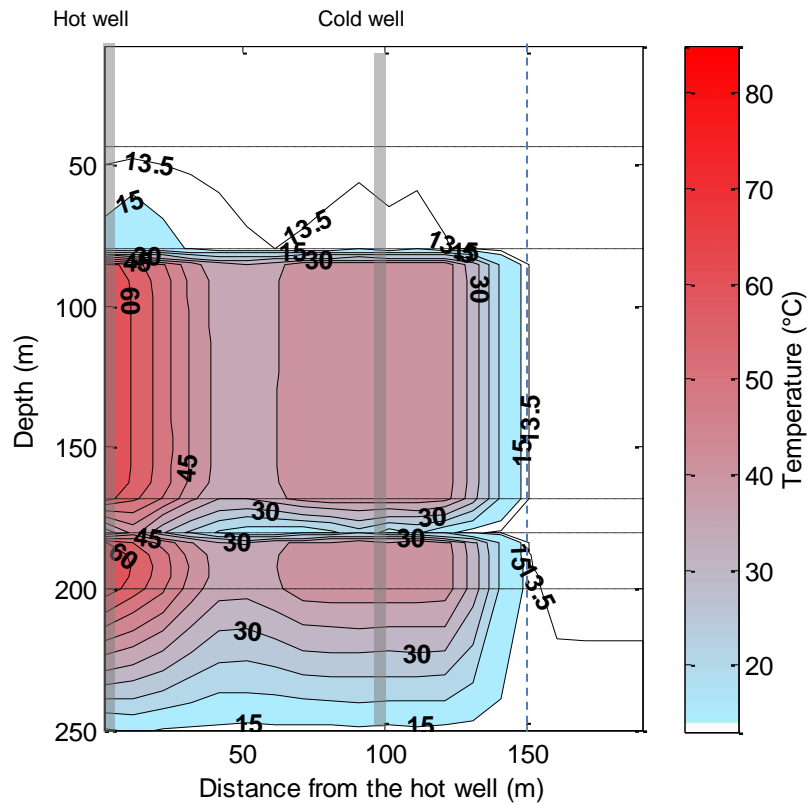


Figure 4.18. Energy balance ratio for the different types of model with injection temperature 84C

### 4.2.3 Density effect

The figure 4.17 shows cross-sections for the reference case, without and with the density effect respectively, at t = 1800 days. The density effect is clearly visible for the first model, with the accumulation of hot water at the top of the aquifer. This leads to a thermal front that extends further in the upper 30 meters of the aquifer. The density effect is mainly visible around the hot well since the injected temperature is higher and thus the density contrast.

According to the relation between density and temperature used in the model ( $\frac{\delta\rho}{\delta T} = -0.375$ ), the density is expected to vary between 973.1 and 999.7 kg/m<sup>3</sup>, which impacts the hydraulic flow. This is visible when looking at the hydraulic heads (Figure 4.20).



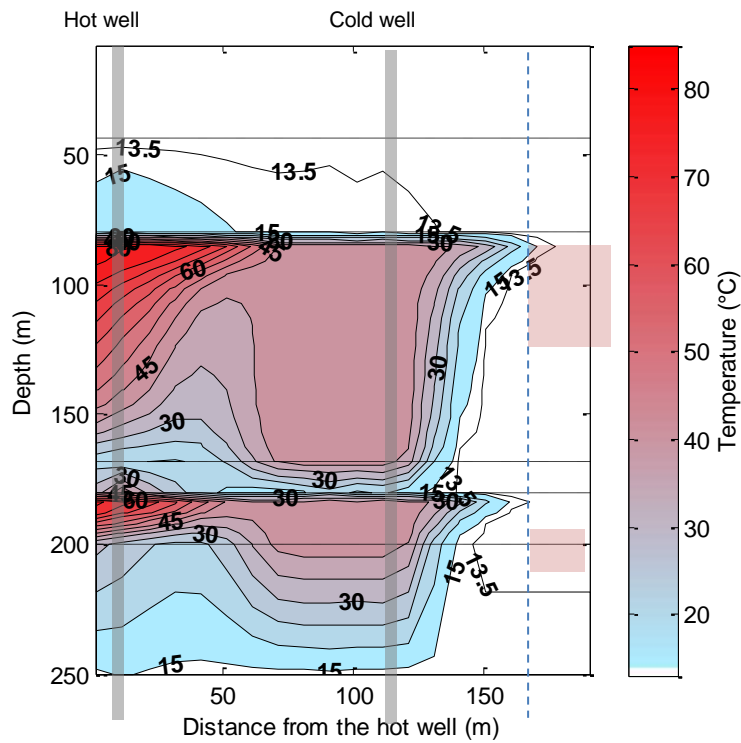


Figure 4.19. Comparison between no density effect (top figure) and density effect included (bottom figure). The red zones indicate the supplementary thermal plume extent.

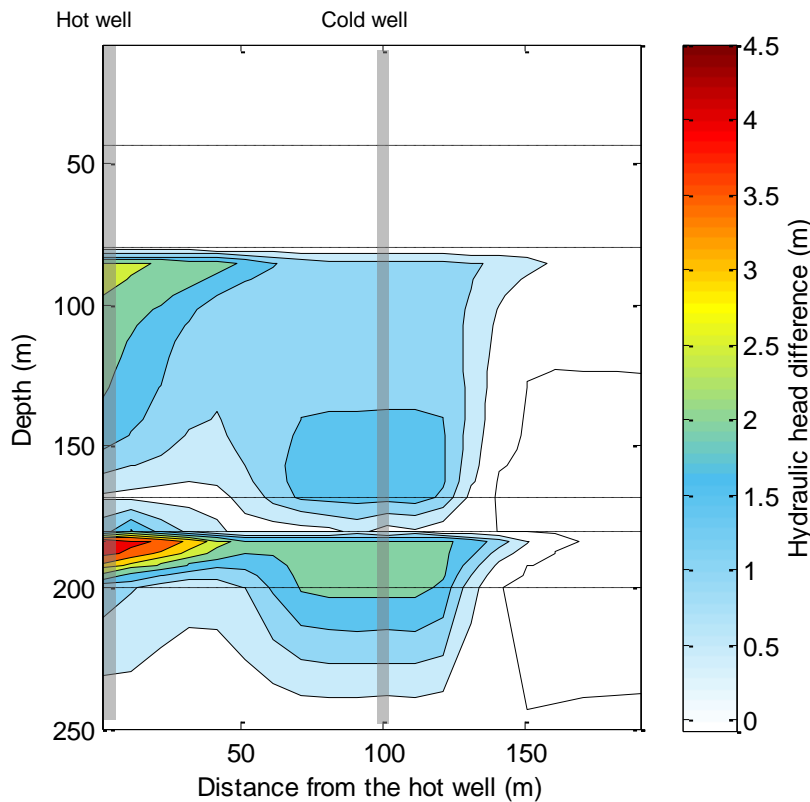


Figure 4.20. Difference in hydraulic heads between the runs with and without density effect

Two different solution schemes were used to represent the density effect concerning the advection package: the method of characteristics (MOC), based on particle tracking and widely used in modeling, and the third-order total-variation-diminishing (TVD) method, which is a finite difference method and conserves mass. It is interesting to note that the MOC method did not show a significant density effect, although a change in hydraulic head was clearly visible. Therefore the TVD method was preferred.

The figure 4.19 shows the difference between models considering density effect or not, i.e. the subtraction of the results, for the first model and one realization of the third model respectively, using the same color scale. It is then clearly visible that the effect of variable density is much more present in the first model. While the absolute difference can reach  $-40^{\circ}\text{C}$  in the homogeneous model (model 1), it reach barely  $5^{\circ}\text{C}$  in the heterogeneous one (model 3a). This is likely due to the presence of less permeable layers in the aquifer that block high-density water up-flowing, with the average vertical conductivity being the same than in the homogeneous model.

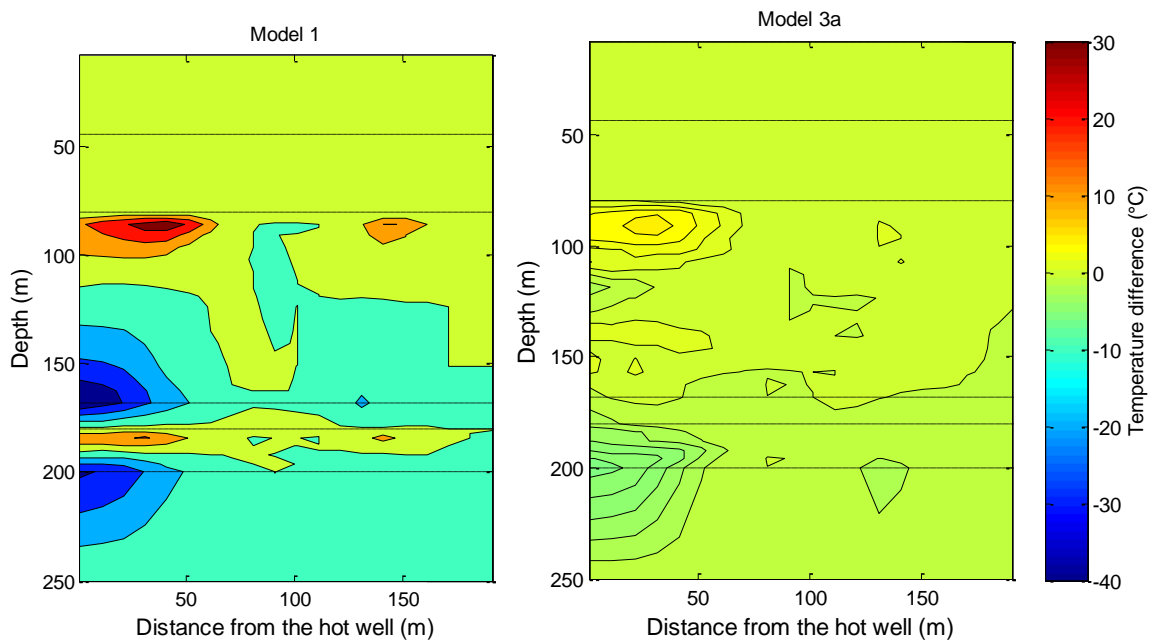


Figure 4.21. Difference in resulting temperature between the runs with and without density effect for model 1 and 3a.

#### 4.2.4 Impact of the ATEs design: different storage temperature

##### 4.2.4.1 Thermal recovery and energy balance ratio

The four following figures (Figure 4.22) show the thermal recovery (TR) and energy balance ratio (EBR) calculated for the three different models respectively. They permit to compare a high-temperature storage system with a medium-temperature storage system.

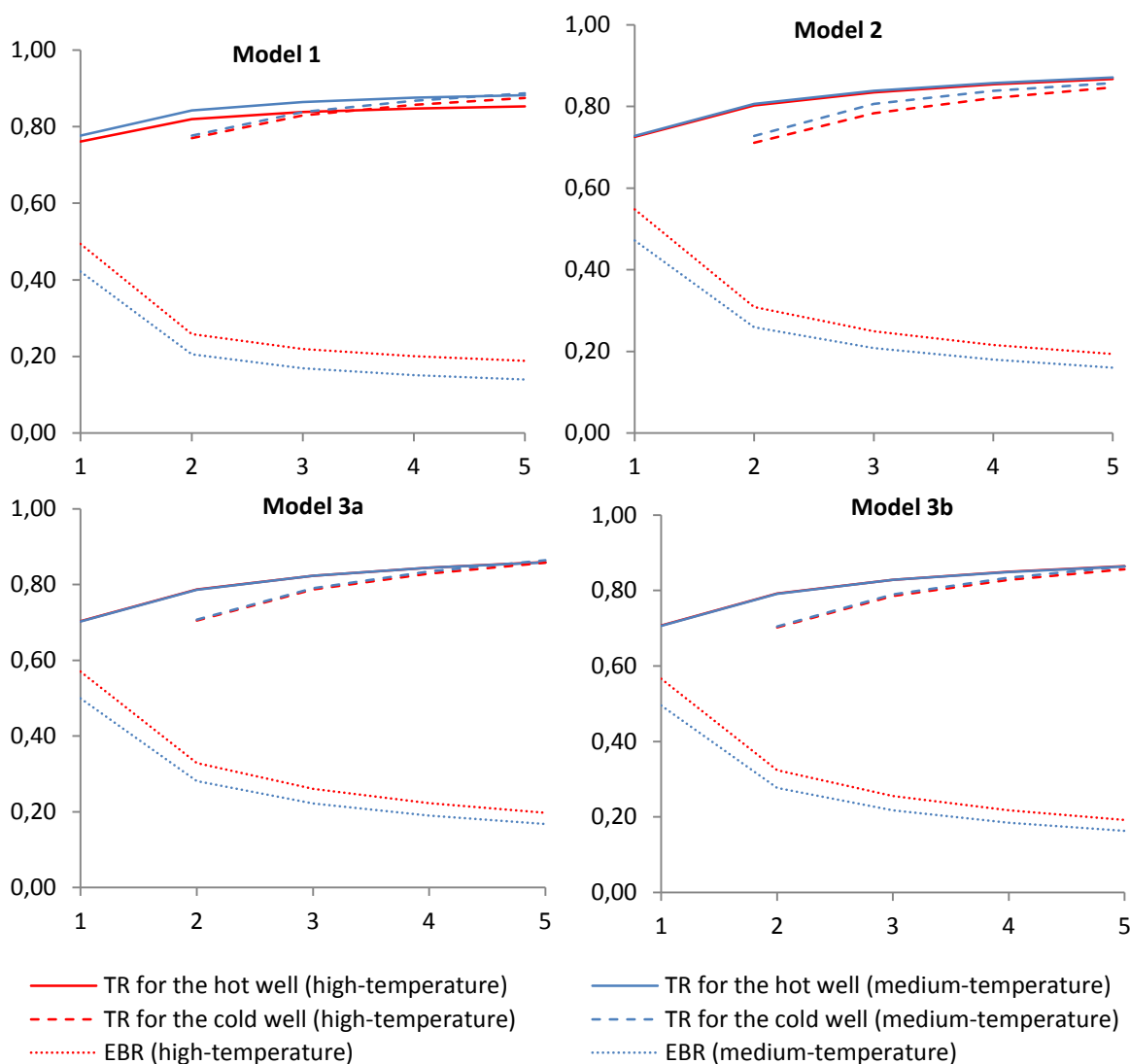


Figure 4.22. Thermal recoveries and energy balance ratio for the different types of model and different injection temperature. The same legend is used for the four figures.

When comparing the models, only the heterogeneous model (model 1) seems to show different thermal recoveries depending on the storage temperature. The difference is low though, about 2,5%, where the medium-temperature storage is more efficient. Concerning the energy balance ratio, the medium-temperature storage system gives lower values for each model. This is logical since the injected temperature is lower and thus the warming lesser.

#### 4.2.5 Impact on the overlying aquifer

It is interesting to see whether the first aquifer unit was affected or not by the heat storage since this unit is probably used for others purposes. Also the permit requires that the temperature in this layer does not exceed 25°C, although this level is far from being achieved. The following table shows the maximum temperature calculated in the layer 2 which corresponds to the first aquifer unit for the different tested scenarios (Table 4.5). Concerning the third model, the mean of the five realizations is here indicated.

Table 4.5. Maximum resulting temperature in layer 2 corresponding to the first aquifer unit

(°C)	Density effect off		Density effect on	
Injection temperature	60°C	84°C	60°C	84°C
Model 1	13,00	13,00	13,00	13,00
Model 2	13,28	13,42	13,29	13,45
Model 3a			13,34	13,53
Model 3b			13,34	13,54

Regarding the heterogeneity, the more the model is, the highest the temperature in the first aquifer, varying of 0,5°C between the two extreme case (model 1 and 3b). When the density variation is taken into account, this also increases the temperature in this unit, but to a much lesser extent. This is an effect of the low density bubble drift, but hampered by the confining layer present between the two aquifers. As expected, the high-temperature storage system gives higher temperature than the medium-temperature system in the first aquifer.

#### 4.2.6 Summary

Analysis of the results showed that heterogeneity and density-effect are interdependent and can impact significantly heat transport and spreading. When comparing different injection temperatures, they would show the same recovery if the density effect is not considered. This is because heat loss is linear with temperatures differences. When the density effect is included in the calculations, a difference is then expected and the density-driven flow would increase heat spreading and thus heat loss. This was indeed observed in the case of the homogeneous model (model 1, Figure 4.19), although to a small extent. However, in the case of aquifer heterogeneity, thermal recovery showed similar levels for a high-temperature ATES and a medium-temperature ATES. At the same time, results showed that heterogeneity hampers the density effect. Low permeable sublayers act as a barrier to the vertical density-driven flow and inhibit upward bubble drift. Therefore, a high temperature difference and its related density difference do not seem to influence thermal recovery. If this is true, it would mean that heterogeneous aquifers are particularly interesting for high-temperature ATES system because for the same thermal recovery and efficiency, more thermal energy can be extracted after storage, as presented in the following table.

Table 4.6. Summary of thermal recovery and extracted energy for the heterogeneous model (3a) after 5 years of exploitation

ATES design	15°C	60°C	84°C
Extracted energy from the hot well (MW)	100	265	347
Thermal recovery of the hot well (-)	0,867	0,866	0,858

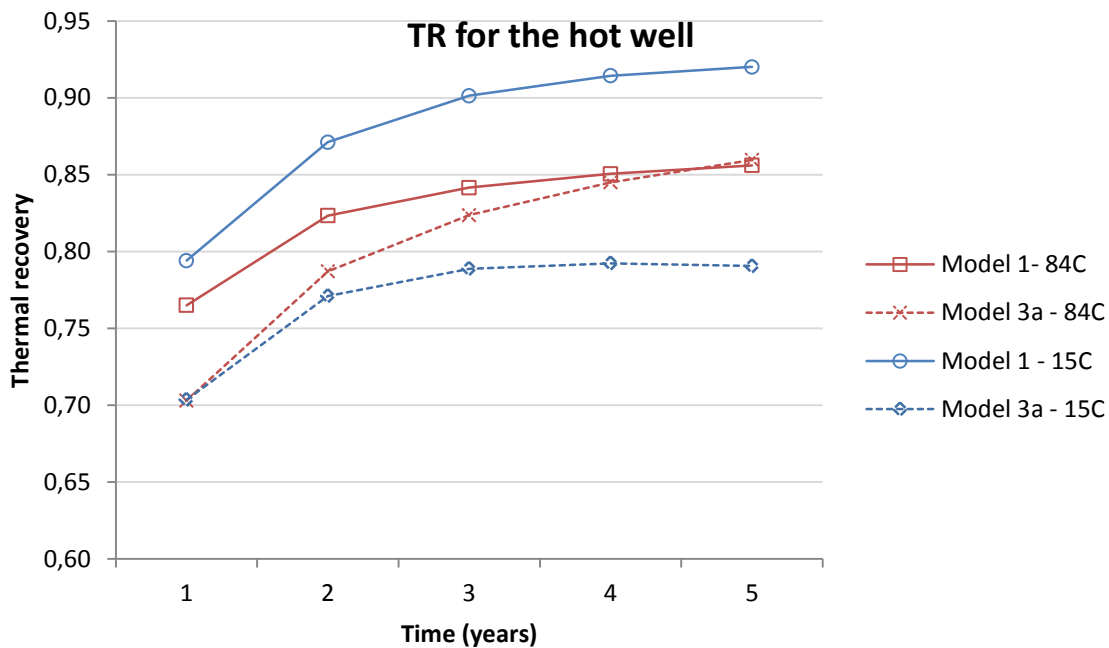


Figure 4.23. Thermal recovery of the hot well for the homogeneous aquifer (model 1) and for the heterogeneous (model 3a) for two different injection temperatures (84C and 15C). In both cases, density-effect is included.

The role of heterogeneity seems to be therefore major for the low-temperature systems but less important when it comes to higher injection temperature. On the contrary, it has a positive impact over the exploitation years (Figure 4.23). Consideration of heterogeneity in design calculation is important, but mainly during the first years of exploitation.

### 4.3 Discussion

Various previous studies studied the efficiency and recovery of thermal energy storage in aquifers, in which though heterogeneity and density effect impacts are rarely addressed at the same time. In Sommer et al. (2013), heterogeneity of the aquifer was also simulated with stochastic simulation. The modeled ATEs system is a low-temperature storage system, so the density effect was not considered. The results showed that thermal recovery decreases with increasing heterogeneity, of 5.8% for the reference case. Ferguson (2007) studied two different aquifers, a sandy aquifer with a hydraulic conductivity variance of 0.261 and a carbonate aquifer with a variance of 1.6. The temperature injection was then 20°C in a 10°C aquifer. The heterogeneous case showed a recovery of 5.5% less than the homogeneous case for the sandy aquifer and 8.2% less for the carbonate one.

The figure 4.24 shows the thermal recovery for the hot well with an increasing heterogeneity for a case similar to the ones in Sommer and Ferguson, i.e. low-temperature injection of 15°C. This confirms what has been shown in the previous studies: the more heterogeneous the model is, the less the recovery. In our case, the difference is even higher, more than 10%.



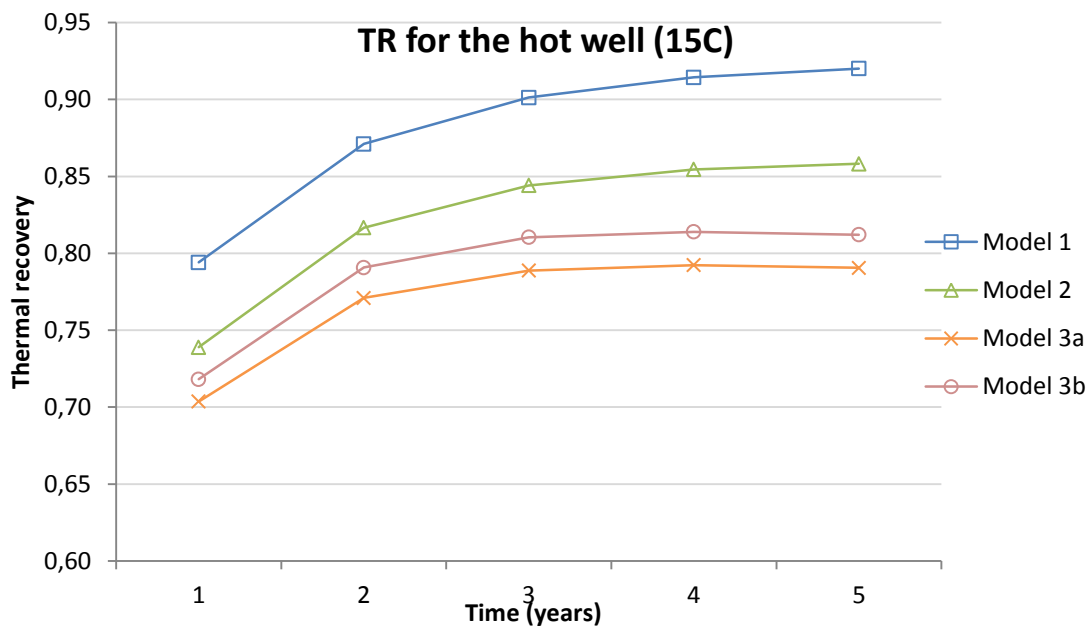


Figure 4.24. Thermal recoveries for the different types of model for injection temperature = 15C

Schout et al. (2013) studied high-temperature ATEs and included the impact of density-driven flow. He compared different injection temperatures: 55°C and 90°C, and showed that recovery efficiency is 10% higher with the lower temperature. However this was demonstrated for an aquifer assumed to be homogeneous. In the present study, comparison with 84°C and 60°C injected gives a difference of 2% in recovery: 86% for the high-temperature system versus 88% for the medium-temperature one after five years of exploitation in the case of the homogeneous model. Schout also showed that density effect is smaller when vertical conductivity is small, which is consistent with our results.

Further investigations would improve the accuracy of the results. The results show relatively small differences between the models considering two different horizontal correlation ranges (3a and 3b). One can assume that the processes impacting thermal recovery play a role at a smaller scale. Moreover, the model domain only extends to 500 m while the horizontal correlation range reaches 1000 m; one can wonder if this has an effect on the resulting realizations. Also, it would be worth performing simulations with more stochastic realizations. The five realizations used in this study might not be representative of the complete range of possible hydraulic conductivity fields and neither statistically significant. The modeling results must then always be considered critically. The uncertainty in thermal recovery due to the unknown geological heterogeneity is here evaluated at  $\pm 1,5\%$ . Also no thorough calibration was performed due to the lack of data, the project not having operating yet. Further modeling with more precise data would confirm the theoretical analysis performed here, with for example temperature logging. It would also be interesting to test a longer exploitation period to see if a common recovery becomes reached for the different models. In the same, simulations with a refined grid would confirm the results are not linked to the discretization.

The choice of stochastic simulation with sequential Gaussian algorithm to generate hydraulic conductivity field can be discussed. For example, Fogg argued that hydraulic conductivity field should not be assumed to be log-normally distributed (Fogg, 1997). Then, another way to treat this parameter distribution would be to consider different facies based on environmental deposit context and texture. In Fogg (1997), the method proposed for this is

the Markov chain modeling, based on transition probability. Another method used by Bierkens and Weerts (1993) applied indicator simulation to modeling heterogeneity. The upscaling approach used by Bierkens (1994) would also provide an interesting insight to this study. It would be interesting to try these different methods to better assess heterogeneity in line with the real site geology. The issue of scale dependence of the two phenomena that influence groundwater and heat flow (heterogeneity, density-driven flow) was not fully addressed here. It should be also remembered that background flow has a minor influence on this site. This could, however, be different at the potential sites for storage of hot water. Its impact should then be combined with the other impacts to further investigate the efficiency of HT-ATES.

Finally, this study is to relate to the current work that is done concerning the Maassluis formation in general, especially by the Geological Survey of the Netherlands. Future results from this will give more accurate data that could be used as input in the models. Correlation analysis on borehole logs is an effort worth being done to characterize the Maassluis Formation and particularly its vertical heterogeneity, since it represents an interesting target for ATES systems. The same resolution that was achieved for Geotop, the detailed three-dimensional model of the Dutch subsurface (Stafleu et al., 2011), represent a stimulating objective for the future investigations. In this direction, grain-size analyses have proven to be an effective way to assess and consider vertical heterogeneity in future efficiency studies, both in term of time and costs, since TGA showed that treatment were not indispensable.

## 5 Conclusion

The impact of heterogeneity on high-temperature thermal energy storage in aquifer has been investigated. For this, an ongoing pilot project in the western part of the Netherlands has been chosen as an example to study this issue on a real site. As a first step, diverse type of data has been collected and analyzed in an attempt to characterize and understand the storage aquifer architecture. At different scale, from the core scale to the regional scale, heterogeneity of the geological formation has been assessed. Grain-size analyses were performed on samples originating from cuttings and cores material. Using the Komeny-Carmen relation to determine hydraulic conductivity from median grain-size, a standard deviation of the logarithm of hydraulic conductivity of 0.75 was reached along one meter core. This showed that heterogeneity in hydraulic conductivity can be important at a small scale. The same exercise was performed at the borehole scale along the entire formation, giving a standard deviation of 0.79 and 0.86. The heterogeneity is then even more important at a larger scale. Another way to understand the spatial structure of the formation was the building of variograms, from gamma-ray logs. The comparison of several boreholes permitted to give a general variogram that can be applied to the formation. Two major structures emerged from this analysis, one with a vertical correlation range of about 3.5 meters and a larger one with a vertical range of 8 meters. Concerning the horizontal heterogeneity, the small density of information in this dimension made this assessment difficult. The analysis of boreholes that are close to each other showed that lithology seems similar within a distance of few meters but more difficult to correlate when separated from more than hundred meters. An attempt to build lithological cross-sections showed that layers are hardly continuous over few kilometers. However, this exercise cannot be complete with only lithological data. These first analyses resulted in parameters for stochastic simulation. Three-dimensional field of hydraulic conductivities were generated using the sequential Gaussian simulation. Five realizations were generated, with conditional data obtained from a test well drilled at the site, for two different horizontal correlation ranges (1000 m and 100 m) and a common vertical range of 10 m.

In a second phase, three types of groundwater and transport model were simulated in order to test an increasing level of heterogeneity : a first homogeneous model, a layered model taking into account vertical heterogeneity and a stochastic model using the generated fields as input to take into account both horizontal and vertical heterogeneity. For all this model, different ATES design were tested: a high-temperature system as designed in the pilot project, with injection of 84°C water, a medium-temperature system with injection of 60°C and a low-temperature system with injection of 15°C. Finally, the density-driven flow was also investigated, by running the models both with and without including the density effect. The results showed small differences in the extent of the thermal plume. However, it was clearly visible that the density effect was only active in the homogeneous model. The low permeability sublayers present in the heterogeneous models act as a barrier to the vertical density-driven flow, reducing the heat loss expected for high temperature difference. When looking at the thermal recovery, it is noticed that different injection temperature in the heterogeneous aquifer gives about the same thermal recovery. This means that for a similar efficiency, a high-temperature system in a heterogeneous aquifer as the Maassluis Formation and with similar conditions would be able to store more energy.

In this study, two currently hot topics were reunited: water resources and energy issues. These two were also reunited for the last World Water Week, showing this an actual

challenge at a world scale. High-temperature aquifer thermal energy storage is one of the solutions newly developed that integrates those two issues. However, its impacts on the environment and its efficiency still have to be properly assessed to make it competitive. A multidisciplinary approach as the one developed in this study is necessary to understand and evaluated those impacts.

## 6 Bibliography

- Batu, V. (1998). *Aquifer Hydraulics: A Comprehensive Guide to Hydrogeologic Data Analysis*. New York: John Wiley & Sons.
- Bear, J. (1979). *Hydraulics of groundwater*. McGraw-Hill Series in water Resources and Environmental Engineering.
- Bierkens, M. F., & van Geer, F. C. (n.d.). *Stochastic Hydrology*. Retrieved from [http://www.earthsurfacehydrology.nl/wp-content/uploads/2012/01/Syllabus\\_Stochastic-Hydrology.pdf](http://www.earthsurfacehydrology.nl/wp-content/uploads/2012/01/Syllabus_Stochastic-Hydrology.pdf)
- Bierkens, M. F., & Weerts, H. J. (1994). Application of indicator simulation to modelling the lithological properties of a complex confining layer. *Geoderma*, vol. 62, 265-284.
- Bridger, D., & Allen, D. (2010). Heat transport simulations in a heterogeneous aquifer used for aquifer thermal energy storage (ATES). *Canadian Geotechnical Journal*, vol. 47, no. 1, 96-115.
- Buik, N. A., & Godschalk, M. (2011). *Hoge temperatuuropslag GeoMEC Vier- polders te Vierpolders (gemeente Brielle) - Effectenstudie grondwatersysteem*. Arnhem: IF Technology.
- Chevalier, S., Gauthier, J., & Banton, O. (1997). Evaluation du potentiel géothermique des nappes aquifères avec stockage thermique : revue de littérature et application en deux contextes typiques du Québec. *Canadian Journal of Civil Engineering*, vol. 24, 611-620.
- Chiles, J., & Delfine, P. (1999). *Geostatistics—modeling spatial uncertainty*. Wiley-Interscience.
- Dalrymple, R. W., & Choi, K. (2007). Morphologic and facies trends through the fluvial–marine transition in tide-dominated depositional systems: A schematic framework for environmental and sequence-stratigraphic interpretation. *Earth-Science Reviews*, vol. 81, no 3, 135-174.
- Dell'Arciprete, D., Vassena, C., Baratelli, F., Giudici, M., Bersezio, R., & Felletti, F. (2014). Connectivity and single/dual domain transport models: tests on a point-bar/channel aquifer analogue. *Hydrogeology Journal*, vol. 22, no. 4, 761-778.
- Deutsch, C. V., & Journel, A. G. (1992). *GSLIB, Geostatistical Software Library and User's Guide*. New York: Oxford University Press.
- Dickinson, J., Buik, N., Matthews, M., & Snijders, A. (2009). ATES: theoretical operational analysis. *Geotechnique*, vol. 59, no. 3, 249-260.
- Ferguson, G. (2007). Heterogeneity and Thermal Modeling of Groundwater. *Ground Water*, vol.45, no. 4, 485-490.
- Harbaugh, A., Banta, E., Hill, M., & McDonald, M. (2000). *MODFLOW-2000, the U.S. Geological Survey modular ground water model, user guide to modularization concepts and the ground water flow process*. USGS.
- Hecht-Méndez, J., Molina-Giraldo, N., Blum, P., & Bayer, P. (2010). Evaluating MT3DMS for Heat Transport: Simulation of closed geothermal systems. *Ground Water*, vol. 48, no. 5, 741-56.
- Kessler, T. C., Comunian, A., Oriani, F., Renard, P., Nilsson, B., Klint, K. E., et al. (2013). Modeling fine-scale geological heterogeneity-examples of sand lenses in tills. *Groundwater*, vol. 51, no. 5, 692-705.
- Krumbein, W., & Monk, G. (1943). Permeability as a function of the size parameters of unconsolidated sands. *Transactions of the American Institute of Mining, Metallurgical and Petroleum Engineers*, vol. 151, 153-163.

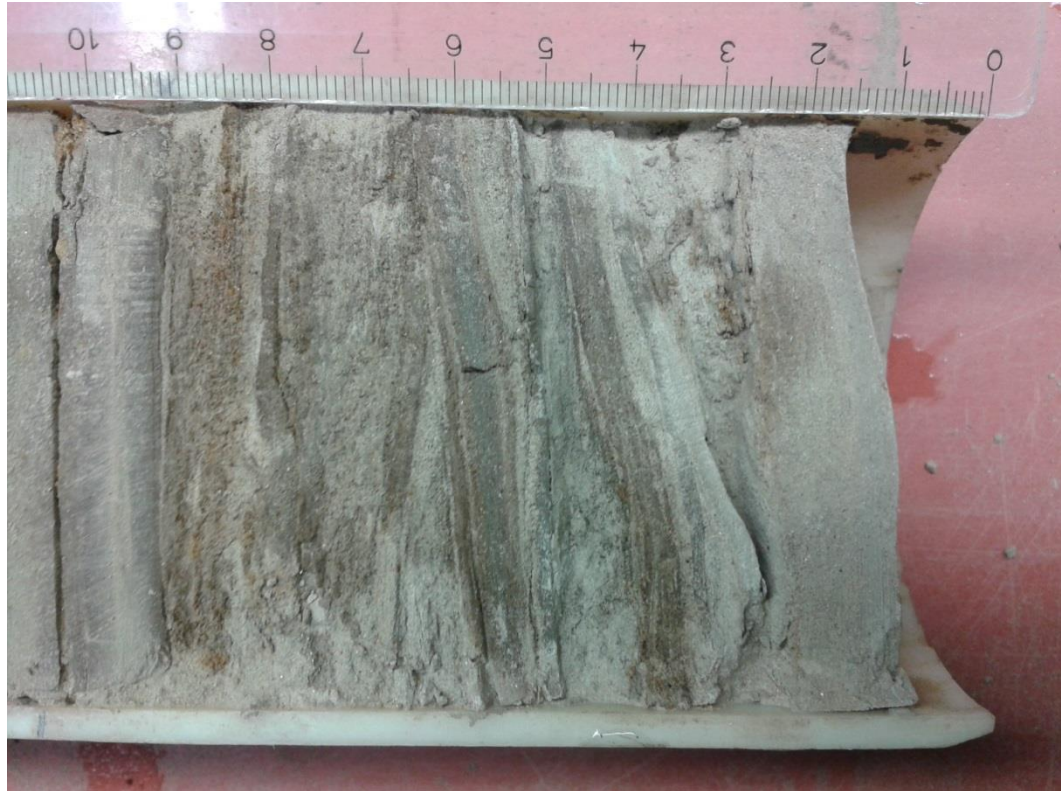
- Langevin, C. D., Thorne, D., Dausman, A. M., Sukop, M. C., & Guo, W. (2008). *SEAWAT Version 4: A Computer Program for Simulation of Multi-Species Solute and Heat Transport*. U.S. Geological Survey.
- Mulder, E. d., Geluk, M., Ritsema, I., Westerhoff, W., & Wong, T. (2003). *Digitaal Geologisch Model, De ondergrond van Nederland. Geologie van Nederland*. Utrecht: TNO.
- Noorbergen, L. (2013). *Shallow marine and near shore successions in the Lower Pleistocene Maassluis Formation*. Unpublished.
- Pyrzcz, M. J., & Deutsch, C. V. (n.d.). *The Whole Story on the Hole Effect*. Edmonton: University of Alberta.
- Roskam, G. D., & Klaver, G. G. (2009). *Methodeontwikkeling voor het bepalen van het gehalte reactief ijzer*. Utrecht: TNO Bouw en Ondergrond.
- Sagal, E., Shouse, P. J., & Corwin, D. L. (2009). Measuring particle size distribution using laser diffraction: implications for predicting soil hydraulic properties. *Soil Science*, vol. 174, no. 12, 639-645.
- Schout, G., Drijver, B., Gutierrez-Neri, M., & Schotting, R. (2013). Analysis of recovery efficiency in high-temperature aquifer thermal energy storage: a Rayleigh-based method. *Hydrogeology Journal*.
- Shepherd, R. G. (1989). Correlations of permeability and grain-size. *Ground water*, vol. 27, no. 5, 633-638.
- Sommer, W., Valstar, J., Van Gaans, P., Grotenhuis, T., & Rijnaarts, H. (2013). The impact of aquifer heterogeneity on the performance of aquifer thermal energy storage. *Water resources research*, vol. 49, no. 12, 8128-8138.
- Stafleu, J., Maljers, D., Gunnink, J. L., Menkovic, A., & Busschers, F. S. (2011). 3D modelling of the shallow subsurface of Zeeland, the Netherlands. *Netherlands Journal of Geosciences*, vol. 90, no. 4, 293-310.
- Stolk, P. (2000). *Analyse van temperatuurmetingen in de Nederlandse ondergrond (20-300 m beneden maaiveld) in relatie tot hydrologische en meteorologische omstandigheden in heden en verleden*. Arnhem and Amsterdam: IF Technology/Vrije Universiteit.
- Stuurman, R. (1995). Groundwater flow systems analysis on a regional and nation-wide scale in The Netherlands; The use of flow systems analysis in wetland management. *Water Science and Technology*, vol. 31, no.8, 375-378.
- Thorne, D., Langevin, C. D., & Sukop, M. C. (2006). Addition of simultaneous heat and solute transport and variable fluid viscosity to SEAWAT. *Computers & Geosciences*, vol. 32, no. 10, 1758-1768.
- van Gaans, P. F., Griffioen, J., Mol, G., & Klaver, G. (2010). Geochemical reactivity of subsurface sediments as potential buffer to anthropogenic inputs: a strategy for regional characterization in the Netherlands. *Journal of Soils and Sediments*, vol. 11, no.2, 336-351.
- van Heekeren, V., & Bakema, G. (2013). Geothermal Energy Use, 2013 Country Update for the Netherlands. *European Geothermal Congress*, (pp. 3-7). Pisa.
- Vernes, R., Hummelman, H., & Menkovic, A. (2010). *REGIS Zeeland, Deelrapport B: Hydrogeologische opbouw en hydraulische eigenschappen van Holocene afzettingen*. Utrecht: TNO.
- Vis, G.-J., van Gessel, S., Mijnlief, H., Pluymaekers, M., Hettelaar, J., & Stegers, D. (2010). *Lower Cretaceous Rijnland Group aquifers in the West Netherlands Basin: suitability for geothermal energy*. Utrecht: TNO.
- Westerhoff, W. (2009). *Stratigraphy and sedimentary evolution: The lower Rhine-Meuse system during the Late Pliocene and Early Pleistocene (southern North Sea Basin)*. Utrecht: TNO - Geological Survey of the Netherlands.

Zheng, C., & Wang, P. (1999). *MT3DMS—A modular three-dimensional multispecies transport model for simulation of advection, dispersion and chemical reactions of contaminants in ground-water systems: Documentation and user's guide*. U.S. Army Corps of Engineers.

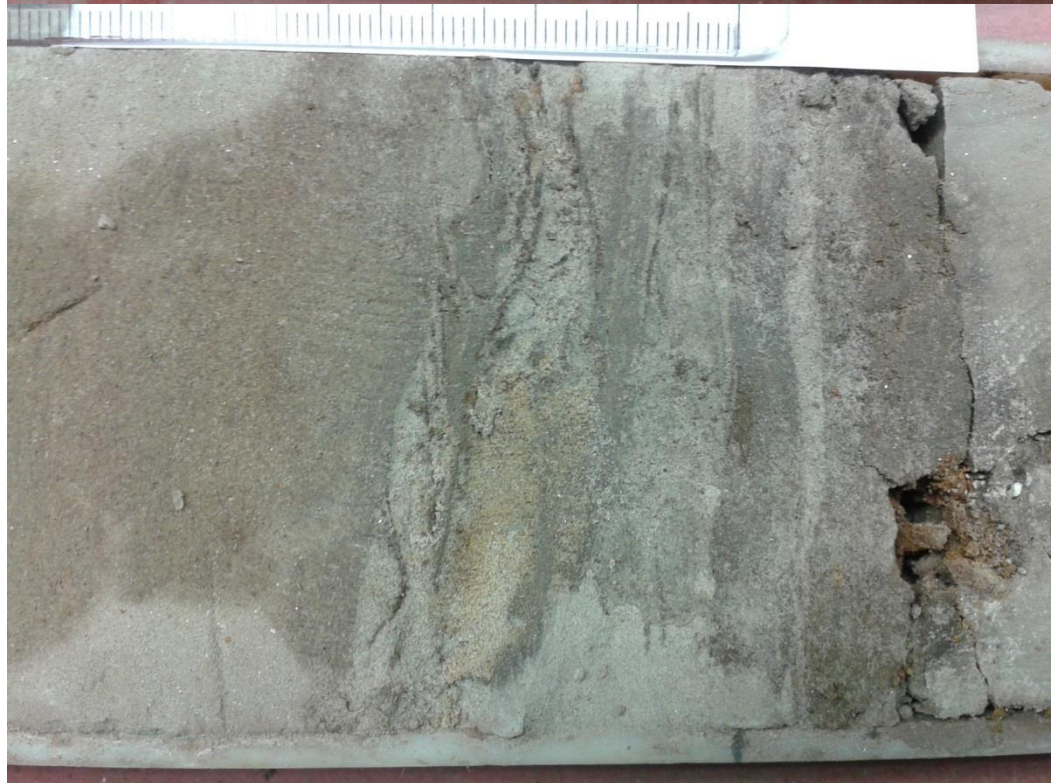




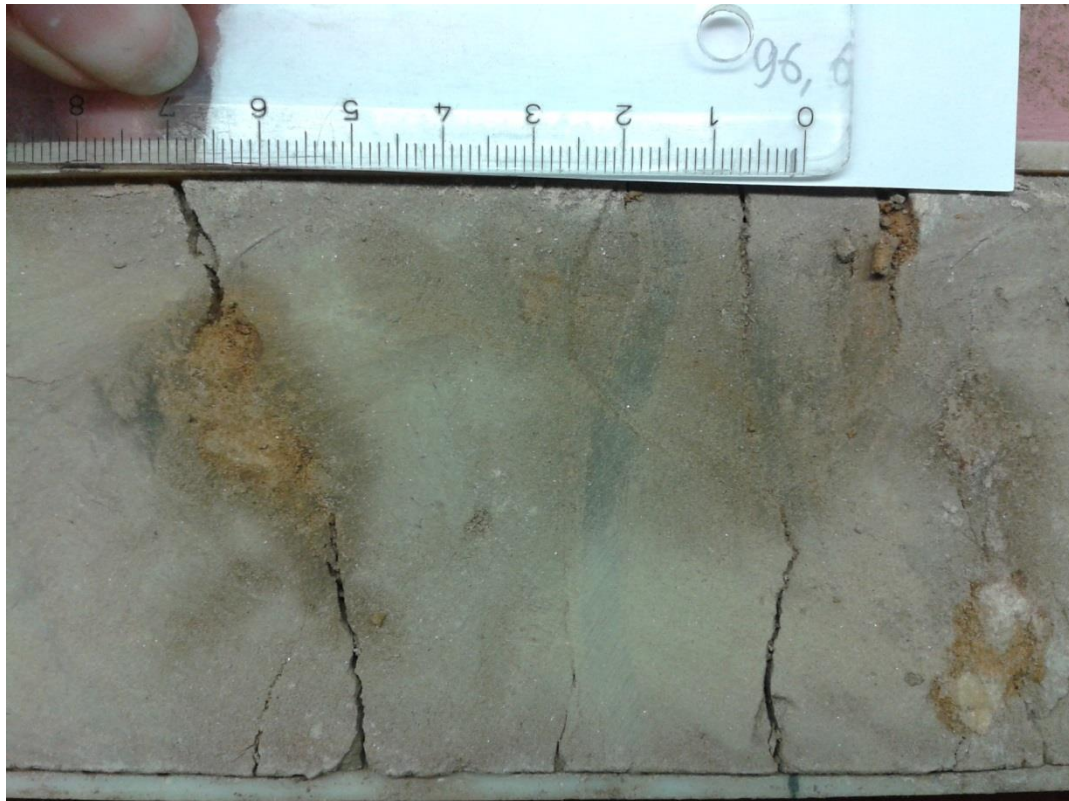
## Appendix 1. Detailed description of core H0637 and photographs



(1)



(2)



(3)



(4)

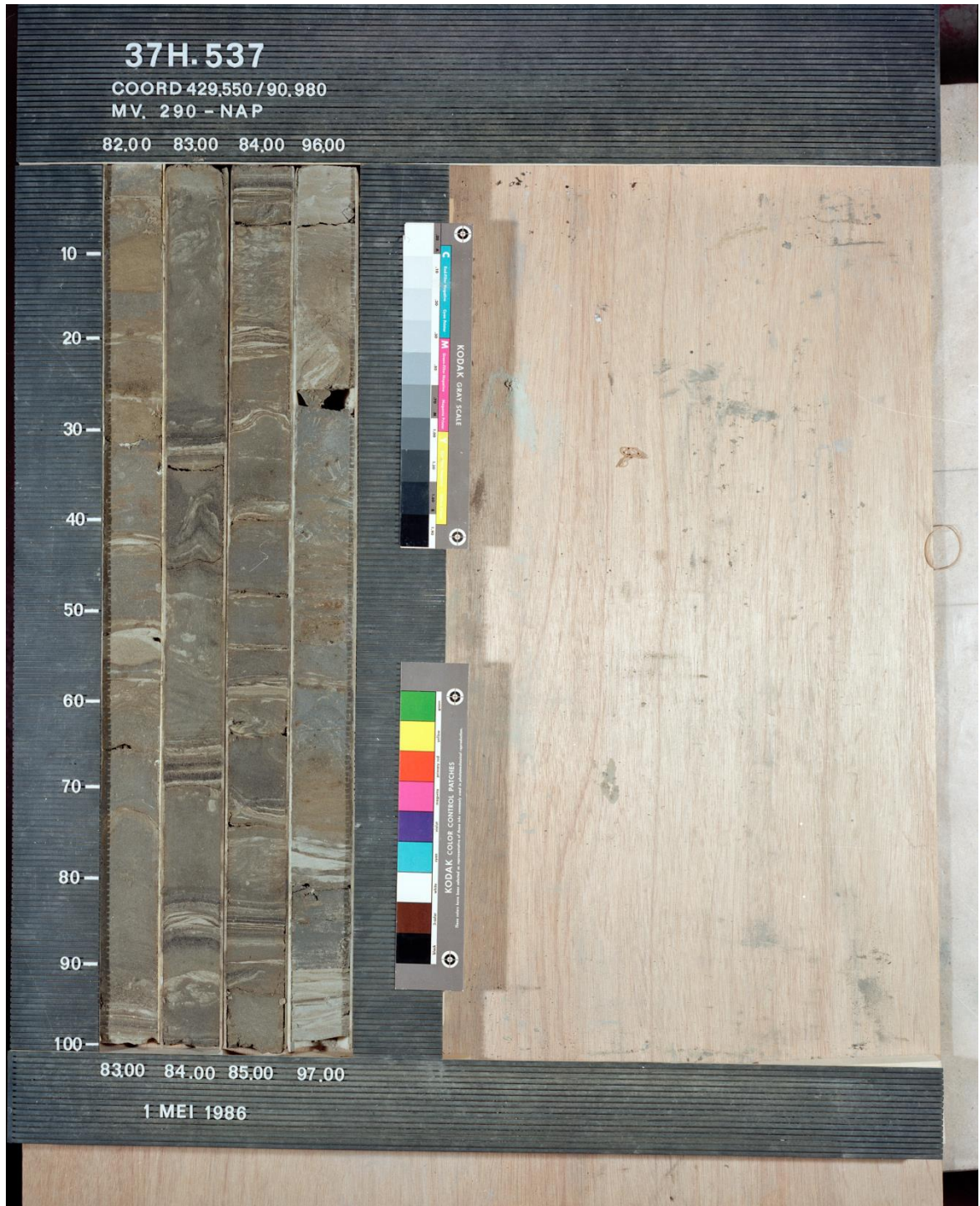
Core ID: 0.39.606  
 Borehole: 37H0537  
 Core depth: 96m-97m

Depth	Sedimentary texture and structures					Core recovery	Physical characteristics				Stratification type				Description (fining-up?)			
	Clay	Silt	Fine sand	Medium sand	Coarse sand		Gravel	Color	Shell	Bioturbation	Sorting	Wavy	Flaser	Lenticular		Cross bed	Massive bed	Inclined bed
96																		
96.1							w											
96.2							(4) b and w											Deformation
96.3							g											
96.4							(3) b											
96.5																		
96.6							g											Silty layer in clay Fining-up
96.7							b-ish											
96.8							(2) w											
96.9							g											Oxydation
97							(1) w											

w: white  
 g: grey  
 b: brown



## Appendix 2. Original photographs of the core H0537





### **Appendix 3. Original core descriptions of H0537 and D0227**





-

# Boorstaat

-

<b>NITG-Boornummer</b>	B37D0227	<b>Coördinatenstelsel</b>	Rijksdriehoeksmeting
<b>X-coördinaat</b>	78900	<b>Bepaling lokatie</b>	
<b>Y-coördinaat</b>	426900	<b>Beschrijvingsmethode</b>	Onbekend
<b>Maaiveld (m tov NAP)</b>	-0.70	<b>Vertrouwelijkheid</b>	Openbaar
<b>Datum boring</b>	26-08-1986	<b>Werknummer</b>	37DR0227
<b>Plaatsnaam</b>	Geervliet		
<b>Provincie</b>	Zuid-Holland		
<b>Kaartblad</b>	37D		
<b>Soort boring</b>	Matig diepe boring derden		
<b>Einddiepte (m)</b>	130.00		
<b>Uitvoerder</b>	RGD - BTD		
<b>Boormethode</b>	Pulsboring		
<b>Opmerkingen</b>			

## Lithologie

<b>Beschrijver lagen</b>	Holst, H. van der / Mensink, H
<b>Organisatie beschrijver</b>	RGD
<b>Nat/droog</b>	Onbekend

## Stratigrafie 1975

<b>Beschrijver stratigrafie</b>	Veld, G. in het
<b>Organisatie beschrijver</b>	
<b>Datum stratigrafie</b>	
<b>Versie stratigrafie</b>	1

## Stratigrafie 2003

<b>Beschrijver stratigrafie</b>	Harting, R.
<b>Organisatie beschrijver</b>	Geologische Dienst Nederland
<b>Datum stratigrafie</b>	14-04-2011
<b>Versie stratigrafie</b>	3

## Oude beschrijving

\$8:Opmerkingen =8-5-1992. STRATIGRAFIE I.V.M. REGIS II. \$D:Boordatum =ONBEKEND \$G:Boormethode =PULSBORING \$H:Boorlokatie =SIMONSHAVEN \$O:Kwaliteitsnr=211001 \$R:Rapportnr =BOORGATMETING RGD. \$S:Typist =J KRAAKMAN \$T:Collationnr =37D

## Laagbeschrijving

Boven	Onder	Grondsoort	Omschrijving	M63	LU	SI	ZA	GR	OR	CA
0.00	0.45	klei	sterk siltig, bruin, stevig, ijzeroxide, omgewerkte grond		30					3
		<i>oude omschr.</i>	<i>[KLEI,30,****,3] licht, bruin, roestig, zeer stug, geroerd.</i>							
0.45	0.95	klei	zwak siltig, bruin, ijzeroxide, insluitsels zand		36					3
		<i>oude omschr.</i>	<i>[KLEI,36,****,3] matig zwaar, bruin, roestvlekjes, ENKELE zandnestjes, OP 75 enkele zandlaagjes, BASIS LICHTER {30%}.</i>							
0.95	1.00	zand	licht-geel-grijs, Zand: uiterst fijn (O), ijzeroxide		90					3
		<i>oude omschr.</i>	<i>[ZAND,***,90,3] uiterst fyn, beige, roestvlekjes.</i>							
1.00	1.35	klei	sterk siltig, bruin, ijzeroxide		30					3
		<i>oude omschr.</i>	<i>[KLEI,30,****,3] licht, bruin, roestig, enkele dunne zandlaagjes.</i>							
1.35	1.95	klei	sterk siltig, zandig, grijs, Organisch materiaal: verspoelde plantenresten, gelaagd		28					3
		<i>oude omschr.</i>	<i>[KLEI,28,****,3] licht, grysg, gelaagd met zand- {m 90} EN detrituslaagjes.</i>							
1.95	3.20	veen	onbekend, Organisch materiaal: zeggeveen, weinig hout, riet, erosieve top							
		<i>oude omschr.</i>	<i>[VEEN,***,****,*] rietzeggeveen, top erosief, enkele houtrestjes.</i>							
3.20	3.45	veen	onbekend, Organisch materiaal: rietveen							
		<i>oude omschr.</i>	<i>[VEEN,***,****,*] rietveen.</i>							
3.45	3.70	klei	zwak siltig, bruin-grijs, Organisch materiaal: rietveen		38					1
		<i>oude omschr.</i>	<i>[KLEI,38,****,1] matig zwaar, bruingrysg, sterk rietvenig, OP 350 EEN ONTKALKT LAAGJE.</i>							
3.70	4.00	klei	zwak siltig, groen-grijs, Organisch materiaal: wortels, top kalkloos		36					3
		<i>oude omschr.</i>	<i>[KLEI,36,****,3] matig zwaar, groengrysg, vet, doorworteld, VANAF 390 enkele dunne zandlaagjes, BASIS LICHTER {30%}, top ontkalkt.</i>							
4.00	5.00	klei	sterk siltig, grijs, Organisch materiaal: plantenresten, verspoelde plantenresten, Schelpen: spoor schelpen, spoor schelpresten, glimmer, sterk gelaagd		20					3

Boven	Onder	Grondsoort	Omschrijving	M63	LU	SI	ZA	GR	OR	CA
		<i>oude omschr.</i>	<i>[KLEI,20,***,3] licht, grys, sterk gelaagd MET UITERST fyne zandlaagjes, FYNE glimmers EN detrituslaagjes, FYNE plantenrestjesM enkele schelpGRUISJES, BASIS LICHTER {10%}.</i>							
5.00	6.00	klei	sterk siltig, grijs, Organisch materiaal: plantenresten, Schelpen: spoor schelpen, spoor schelpresten		28					3
		<i>oude omschr.</i>	<i>[KLEI,28,***,3] licht, grys, fynzandig gelaagd, fyne plantenresten, spoor fyn schelpgruis.</i>							
6.00	8.00	zand	sterk kleilig, grijs, Zand: uiterst fijn (O), Schelpen: spoor schelpen, spoor schelpresten		80					3
		<i>oude omschr.</i>	<i>[ZAND,***,80,3] uiterst fyn, grys, ZEER sterk kleihoudend, spoor fyn schelpgruis.</i>							
8.00	9.00	zand	kleilig, grijs, Zand: uiterst fijn (O), Organisch materiaal: plantenresten, Schelpen: spoor schelpen, spoor schelpresten		80					3
		<i>oude omschr.</i>	<i>[ZAND,***,80,3] uiterst fyn, grys, kleihoudend, spoor uiterst fyn schelpgruis, UITERST fyne plantenresten.</i>							
9.00	13.00	zand	grijs, Zand: uiterst fijn (O), Organisch materiaal: plantenresten, Schelpen: schelpen, schelpresten		90					3
		<i>oude omschr.</i>	<i>[ZAND,***,90,3] uiterst fyn, grys, SPOOR UITERST FYN schelpresten, ZEER fyne plantenresten.</i>							
13.00	14.00	klei	sterk siltig, sterk zandig, grijs, Zand: fijne categorie (O), Organisch materiaal: plantenresten		24					3
		<i>oude omschr.</i>	<i>[KLEI,24,***,3] licht, grys, sterk fynzandig, SPOOR ZEER fyne plantenresten.</i>							
14.00	16.00	zand	zwak kleilig, licht-grijs-geel, Zand: uiterst fijn (O)		75					3
		<i>oude omschr.</i>	<i>[ZAND,***,75,3] uiterst fyn, grysblond, zwak kleihoudend.</i>							
16.00	17.00	zand	zwak kleilig, licht-grijs-geel, Zand: uiterst fijn (O), veenbrokjes		75					3
		<i>oude omschr.</i>	<i>[ZAND,***,75,3] uiterst fyn, grysblond, ZEER zwak kleihoudend, ENKELE stugGE veenbrokken.</i>							
17.00	18.00	zand	licht-grijs-geel, Zand: uiterst fijn (O)		80					3
		<i>oude omschr.</i>	<i>[ZAND,***,80,3] uiterst fyn, grysblond.</i>							
18.00	19.00	zand	licht-grijs-geel, Zand: uiterst fijn (O), tweetoppige spreiding, Schelpen: spoor schelpen, spoor schelpresten, Hydrobiidae, weinig insluitsels veen		80					3
		<i>oude omschr.</i>	<i>[ZAND,***,80,3] uiterst fyn, grysblond, tweetoppig {m 80/300}, spoor uiterst fyn schelpgruis, EEN enkele schelp O.A. hydrobia, EEN ENKEL kleilig veenBROKJE.</i>							
19.00	20.00	zand	licht-grijs-geel, Zand: uiterst fijn (O), tweetoppige spreiding, Organisch materiaal: weinig hout, Schelpen: spoor schelpen, weinig Cerastoderma sp., Hydrobiidae		80					3
		<i>oude omschr.</i>	<i>[ZAND,***,80,3] uiterst fyn, grysblond, tweetoppig {m 80/300}, enkele schelpen O.A. cardium EN hydrobia, ENKELE ZOETWATERSLAKJES O.A. VALVATA, weinig houtresten.</i>							
20.00	21.00	zand	zwak grindig, licht-geel-grijs, Zand: uiterst fijn (O), tweetoppige spreiding, Grind: witte kwarts, zandsteen, Schelpen: spoor schelpen, spoor schelpresten		80					3
		<i>oude omschr.</i>	<i>[ZAND,***,80,3] uiterst fyn, blondgrys, tweetoppig {m 80/300}, spoor schelpgruis, enkele grindjes O.A. gangkwarts EN zandsteen.</i>							
21.00	22.00	zand	zwak grindig, licht-geel-grijs, Zand: matig grof (O), tweetoppige spreiding, Grind: kwartsiet, witte kwarts		300					3
		<i>oude omschr.</i>	<i>[ZAND,***,300,3] matig grof, blondgrys, tweetoppig {m 300/80}, grindjeS O.A. gangkwarts EN kwartsiet.</i>							
22.00	23.00	zand	grindig, licht-geel-grijs, Zand: uiterst grof (O), matig grote spreiding, Grind: kalksteen, kwartsiet, witte kwarts, zandsteen, Schelpen: spoor schelpen, spoor schelpresten, weinig Cerastoderma sp.		580					3
		<i>oude omschr.</i>	<i>[ZAND,***,580,3] uiterst grof, blondgrys, grote spreiding, MET UITERST FYNE {m 80} KORRELS, grindhoudend O.A. gangkwarts, rookkwarts, kwartsiet, zandsteen EN kalksteen, enkele schelpresten O.A. cardium.</i>							
23.00	24.00	zand	grindig, grijs, Zand: zeer grof (O), tweetoppige spreiding, Grind: fijn grind, witte kwarts, Schelpen: weinig schelpen, weinig Cerastoderma sp., Scrobicularia plana		380					3
		<i>oude omschr.</i>	<i>[ZAND,***,380,3] zeer grof, grys, grote spreiding, tweetoppig {m 380/80}, fyne grindjes O.A. gangkwarts, weinig schelpen EN RESTEN O.A. cardium EN scrobicularia {marien} EN PLANORBIS {zoet}.</i>							
24.00	25.00	zand	grindig, licht-grijs, Zand: uiterst grof (O), Grind: fijn grind, witte kwarts, zandsteen, Schelpen: weinig schelpen, weinig Cerastoderma sp., Scrobicularia plana		440					3
		<i>oude omschr.</i>	<i>[ZAND,***,440,3] uiterst grof, lichtgrys, fyne grindjes O.A. gangkwarts EN zandsteen, schelpen EN RESTEN O.A. cardium EN scrobicularia.</i>							
25.00	26.00	zand	zwak grindig, licht-geel, Zand: zeer grof (O), Grind: witte kwarts, zandsteen, Organisch materiaal: spoor hout, Schelpen: weinig schelpen, weinig schelpresten, weinig Cerastoderma sp.		360					3
		<i>oude omschr.</i>	<i>[ZAND,***,360,3] zeer grof, blond, weinig grindJES O.A. gangkwarts EN zandsteen, weinig schelpresten O.A. cardium, spoor houtresten.</i>							

Boven	Onder	Grondsoort	Omschrijving	M63	LU	SI	ZA	GR	OR	CA
26.00	27.00	zand	licht-geel-grijs, Zand: zeer grof (O), Grind: spoor fijn grind, witte kwarts, Schelpen: spoor schelpen, spoor schelpresten	310						3
		<i>oude omschr.</i>	<i>[ZAND,***,310,3] zeer grof, blondgrys, spoor schelpgruis, spoor fyn grind O.A. gangkwarts.</i>							
27.00	28.00	zand	licht-grijs-geel, Zand: zeer grof (O), Organisch materiaal: plantenresten, Schelpen: schelpen, schelpresten, weinig Cerastoderma sp., Hydrobiidae	380						3
		<i>oude omschr.</i>	<i>[ZAND,***,380,3] zeer grof, grysblood, FINE schelpresten O.A. cardium EN hydrobia, fyne plantenresten.</i>							
28.00	29.00	zand	grijs, Zand: matig grof (O), matig grote spreiding, Schelpen: veel schelpen, weinig Cerastoderma sp., Macoma sp., Spisula sp., kleibrokjes	280						3
		<i>oude omschr.</i>	<i>[ZAND,***,280,3] matig grof, grys, grote spreiding, kleibrokken, veel schelpen EN RESTEN O.A. cardium, macoma EN spisula.</i>							
29.00	30.00	zand	grindig, grijs, Zand: matig grof (O), matig grote spreiding, Grind: fijn grind, kwartsiet, witte kwarts, Schelpen: weinig schelpen, weinig Cerastoderma sp., Hydrobiidae, Mytilus edulis	240						3
		<i>oude omschr.</i>	<i>[ZAND,***,240,3] matig grof, grys, grote spreiding, schelpen EN RESTEN O.A. cardium, hydrobia EN mytilus, WEINIG fyne grindjes O.A. gangkwarts EN kwartsiet.</i>							
30.00	31.00	zand	zwak kleilig, grijs, Zand: matig fijn (O), Schelpen: weinig schelpen, weinig Cerastoderma sp., Macoma sp., Mytilus edulis, veenbrokjes	160						3
		<i>oude omschr.</i>	<i>[ZAND,***,160,3] matig fyn, grys, zwak kleihoudend, schelpen EN RESTEN O.A. cardium, mytilus EN macoma, ENKELE GEROLDE veenbrokken.</i>							
31.00	32.00	zand	zwak kleilig, zwak grindig, grijs, Zand: zeer fijn (O), Grind: kwartsiet, vuursteen, witte kwarts, zandsteen, Schelpen: veel schelpen, weinig Cerastoderma sp., Macoma sp., Mytilus edulis, Scrobicularia plana	140						3
		<i>oude omschr.</i>	<i>[ZAND,***,140,3] zeer fyn, grys, zwak kleihoudend, ZEER veel schelpen EN RESTEN O.A. cardium, scrobicularia, macoma EN mytilus, weinig grindjes O.A. gangkwarts, kwartsiet, GRYZE zandsteen EN ZWARTE vuursteen.</i>							
32.00	35.00	zand	grijs, Zand: zeer fijn (O), Schelpen: weinig schelpen, weinig schelpresten, weinig Cerastoderma sp.	140						3
		<i>oude omschr.</i>	<i>[ZAND,***,140,3] zeer fyn, grys, weinig schelpresten O.A. cardium.</i>							
35.00	37.00	zand	grijs, Zand: zeer fijn (O)	140						3
		<i>oude omschr.</i>	<i>[ZAND,***,140,3] zeer fyn, grys.</i>							
37.00	38.00	zand	licht-grijs, Zand: zeer fijn (O), Organisch materiaal: hout, Schelpen: weinig schelpen, weinig schelpresten, weinig Cerastoderma sp., kleistenen	140						3
		<i>oude omschr.</i>	<i>[ZAND,***,140,3] zeer fyn, lichtgrys, weinig schelpresten O.A. cardium, houtresten, ENKELE GEROLDE kleistenen.</i>							
38.00	39.00	zand	licht-geel-grijs, Zand: zeer fijn (O), Grind: spoor fijn grind, witte kwarts, Organisch materiaal: weinig hout, Schelpen: spoor schelpen, spoor schelpresten, weinig Cerastoderma sp., kleistenen	140						3
		<i>oude omschr.</i>	<i>[ZAND,***,140,3] zeer fyn, blondgrys, spoor schelpgruis O.A. cardium, enkele houtresten, enkele fyne grindjes O.A. gangkwarts EN ENKELE kleisteentjes.</i>							
39.00	43.00	zand	licht-geel, Zand: zeer fijn (O), spoor glimmer	140						3
		<i>oude omschr.</i>	<i>[ZAND,***,140,3] zeer fyn, blond, spoor glimmer.</i>							
43.00	44.00	zand	licht-geel, Zand: matig fijn (O), tweetoppige spreiding, Organisch materiaal: weinig hout, Schelpen: spoor schelpen, spoor schelpresten, Hydrobiidae	180						3
		<i>oude omschr.</i>	<i>[ZAND,***,180,3] matig fyn, blond, tweetoppig {m 140/280}, enkele houtresten, spoor zeer fyn schelpgruis O.A. hydrobia.</i>							
44.00	45.00	zand	licht-geel, Zand: zeer fijn (O), matig grote spreiding, Schelpen: spoor schelpen, spoor schelpresten, spoor glimmer, kleibrokjes	110						3
		<i>oude omschr.</i>	<i>[ZAND,***,110,3] zeer fyn, blond, grote spreiding, kleibrokken, spoor zeer fyn schelpgruis, spoor glimmer.</i>							
45.00	50.00	klei	sterk siltig, uiterst zandig, grijs, Zand: fijne categorie (O), Schelpen: spoor schelpen, spoor schelpresten, spoor glimmer	18						3
		<i>oude omschr.</i>	<i>[KLEI,18,****,3] licht, grys, spoor zeer fyn schelpgruis, STERK uiterst fynzandig, spoor glimmer TOT glimmerhoudend.</i>							
50.00	54.00	klei	sterk siltig, grijs, Organisch materiaal: verspoelde plantenresten, veel glimmer, sterk gelaagd	20						3
		<i>oude omschr.</i>	<i>[KLEI,20,****,3] licht, grys, sterk gelaagd MET UITERST FINE {m 90} zandlaagjes, glimmer, FINE detrituslaagjes, VAN 51.10 - 51.60 WITGRYS, MINDER zandlaagjes, NA 52.00 MET vette, LICHTGRYZE kleilaagjes, NA 53.20 LICHTER {15%} EN veel glimmer.</i>							
54.00	55.00	klei	sterk siltig, sterk zandig, grijs, Zand: fijne categorie (O)	15						3
		<i>oude omschr.</i>	<i>[KLEI,15,****,3] licht, grys, sterk fynzandig.</i>							
55.00	58.00	zand	licht-geel, Zand: uiterst fijn (O)	90						
		<i>oude omschr.</i>	<i>[ZAND,***,90,*] uiterst fyn, blond.</i>							
58.00	59.00	zand	zwak kleilig, licht-grijs-geel, Zand: uiterst fijn (O), spoor kleibrokjes	100						3
		<i>oude omschr.</i>	<i>[ZAND,***,100,3] uiterst fyn, grysblood, enkele kleibrokken, zwak kleihoudend.</i>							

Boven	Onder	Grondsoort	Omschrijving	M63	LU	SI	ZA	GR	OR	CA
59.00	61.00	zand	licht-grijs-geel, Zand: uiterst fijn (O)	90						3
		<i>oude omschr.</i>	<i>[ZAND,***,90,3] uiterst fyn, grysblond.</i>							
61.00	63.00	zand	kleilig , licht-grijs, Zand: uiterst fijn (O), kleibrokjes	100						3
		<i>oude omschr.</i>	<i>[ZAND,***,100,3] uiterst fyn, lichtgrys, kleihoudend, kleibrokken.</i>							
63.00	65.00	zand	licht-grijs-geel, Zand: zeer fijn (O)	120						3
		<i>oude omschr.</i>	<i>[ZAND,***,120,3] zeer fyn, grysblond.</i>							
65.00	66.00	zand	licht-grijs-geel, Zand: uiterst fijn (O), Organisch materiaal: hout, Schelpen: spoor schelpen, spoor schelpresten	90						3
		<i>oude omschr.</i>	<i>[ZAND,***,90,3] uiterst fyn, grysblond, ENKELE FYNE houtresten, enkele fyne schelprestjes.</i>							
66.00	68.00	zand	zwak grindig, licht-grijs-geel, Zand: uiterst fijn (O), Grind: witte kwarts, Organisch materiaal: weinig hout, Schelpen: schelpen, schelpresten, kleistenen	100						3
		<i>oude omschr.</i>	<i>[ZAND,***,100,3] uiterst fyn, grysblond, ENKELE STERK VERWEERDE schelpresten, weinig houtresten, EEN enkel grindje O.A. gangkwarts EN kleisteenjes.</i>							
68.00	69.00	zand	licht-grijs-geel, Zand: matig grof (O), matig grote spreiding, Grind: spoor fijn grind, witte kwarts, Organisch materiaal: hout, Schelpen: schelpen, schelpresten, Turritella sp.	220						3
		<i>oude omschr.</i>	<i>[ZAND,***,220,3] matig grof, grysblond, grote spreiding, STERK VERWEERDE schelpresten O.A. turritella, FYNE houtresten, enkele fyne grindjes O.A. gangkwarts.</i>							
69.00	70.00	zand	zwak grindig, licht-grijs-geel, Zand: matig grof (O), matig grote spreiding, Grind: kwartsiet, Schelpen: spoor schelpen, spoor schelpresten	220						3
		<i>oude omschr.</i>	<i>[ZAND,***,220,3] matig grof, grysblond, grote spreiding, spoor schelpgruis, EEN enkel grindje O.A. kwartsiet.</i>							
70.00	72.00	zand	licht-grijs-geel, Zand: matig grof (O), matig grote spreiding, Schelpen: spoor schelpen, spoor schelpresten, kleibrokjes, veenbrokjes	240						3
		<i>oude omschr.</i>	<i>[ZAND,***,240,3] matig grof, grysblond, grote spreiding, spoor schelpgruis, ENKELE GEROLDE kleibrokken, ENKELE FYNE veenbrokjes.</i>							
72.00	74.00	zand	licht-grijs-geel, Zand: matig grof (O), Schelpen: spoor schelpen, spoor schelpresten, veel kleibrokjes	240						3
		<i>oude omschr.</i>	<i>[ZAND,***,240,3] matig grof, grysblond, spoor schelpgruis, VRY veel kleibrokjes.</i>							
74.00	75.00	zand	licht-geel-grijs, Zand: matig grof (O), Organisch materiaal: hout	240						3
		<i>oude omschr.</i>	<i>[ZAND,***,240,3] matig grof, blondgrys, houtresten.</i>							
75.00	76.00	zand	licht-geel-grijs, Zand: matig grof (O), Organisch materiaal: hout	240						3
		<i>oude omschr.</i>	<i>[ZAND,***,240,3] matig grof, blondgrys, SPOOR FYNE houtresten.</i>							
76.00	78.00	zand	licht-geel, Zand: matig fijn (O)	180						3
		<i>oude omschr.</i>	<i>[ZAND,***,180,3] matig fyn, blond.</i>							
78.00	80.00	zand	licht-geel, Zand: zeer fijn (O)	130						3
		<i>oude omschr.</i>	<i>[ZAND,***,130,3] zeer fyn, blond.</i>							
80.00	81.00	zand	licht-geel, Zand: matig fijn (O), matig grote spreiding, Organisch materiaal: weinig hout	180						3
		<i>oude omschr.</i>	<i>[ZAND,***,180,3] matig fyn, blond, grote spreiding, weinig houtresten.</i>							
81.00	82.00	zand	licht-geel, Zand: matig grof (O), Schelpen: spoor schelpen, spoor schelpresten	300						3
		<i>oude omschr.</i>	<i>[ZAND,***,300,3] matig grof, blond, spoor schelpgruis.</i>							
82.00	83.00	zand	kleilig , licht-geel, Zand: matig grof (O), matig grote spreiding, Schelpen: schelpen, schelpresten, spoor kalkconcreties	300						3
		<i>oude omschr.</i>	<i>[ZAND,***,300,3] matig grof, blond, grote spreiding, kleihoudend, FYNE schelpresten, enkele kalkconcreties.</i>							
83.00	84.00	zand	licht-geel-grijs, Zand: matig grof (O), matig grote spreiding, Schelpen: schelpen, schelpresten	260						3
		<i>oude omschr.</i>	<i>[ZAND,***,260,3] matig grof, blondgrys, grote spreiding, FYNE schelpresten.</i>							
84.00	86.00	zand	licht-geel-grijs, Zand: matig fijn (O), Schelpen: spoor schelpen, spoor schelpresten, kleibrokjes	200						3
		<i>oude omschr.</i>	<i>[ZAND,***,200,3] matig fyn, blondgrys, ENKELE FYNE kleibrokjes, spoor schelpresten.</i>							
86.00	87.00	zand	zwak grindig, licht-grijs-geel, Zand: matig fijn (O), Grind: witte kwarts, Schelpen: schelpen, schelpresten, weinig Cerastoderma sp.	155						3
		<i>oude omschr.</i>	<i>[ZAND,***,155,3] matig fyn, grysblond, schelpresten O.A. cardium, enkele grindjes O.A. gangkwarts.</i>							
87.00	88.00	zand	licht-grijs-geel, Zand: matig fijn (O), matig grote spreiding, Organisch materiaal: hout, Schelpen: schelpen, schelpresten, weinig Cerastoderma sp.	155						3
		<i>oude omschr.</i>	<i>[ZAND,***,155,3] matig fyn, grysblond, grote spreiding, WEINIG FYNE schelpresten O.A. cardium, FYNE houtresten.</i>							

Boven	Onder	Grondsoort	Omschrijving	M63	LU	SI	ZA	GR	OR	CA
88.00	89.00	zand	zwak grindig, licht-grijs-geel, Zand: matig fijn (O), matig grote spreiding, Grind: witte kwarts, Organisch materiaal: weinig hout, Schelpen: weinig schelpen, weinig schelpresten, weinig Cerastoderma sp., Macoma sp., Mytilus edulis, kleistenen	180						3
		<i>oude omschr.</i>	<i>[ZAND,***,180,3] matig fyn, grysblond, grote spreiding, weinig schelpresten O.A. mytilus, macoma EN cardium, weinig houtresten, enkele grindjes O.A. gangkwarts, ENKELE GEROLDE kleistenen.</i>							
89.00	90.00	zand	licht-grijs-geel, Zand: matig fijn (O), matig grote spreiding, Schelpen: spoor schelpen, spoor schelpresten	160						3
		<i>oude omschr.</i>	<i>[ZAND,***,160,3] matig fyn, grysblond, grote spreiding, spoor schelpgruis.</i>							
90.00	91.00	zand	grijs, Zand: zeer grof (O), Organisch materiaal: hout, Schelpen: schelpen, schelpresten, weinig Cerastoderma sp.	310						3
		<i>oude omschr.</i>	<i>[ZAND,***,310,3] zeer grof, grys, WEINIG FYNE schelpresten O.A. cardium, FYNE houtresten.</i>							
91.00	92.00	zand	grijs, Zand: matig fijn (O), matig grote spreiding, Organisch materiaal: hout, Schelpen: weinig schelpen, weinig schelpresten, weinig Cerastoderma sp., Macoma sp., Mytilus edulis, kleibrokjes	210						3
		<i>oude omschr.</i>	<i>[ZAND,***,210,3] matig fyn, grys, grote spreiding, weinig schelpresten O.A. mytilus, cardium EN macoma OBLIGUA, FYNE houtresten, kleibrokken {stenen}.</i>							
92.00	93.00	zand	licht-grijs-geel, Zand: zeer fijn (O), Schelpen: spoor schelpen, spoor schelpresten, spoor kleibrokjes	145						3
		<i>oude omschr.</i>	<i>[ZAND,***,145,3] zeer fyn, grysblond, spoor schelpgruis, enkele kleibrokken.</i>							
93.00	94.00	zand	licht-geel, Zand: matig fijn (O), Organisch materiaal: weinig hout, Schelpen: weinig schelpen, Ensis sp., Macoma sp., Mytilus edulis, kleibrokjes	155						3
		<i>oude omschr.</i>	<i>[ZAND,***,155,3] matig fyn, blond, schelpen EN RESTEN O.A. mytilus, ensis EN macoma, enkele houtresten, kleibrokken {-stenen}.</i>							
94.00	95.00	zand	grijs, Zand: zeer fijn (O), matig grote spreiding, Schelpen: veel schelpen, veel schelpresten, Arctica islandica, weinig Cerastoderma sp., Ensis sp., Macoma sp., Mytilus edulis	145						3
		<i>oude omschr.</i>	<i>[ZAND,***,145,3] zeer fyn, grys, grote spreiding, veel schelpresten O.A. ensis, mytilus, cyprina, macoma EN cardium.</i>							
95.00	96.00	zand	grijs, Zand: matig grof (O), matig grote spreiding, Schelpen: weinig schelpen, weinig Cerastoderma sp., Ensis sp., Macoma sp.	280						3
		<i>oude omschr.</i>	<i>[ZAND,***,280,3] matig grof, grys, grote spreiding, schelpen EN RESTEN O.A. cardium, ensis EN macoma.</i>							
96.00	97.00	zand	grijs, Zand: matig grof (O), matig grote spreiding, Schelpen: veel schelpen, weinig Cerastoderma sp., Ensis sp., Macoma sp., Mya sp., Mytilus edulis	280						3
		<i>oude omschr.</i>	<i>[ZAND,***,280,3] matig grof, grys, grote spreiding, veel schelpen EN RESTEN O.A. cardium, ensis, mytilus, macoma EN mya ORENASIA.</i>							
97.00	98.00	klei	sterk siltig, licht-grijs, Schelpen: veel schelpen, veel schelpresten, weinig Cerastoderma sp., Ensis sp., Macoma sp., Mytilus edulis		30					3
		<i>oude omschr.</i>	<i>[KLEI,30,***,3] licht, lichtgrys, veel schelpresten O.A. cardium, ensis, mytilus EN macoma.</i>							
98.00	99.00	zand	zwak siltig, licht-geel-grijs, Zand: matig grof (O), Schelpen: veel schelpen, veel schelpresten, gelaagd	300						3
		<i>oude omschr.</i>	<i>[ZAND,***,300,3] matig grof, beige, gelaagd MET vette, taaiE, GRYZE kleilaagjes, ZEER veel schelpresten TOT 98.50</i>							
99.00	100.00	zand	siltig, grijs, Zand: matig grof (O), Schelpen: spoor schelpen, spoor schelpresten, kleibrokjes	260						3
		<i>oude omschr.</i>	<i>[ZAND,***,260,3] matig grof, grys, enkele schelpresten, ENKELE lemigE kleibrokken.</i>							
100.00	102.00	zand	grijs, Zand: matig fijn (O)	155						3
		<i>oude omschr.</i>	<i>[ZAND,***,155,3] matig fyn, grys.</i>							
102.00	104.00	zand	licht-grijs-geel, Zand: matig grof (O), matig grote spreiding, Schelpen: weinig schelpen, weinig schelpresten, weinig Cerastoderma sp., Macoma sp.	260						3
		<i>oude omschr.</i>	<i>[ZAND,***,260,3] matig grof, grysblond, grote spreiding, weinig schelpresten O.A. macoma EN cardium.</i>							
104.00	105.00	zand	licht-grijs-geel, Zand: zeer grof (O), matig grote spreiding, Schelpen: weinig schelpen, weinig schelpresten, weinig Cerastoderma sp., Macoma sp.	340						3
		<i>oude omschr.</i>	<i>[ZAND,***,340,3] zeer grof, grysblond, grote spreiding, weinig schelpresten O.A. macoma EN cardium.</i>							
105.00	106.00	zand	zwak grindig, licht-grijs-geel, Zand: zeer grof (O), matig grote spreiding, Grind: kwartsiet, witte kwarts, Schelpen: weinig schelpen, Arctica islandica, weinig Cerastoderma sp., Macoma sp., spoor veenbrokjes	380						3
		<i>oude omschr.</i>	<i>[ZAND,***,380,3] zeer grof, grysblond, grote spreiding, schelpen EN RESTEN O.A. cardium, macoma EN cyprina, enkele veenbrokjes, enkele grindjes O.A. gangkwarts EN kwartsiet.</i>							

Boven	Onder	Grondsoort	Omschrijving	M63	LU	SI	ZA	GR	OR	CA
106.00	107.00	zand	zwak grindig, licht-grijs-geel, Zand: uiterst grof (O), Grind: kwartsiet, vuursteen, witte kwarts, Schelpen: veel schelpen, Arctica islandica, weinig Cerastoderma sp., zandverkitting	430						3
		<i>oude omschr.</i>	<i>[ZAND,***,430,3] uiterst grof, grysblood, VRY veel schelpen EN RESTEN O.A. cyprina EN cardium, grindjeS O.A. gangkwarts, zandverkittingen, ZWARTE vuursteen EN kwartsiet.</i>							
107.00	110.00	zand	licht-geel, Zand: zeer grof (O), Organisch materiaal: spoor plantenresten, Schelpen: veel schelpen, Arctica islandica, Astartidae, Turritella sp., glimmer, kleistenen	380						3
		<i>oude omschr.</i>	<i>[ZAND,***,380,3] zeer grof, blond, VRY veel schelpen EN RESTEN O.A. cyprina, turritella, CORBULA EN astarte, GEROLDE kleistenen, spoor plantenresten, glimmers.</i>							
110.00	113.00	zand	licht-grijs-geel, Zand: zeer grof (O), Schelpen: schelpen, schelpresten, Arctica islandica, weinig Cerastoderma sp., zandverkitting, spoor leembrokjes	320						3
		<i>oude omschr.</i>	<i>[ZAND,***,320,3] zeer grof, grysblood, schelpresten O.A. cardium EN cyprina, zandverkittingen, enkele leembrokjes.</i>							
113.00	115.00	zand	licht-grijs-geel, Zand: matig grof (O), kleistenen	240						3
		<i>oude omschr.</i>	<i>[ZAND,***,240,3] matig grof, grysblood, kleistenen.</i>							
115.00	120.00	zand	grijs, Zand: matig fijn (O), glimmer, kleistenen	160						3
		<i>oude omschr.</i>	<i>[ZAND,***,160,3] matig fyn, grysblood, ENKELE kleisteentjes, glimmerhoudend.</i>							
120.00	121.00	zand	grijs, Zand: matig fijn (O), Schelpen: spoor schelpen, spoor schelpresten, glimmer, spoor kleibrokjes	160						3
		<i>oude omschr.</i>	<i>[ZAND,***,160,3] matig fyn, grysblood, glimmerhoudend, spoor schelpgruis, enkele kleibrokjes.</i>							
121.00	122.00	zand	sterk kleiig, grijs, Zand: matig fijn (O), Organisch materiaal: plantenresten, Schelpen: schelpen, schelpresten, weinig Cerastoderma sp.	200						3
		<i>oude omschr.</i>	<i>[ZAND,***,200,3] matig fyn, grysblood, sterk kleihoudend, kleilaagjes {brokken}, schelpresten O.A. cardium, ENKELE ZWARTE plantenresten.</i>							
122.00	123.00	zand	licht-grijs-geel, Zand: matig fijn (O), Schelpen: schelpen, schelpresten, Arctica islandica, weinig Cerastoderma sp., Macoma sp., spoor glimmer, spoor kleibrokjes	160						3
		<i>oude omschr.</i>	<i>[ZAND,***,160,3] matig fyn, grysblood, schelpresten O.A. cyprina, macoma EN cardium, enkele kleibrokken, zwak glimmerhoudend.</i>							
123.00	126.00	zand	licht-geel, Zand: matig fijn (O), Organisch materiaal: spoor plantenresten, Schelpen: spoor schelpen, spoor schelpresten, glimmer	155						3
		<i>oude omschr.</i>	<i>[ZAND,***,155,3] matig fyn, blond, spoor schelpresten, spoor plantenresten, glimmers.</i>							
126.00	127.00	zand	kleiig, licht-grijs-geel, Zand: matig fijn (O), Organisch materiaal: spoor plantenresten, Schelpen: schelpen, schelpresten, glimmer	180						3
		<i>oude omschr.</i>	<i>[ZAND,***,180,3] matig fyn, grysblood, schelpresten, glimmers, ENKELE kleiVERKITTINGEN, spoor plantenresten.</i>							
127.00	130.00	zand	licht-grijs-geel, Zand: matig fijn (O), Organisch materiaal: spoor plantenresten, Schelpen: spoor schelpen, spoor schelpresten, glimmer	160						3
		<i>oude omschr.</i>	<i>[ZAND,***,160,3] matig fyn, grysblood, spoor schelpgruis, spoor plantenresten, glimmers.</i>							

### Stratigrafie 1975

Boven	Onder	S	AS	LF	ST	Omschrijving
0.00	1.95	WED				Westland Formatie, Afzettingen van Duinkerke
1.95	3.45	WEH				Westland Formatie, Hollandveen
3.45	21.00	WEC				Westland Formatie, Afzettingen van Calais
21.00	39.70	KR				Formatie van Kreftenheye
39.70	65.00	KE	TE			Formatie van Kedichem of Formatie van Tegelen
65.00	86.00	TE	MS			Formatie van Tegelen of Formatie van Maassluis
86.00	130.00	MS				Formatie van Maassluis

### Stratigrafie 2003

Boven	Onder	S	AS	LF	ST	Omschrijving
0.00	1.95	NAWA				Formatie van Naaldwijk, Laagpakket van Walcheren
1.95	3.45	NIHO				Formatie van Nieuwkoop, Hollandveen Laagpakket
3.45	13.00	NAWO				Formatie van Naaldwijk, Laagpakket van Wormer
13.00	21.00	EC				Formatie van Echteld
21.00	30.00	KROC				Formatie van Kreftenheye, Laagpakket van Ockenburg

30.00 39.00 KR

Formatie van Kreftenheye

39.00 81.00 WA

Formatie van Waalre

81.00 130.00 MS

Formatie van Maassluis



-

# Boorstaat

-

<b>NITG-Boornummer</b>	B37H0537	<b>Coördinatenstelsel</b>	Rijksdriehoeksmeting
<b>X-coördinaat</b>	90980	<b>Bepaling lokatie</b>	
<b>Y-coördinaat</b>	429550	<b>Beschrijvingsmethode</b>	Onbekend
<b>Maaiveld (m tov NAP)</b>	-0.60	<b>Vertrouwelijkheid</b>	Openbaar
<b>Datum boring</b>	24-06-1986	<b>Werknummer</b>	37HR0537
<b>Plaatsnaam</b>	Rhoon		
<b>Provincie</b>	Zuid-Holland		
<b>Kaartblad</b>	37H		
<b>Soort boring</b>	Matig diepe boring derden		
<b>Einddiepte (m)</b>	135.00		
<b>Uitvoerder</b>	RGD - BTD		
<b>Boormethode</b>	Pulsboring		
<b>Opmerkingen</b>			

## Lithologie

<b>Beschrijver lagen</b>	Mensink, H.
<b>Organisatie beschrijver</b>	RGD
<b>Nat/droog</b>	Onbekend

## Stratigrafie 1975

<b>Beschrijver stratigrafie</b>	Zwaan, H.
<b>Organisatie beschrijver</b>	RGD
<b>Datum stratigrafie</b>	
<b>Versie stratigrafie</b>	1

## Stratigrafie 2003

<b>Beschrijver stratigrafie</b>	Kok, H.
<b>Organisatie beschrijver</b>	TNO-NITG
<b>Datum stratigrafie</b>	28-01-2001
<b>Versie stratigrafie</b>	1

## Oude beschrijving

\$8:Opmerkingen =21-5-1992. STRATIGRAFIE I.V.M. REGIS II. \$G:Boormethode =PULSBORING \$H:Boorlokatie =HOEVE JOHANNA  
 \$O:Kwaliteitsnr=211991 \$S:Typist =J KRAAKMAN \$T:Collationnr =37H

## Laagbeschrijving

Boven	Onder	Grondsoort	Omschrijving	M63	LU	SI	ZA	GR	OR	CA
0.00	0.85	klei	zwak siltig, bruin, ijzeroxide, puinresten, omgewerkte grond		36					3
		<i>oude omschr.</i>	<i>[KLEI,36,****,3] matig zwaar, bruin, roestig, geroerd MET puinresten.</i>							
0.85	1.60	klei	sterk siltig, zandig, sterk humeus, donker-bruin, Organisch materiaal: verspoelde plantenresten, Schelpen: schelpen, schelpresten, weinig Cerastoderma sp., glimmer, ijzeroxide, sterk gelaagd		30					3
		<i>oude omschr.</i>	<i>[KLEI,30,****,3] licht, sterk humeus, donkerbruin, gelaagd MET BEIGE zandlaagjes, roestvlekjes, TOP schelpresten O.A. cardium, NA 100 LICHTER {26%}, GRYS, sterk gelaagd MET UITERST FYNE zand- EN detrituslaagjes, glimmerhoudend.</i>							
1.60	2.30	zand	grijs, Zand: uiterst fijn (O), Organisch materiaal: verspoelde plantenresten, glimmer, zee-eggestekels, gelaagd	90	5					3
		<i>oude omschr.</i>	<i>[ZAND,5,90,3] uiterst fyn, gryns, gelaagd MET DUNNE, zandigE kleilaagjes, FYNE detrituslaagjes, glimmer, echinide stekels, BASIS IETS GROVER {m 150} EN BEIGE.</i>							
2.30	2.45	klei	zwak siltig, matig humeus, bruin, Organisch materiaal: spoor riet		36					1
		<i>oude omschr.</i>	<i>[KLEI,36,****,1] matig zwaar, humeus, bruin, FYNE rietrestjeS.</i>							
2.45	3.10	veen	zwak kleiig, onbekend, Organisch materiaal: zeggeveen, elzenhout, weinig hout, riet							
		<i>oude omschr.</i>	<i>[VEEN,***,****,*] rietzeggeveen, TOP iets kleiig, enkele houtrestjes O.A. els.</i>							
3.10	4.00	veen	onbekend, Organisch materiaal: rietveen, spoor hout							
		<i>oude omschr.</i>	<i>[VEEN,***,****,*] rietveen, OP 3.29 EEN kleilaagje, TOP EN BASIS EROSIEF, EEN ENKEL houtrestJE.</i>							
4.00	4.35	veen	onbekend, Organisch materiaal: bosveen							
		<i>oude omschr.</i>	<i>[VEEN,***,****,*] bosveen.</i>							
4.35	4.80	klei	matig siltig, humeus, donker-bruin, Organisch materiaal: hout, riet, zegge							

Boven	Onder	Grondsoort	Omschrijving	M63	LU	SI	ZA	GR	OR	CA
		<i>oude omschr.</i>	<i>[KLEI,***,***,*] matig zwaar, venig, donkerbruin, houtrestjes EN rietzegge.</i>							
4.80	5.00	veen	onbekend, Organisch materiaal: rietveen, weinig hout							
		<i>oude omschr.</i>	<i>[VEEN,***,***,*] rietveen, enkele houtrestjes.</i>							
5.00	5.30	veen	onbekend, Organisch materiaal: bosveen							
		<i>oude omschr.</i>	<i>[VEEN,***,***,*] bosveen.</i>							
5.30	6.30	klei	zwak siltig, grijs, Organisch materiaal: veel hout		38					1
		<i>oude omschr.</i>	<i>[KLEI,38,***,1] matig zwaar, gryns, veel houtrestjes.</i>							
6.30	6.90	klei	sterk siltig, humeus, grijs, Organisch materiaal: hout, riet, rietwortels, glimmer, gelaagd, top kalkloos		30					3
		<i>oude omschr.</i>	<i>[KLEI,30,***,3] licht, gryns, gelaagd met dunne zandlaagjes, TOP FYNE houtrestjes, NA 650 OOK doorworteld met riet, glimmer, BASIS IETS rietvenig, top ontkalkt.</i>							
6.90	7.40	veen	zwak kleilig, onbekend, Organisch materiaal: rietveen							
		<i>oude omschr.</i>	<i>[VEEN,***,***,*] rietveen, TOP iets kleilig.</i>							
7.40	8.05	klei	zwak siltig, humeus, bruin-grijs, Organisch materiaal: riet, rietwortels, glimmer, gelaagd		38					1
		<i>oude omschr.</i>	<i>[KLEI,38,***,1] matig zwaar, bruingryns, TOP rietvenig, doorworteld met riet, NA 765 LICHTER {32%}, gelaagd MET EEN ENKEL DUN zandlaagje, glimmer EN kalkhoudend {ca 4}.</i>							
8.05	8.50	klei	zwak siltig, grijs, Organisch materiaal: rietwortels		38					1
		<i>oude omschr.</i>	<i>[KLEI,38,***,1] matig zwaar, gryns, STERK doorworteld met riet.</i>							
8.50	12.00	klei	sterk siltig, grijs, Organisch materiaal: plantenresten, verspoelde plantenresten, Schelpen: weinig schelpen, glimmer		30					3
		<i>oude omschr.</i>	<i>[KLEI,30,***,3] licht, gryns, gelaagd met zandlaagjes, detrituslaagjes, FYNE plantenrestjes, glimmerhoudend, ENKELE FLUVIATIELE schelpjes O.A. LYMNIA EN OVATA, BASIS ZWARE ZAVEL {20%}.</i>							
12.00	13.00	klei	sterk siltig, grijs, Organisch materiaal: bladresten, weinig hout, verspoelde plantenresten, Schelpen: schelpen, schelpresten, glimmer, veel vivianiet, gelaagd		30					3
		<i>oude omschr.</i>	<i>[KLEI,30,***,3] licht, gryns, enkele houtrestjes, gelaagd met dunne zandlaagjes EN FYNE detrituslaagjes, FLUVIATIELE schelprestjes, glimmers, veel vivianiet, bladresten.</i>							
13.00	14.20	klei	zwak siltig, grijs, Organisch materiaal: plantenresten, bladresten, hout, verspoelde plantenresten		36					3
		<i>oude omschr.</i>	<i>[KLEI,36,***,3] matig zwaar, gryns, houtresten, plantenresten EN bladresten, detritus.</i>							
14.20	14.45	veen	onbekend, Organisch materiaal: rietveen, bladresten, hout							
		<i>oude omschr.</i>	<i>[VEEN,***,***,*] rietveen, houtresten EN bladresten.</i>							
14.45	15.30	klei	sterk siltig, grijs, Organisch materiaal: weinig plantenresten		28					3
		<i>oude omschr.</i>	<i>[KLEI,28,***,3] licht, gryns, weinig fyne plantenresten, OP 1490 EEN BEIGE zandlaagje {m 180}.</i>							
15.30	15.70	klei	zwak siltig, grijs-bruin, Organisch materiaal: hout, gelaagd		38					3
		<i>oude omschr.</i>	<i>[KLEI,38,***,3] matig zwaar, grynsbruin, FYNE houtrestjes, NA 1550 gelaagd MET MATIG GROVE {m 300}, BEIGE zandlaagjes, PLAATSELYK BLAUWGRYS.</i>							
15.70	17.00	zand	donker-geel-grijs, Zand: matig grof (O), Grind: spoor fijn grind, top kalkloos		300					3
		<i>oude omschr.</i>	<i>[ZAND,***,300,3] matig grof, bruinbeige, ENKELE IETS FYNERE LAAGJES, enkele zeer fyne grindjes, top ontkalkt.</i>							
17.00	20.00	zand	grindig, donker-geel-grijs, Zand: zeer grof (O), Grind: fijn grind, Organisch materiaal: verspoelde plantenresten, Schelpen: spoor schelpen, spoor schelpresten, weinig Cerastoderma sp., Scrobicularia plana		420					3
		<i>oude omschr.</i>	<i>[ZAND,***,420,3] zeer grof, bruinbeige, UITERST fyn grindhoudend, NA 1800 OOK enkele schelprestjes O.A. cardium EN scrobicularia, ENKELE GROVERE grindjes, WEINIG FYNE detritusRESTJES.</i>							
20.00	21.25	zand	donker-geel-grijs, Zand: matig grof (O), glimmer		300					3
		<i>oude omschr.</i>	<i>[ZAND,***,300,3] matig grof, bruinbeige, WAT glimmer, VERDER ALS VOORGAAND.</i>							
21.25	21.40	klei	zwak siltig, matig humeus, bruin, stevig		40					3
		<i>oude omschr.</i>	<i>[KLEI,40,***,3] matig zwaar, lemig, humeus, bruin, zeer taai, BASIS LICHTGRYS.</i>							
21.40	23.00	zand	sterk kleilig, grijs-blauw, Zand: uiterst fijn (O), glimmer, gelaagd		90					3
		<i>oude omschr.</i>	<i>[ZAND,***,90,3] uiterst fyn, grynsblauw, TOP sterk kleihoudend {20%} gelaagd, glimmer, NA 2180 BEIGE, BASIS MINDER kleihoudend {10%}.</i>							
23.00	23.75	zand	donker-geel-grijs, Zand: fijne categorie (O), Organisch materiaal: verspoelde plantenresten, glimmer, gelaagd		60	8				3
		<i>oude omschr.</i>	<i>[ZAND,8,60,3] UITERST fyn, bruinbeige, zeer zacht, glimmerhoudend, gelaagd, VEEL FYNE detritus.</i>							

Boven	Onder	Grondsoort	Omschrijving	M63	LU	SI	ZA	GR	OR	CA
23.75	23.90	klei	zwak siltig, matig humeus, bruin, stevig		36					3
		<i>oude omschr.</i>	<i>[KLEI,36,***,3] matig zwaar, humeus, bruin, zeer taai.</i>							
23.90	27.00	klei	sterk siltig, matig humeus, grijs, stevig		32					3
		<i>oude omschr.</i>	<i>[KLEI,32,***,3] licht, grys, zeer stug, PLAATSELYK IETS LICHTER {28-30%}, NA 2475 BLAUWGRYS, kalkloos {ca 0}, OP 2615 EEN humeus LAAGJE VAN 10 CM.</i>							
27.00	27.50	zand	kleilig, grijs, Zand: uiterst fijn (O), glimmer, zwak gelaagd	90	10					1
		<i>oude omschr.</i>	<i>[ZAND,10,90,1] uiterst fyn, grys, iets gelaagd, glimmer, BASIS MINDER kleihoudend {2%}.</i>							
27.50	27.80	klei	sterk siltig, matig humeus, bruin, gelaagd		26					2
		<i>oude omschr.</i>	<i>[KLEI,26,***,2] licht, humeus, bruin, gelaagd MET UITERST DUNNE EN fyne zandlaagjes {m 90}.</i>							
27.80	27.95	klei	zwak siltig, grijs		36					1
		<i>oude omschr.</i>	<i>[KLEI,36,***,1] matig zwaar, grys, IETS BLAUW, EEN ENKEL DUN zandlaagje</i>							
27.95	28.15	klei	sterk siltig, sterk humeus, bruin, gelaagd		30					1
		<i>oude omschr.</i>	<i>[KLEI,30,***,1] licht, sterk humeus, bruin, gelaagd MET UITERST FYNE EN dunne zandlaagjes, gyttjaachtig.</i>							
28.15	29.80	zand	matig humeus, licht-geel-grijs, Zand: zeer fijn (O), Organisch materiaal: weinig plantenresten, spoor glimmer, gelaagd	110						1
		<i>oude omschr.</i>	<i>[ZAND,***,110,1] zeer fyn, beige, PLAATSELYK M 90, gelaagd, ENKELE humeuze LAAGJES, enkele fyne plantenrestjes, iets glimmerhoudend.</i>							
29.80	30.00	klei	zwak siltig, blauw, stevig		40					1
		<i>oude omschr.</i>	<i>[KLEI,40,***,1] matig zwaar, blauw, zeer stug {leem}.</i>							
30.00	30.80	klei	sterk siltig, licht-geel-grijs		28					1
		<i>oude omschr.</i>	<i>[KLEI,28,***,1] licht, grysbeige, NA 3020 BLAUWGRYS.</i>							
30.80	31.40	klei	sterk siltig, groen-grijs		26					1
		<i>oude omschr.</i>	<i>[KLEI,26,***,1] licht, groengrys, NAAR BASIS LANGZAAM AFLOPEND {15%}.</i>							
31.40	31.80	zand	onbekend, Zand: zeer fijn (O)	110						1
		<i>oude omschr.</i>	<i>[ZAND,***,110,1] zeer fyn, GRAUWBEIGE, TOP EEN ENKEL dun kleilaagje.</i>							
31.80	34.00	zand	zwak kleilig, blauw-grijs, Zand: matig fijn (O), spoor glimmer	180	6					2
		<i>oude omschr.</i>	<i>[ZAND,6,180,2] matig fyn, iets kleihoudend, blauwgrys, NA 3200 MINDER kleihoudend {3%}, zwak glimmerhoudend.</i>							
34.00	35.00	zand	licht-geel, Zand: uiterst fijn (O), spoor glimmer	90						2
		<i>oude omschr.</i>	<i>[ZAND,***,90,2] uiterst fyn, blond, zwak kalkhoudend, spoor glimmer.</i>							
35.00	41.00	zand	zwak kleilig, grijs, Zand: matig fijn (O)	150	3					1
		<i>oude omschr.</i>	<i>[ZAND,3,150,1] matig fyn, grys, enkele kleilaagjes, NA 3700 kalkhoudend {ca 4}, BRUINGRYS, NIET MEER kleihoudend, NA 4000 zwak kleihoudend.</i>							
41.00	42.00	zand	grijs, Zand: zeer fijn (O)	110						3
		<i>oude omschr.</i>	<i>[ZAND,***,110,3] zeer fyn, grys, iets bont.</i>							
42.00	43.00	zand	grijs, Zand: matig fijn (O)	180						3
		<i>oude omschr.</i>	<i>[ZAND,***,180,3] matig fyn, grys, iets bont.</i>							
43.00	44.00	zand	grijs, Zand: matig grof (O), spoor glimmer	300						3
		<i>oude omschr.</i>	<i>[ZAND,***,300,3] matig grof, grys, zwak glimmerhoudend.</i>							
44.00	45.00	zand	licht-geel-grijs, Zand: zeer grof (O), Organisch materiaal: verspoelde plantenresten, Schelpen: spoor schelpen, spoor schelpresten	350						3
		<i>oude omschr.</i>	<i>[ZAND,***,350,3] zeer grof, grysbeige, iets bont, spoor schelpgruis, WAT FYNE detritus.</i>							
45.00	48.80	zand	grindig, bruin-grijs, Zand: zeer grof (O), matig grote spreiding, Grind: fijn grind, spoor zeer grof grind, granuul	420						3
		<i>oude omschr.</i>	<i>[ZAND,***,420,3] zeer grof, bruingrys, grote spreiding {m 150-420}, VEEL FYNERE KORRELS, EEN enkel grindje, AAN BASIS UITERST grove korrels {m 600}, fyn grindhoudend EN enkele grove grindjes.</i>							
48.80	49.00	klei	zwak siltig, groen-grijs		36					2
		<i>oude omschr.</i>	<i>[KLEI,36,***,2] matig zwaar, groengrys.</i>							
49.00	58.00	zand	kleilig, zwak siltig, bruin, Zand: uiterst fijn (O), glimmer, spoor kleibrokjes	105	5					3
		<i>oude omschr.</i>	<i>[ZAND,5,105,3] uiterst fyn, TOP bruin, enkele kleibrokjes, glimmer, TOT 5100 kleihoudend, NA 5300 GRYS, NA 5500 BRUINGRYS, VAN 5700-5800 ENKELE BLAUWGRYZE, vette {40%} kleilaagjes.</i>							
58.00	59.00	zand	grijs-blauw, Zand: matig grof (O), glimmer, kleibrokjes	220						3
		<i>oude omschr.</i>	<i>[ZAND,***,220,3] matig grof, grysbauw, ENKELE BLAUWGRYZE kleibrokjes, glimmer.</i>							
59.00	70.00	zand	bruin-grijs, Zand: matig fijn (O), Organisch materiaal: verspoelde plantenresten	180						3

Boven	Onder	Grondsoort	Omschrijving	M63	LU	SI	ZA	GR	OR	CA
		<i>oude omschr.</i>	[ZAND,***,180,3] matig fyn {m 150-210}, bruingrys, WAT FYNE detritus, VAN 6930-7000 ENKELE GRYZE, LICHTE {30%} kleilaagjes.							
70.00	72.00	zand	donker-geel-grijs, Zand: uiterst fijn (O), glimmer, granuul	105						3
		<i>oude omschr.</i>	[ZAND,***,105,3] uiterst fyn, bruinbeige, OOK ZEER VEEL grovere korrels, ENKELE LICHTE kleilaagjes {28%} TOT 7100, glimmer.							
72.00	73.00	zand	donker-geel-grijs, Zand: matig fijn (O)	150						3
		<i>oude omschr.</i>	[ZAND,***,150,3] matig fyn, bruinbeige.							
73.00	80.00	zand	zwak kleilig, donker-geel-grijs, Zand: uiterst fijn (O), Organisch materiaal: verspoelde plantenresten, veel glimmer, spoor kleibrokjes	105	3					3
		<i>oude omschr.</i>	[ZAND,3,105,3] uiterst fyn, bruinbeige, VRY veel glimmer, FYNE detritus, NA 7600 BRUIN, enkele kleibrokjes OF LAAGJES, iets kleihoudend.							
80.00	82.00	zand	kleilig, sterk zandig, licht-geel-grijs, Zand: matig fijn (O), glimmer	150	3					3
		<i>oude omschr.</i>	[ZAND,3,150,3] matig fyn, zwak kleihoudend, beige, glimmer, NA 8100 sterk kleihoudend {9-15%} TOT sterk zandigE klei, GRYS.							
82.00	85.00	zand	sterk humeus, grijs, Zand: uiterst fijn (O), Organisch materiaal: verspoelde plantenresten, veel glimmer	90	15					3
		<i>oude omschr.</i>	[ZAND,15,90,3] uiterst fyn, grys, sterk glimmerhoudend, PLAATSELYK BEIGE, NA 8290 ENKELE sterk humeuze LAAGJES EN FYNE detrituslaagjes.							
85.00	89.00	zand	kleilig, matig humeus, donker-grijs, Zand: uiterst fijn (O), Schelpen: spoor schelpen, spoor schelpresten, granuul, gelaagd	65						3
		<i>oude omschr.</i>	[ZAND,***,65,3] uiterst fyn, kleihoudend, grauwgrys, spoor fyn schelpgrijs, gelaagd MET DUNNE humeuze kleilaagjes, VERMENGD met grovere korrels.							
89.00	90.00	zand	kleilig, grijs, Zand: zeer fijn (O), zeer grote spreiding, Schelpen: spoor schelpen, kalkconcreties	120						3
		<i>oude omschr.</i>	[ZAND,***,120,3] zeer fyn, kleihoudend, grys, zeer grote spreiding, spoor schelpGGRUIS, kalkconcreties.							
90.00	91.00	zand	kleilig, grijs, Zand: uiterst fijn (O), Schelpen: spoor schelpen, spoor schelpresten, kleibrokjes	90						3
		<i>oude omschr.</i>	[ZAND,***,90,3] uiterst fyn, kleihoudend, grys, kleibrokjes, spoor fyn schelpgrijs.							
91.00	92.00	zand	kleilig, grijs, Zand: uiterst fijn (O), Schelpen: spoor schelpen, spoor schelpresten, spoor kleibrokjes	100						3
		<i>oude omschr.</i>	[ZAND,***,100,3] uiterst fyn, kleihoudend, grys, enkele kleibrokjes, spoor fyn schelpgrijs.							
92.00	93.00	zand	kleilig, grijs, Zand: zeer fijn (O), matig grote spreiding, Schelpen: spoor schelpen, spoor schelpresten	110						3
		<i>oude omschr.</i>	[ZAND,***,110,3] zeer fyn, kleihoudend, grys, grote spreiding, spoor zeer fyn schelpgrijs.							
93.00	94.00	zand	zwak kleilig, grijs, Zand: zeer fijn (O), Schelpen: schelpen, schelpresten, weinig Cerastoderma sp., Macoma sp., veel kleibrokjes	120						3
		<i>oude omschr.</i>	[ZAND,***,120,3] zeer fyn, zwak kleihoudend, grys, veel kleibrokken, schelpresten O.A. cardium EN macoma.							
94.00	95.00	zand	grindig, grijs, Zand: zeer fijn (O), Grind: fijn grind, kwartsiet, lydiet, Schelpen: veel schelpen, weinig Cerastoderma sp., kleibrokjes	140						3
		<i>oude omschr.</i>	[ZAND,***,140,3] zeer fyn, grys, ZEER veel schelpen O.A. cardium, fyne grindjes O.A. kwartsiet EN lydiet, GROVE kleibrokken.							
95.00	96.00	zand	sterk kleilig, grijs-blauw, Zand: uiterst fijn (O), Schelpen: schelpen, schelpresten	100						3
		<i>oude omschr.</i>	[ZAND,***,100,3] uiterst fyn, sterk kleihoudend, grysbauw, FYNE schelpresten.							
96.00	97.00	klei	zwak siltig, grijs, stevig, gelaagd		40					3
		<i>oude omschr.</i>	[KLEI,40,***,3] matig zwaar, grys, zeer taai, gelaagd MET ENKELE UITERST FYNE {m 90}, BEIGE zandlaagjes.							
97.00	98.00	zand	grijs, Zand: matig grof (O), Schelpen: schelpen, schelpresten, weinig Cerastoderma sp., kleibrokjes	300						3
		<i>oude omschr.</i>	[ZAND,***,300,3] matig grof, grys, kleibrokken, FYNE schelpresten O.A. cardium.							
98.00	99.00	zand	zwak kleilig, grijs, Zand: matig grof (O), matig grote spreiding, Schelpen: schelpen, schelpresten, weinig Cerastoderma sp., Macoma sp., Scrobicularia plana, spoor kleibrokjes	300						3
		<i>oude omschr.</i>	[ZAND,***,300,3] matig grof, zwak kleihoudend, grys, grote spreiding, enkele kleibrokjes, schelpresten O.A. cardium, macoma EN scrobicularia.							
99.00	102.00	zand	zwak kleilig, bruin-grijs, Zand: zeer grof (O), matig grote spreiding, Schelpen: schelpen, schelpresten, weinig Cerastoderma sp., Ensis sp., Macoma sp., Spisula sp., kleibrokjes	340						3
		<i>oude omschr.</i>	[ZAND,***,340,3] zeer grof, zwak kleihoudend, bruingrys, grote spreiding, schelpresten O.A. cardium, spisula, macoma EN ensis, kleibrokken.							
102.00	104.00	zand	grijs, Zand: matig grof (O), matig grote spreiding, Schelpen: schelpen, schelpresten, weinig Cerastoderma sp., Macoma sp., Spisula sp.	240						3

Boven	Onder	Grondsoort	Omschrijving	M63	LU	SI	ZA	GR	OR	CA
		<i>oude omschr.</i>	<i>[ZAND,***,240,3] matig grof, grys, grote spreiding, spoor schelpgruis EN schelpresten O.A. macoma, spisula EN cardium.</i>							
104.00	107.00	zand	grijs, Zand: matig fijn (O), Schelpen: weinig schelpen, weinig schelpresten	180						3
		<i>oude omschr.</i>	<i>[ZAND,***,180,3] matig fyn, grys, weinig fyn schelpgruis.</i>							
107.00	111.00	zand	kleilig, grijs, Zand: matig fijn (O), matig grote spreiding, Organisch materiaal: hout, Schelpen: veel schelpen, veel schelpresten, weinig Cerastoderma sp., Macoma sp., Spisula sp., Venerupis sp., kleibrokjes	200						3
		<i>oude omschr.</i>	<i>[ZAND,***,200,3] matig fyn, grys, grote spreiding, VRY veel schelpresten O.A. cardium, macoma, spisula EN venerupis, FYNE houtresten, kleiVERKITTINGEN, kleibrokken.</i>							
111.00	112.00	zand	kleilig, zwak grindig, grijs, Zand: matig grof (O), matig grote spreiding, Grind: kwartsiet, lydiet, schalie, Schelpen: veel schelpen, veel hele schelpen, schelpresten, weinig Cerastoderma sp., Gibbula sp., Macoma sp., Venerupis sp., kleibrokjes	250						3
		<i>oude omschr.</i>	<i>[ZAND,***,250,3] matig grof, kleihoudend, grys, grote spreiding, ZEER veel schelpen EN schelpresten O.A. macoma, cardium, venerupis EN gibbula, kleiVERKITTINGEN, wat grindJES O.A. lydiet, kwartsiet EN Kleisteen.</i>							
112.00	113.00	zand	grijs, Zand: matig fijn (O), Organisch materiaal: hout, Schelpen: schelpen, schelpresten, weinig Cerastoderma sp., Macoma sp., Venerupis sp.	190						3
		<i>oude omschr.</i>	<i>[ZAND,***,190,3] matig fyn, grys, schelpresten O.A. macoma, cardium EN venerupis, FYNE houtresten.</i>							
113.00	117.00	zand	grijs, Zand: matig fijn (O), Schelpen: spoor schelpen, spoor schelpresten, spoor kleibrokjes	175						3
		<i>oude omschr.</i>	<i>[ZAND,***,175,3] matig fyn, grys, spoor fyn schelpgruis, enkele kleibrokjes.</i>							
117.00	118.00	zand	grijs, Zand: matig grof (O), Schelpen: veel schelpen, veel schelpresten, weinig Cerastoderma sp., Macoma sp.	220						3
		<i>oude omschr.</i>	<i>[ZAND,***,220,3] matig grof, grys, veel schelpresten O.A. cardium EN macoma.</i>							
118.00	119.00	zand	grijs, Zand: matig fijn (O), Schelpen: schelpen, schelpresten	160						3
		<i>oude omschr.</i>	<i>[ZAND,***,160,3] matig fyn, grys, VRY VEEL ZEER FYN schelpgruis.</i>							
119.00	120.00	zand	grijs, Zand: matig fijn (O), Schelpen: schelpen, schelpresten, weinig Cerastoderma sp., Macoma sp., kleibrokjes	180						3
		<i>oude omschr.</i>	<i>[ZAND,***,180,3] matig fyn, grys, kleibrokjes, schelpresten O.A. cardium EN macoma.</i>							
120.00	121.00	zand	zwak kleilig, grijs, Zand: matig fijn (O), Schelpen: schelpen, schelpresten	150						3
		<i>oude omschr.</i>	<i>[ZAND,***,150,3] matig fyn, iets kleihoudend, grys, FYN schelpgruis.</i>							
121.00	122.00	zand	grijs, Zand: matig fijn (O), Schelpen: spoor schelpen, spoor schelpresten	150						3
		<i>oude omschr.</i>	<i>[ZAND,***,150,3] matig fyn, grys, spoor zeer fyn schelpgruis.</i>							
122.00	125.00	zand	zwak kleilig, grijs, Zand: matig grof (O), Organisch materiaal: hout, Schelpen: schelpen, schelpresten, Macoma sp., Venerupis sp., spoor kleibrokjes	220						3
		<i>oude omschr.</i>	<i>[ZAND,***,220,3] matig grof, zwak kleihoudend, grys, schelpresten O.A. venerupis EN macoma, enkele kleibrokken, FYNE houtresten.</i>							
125.00	127.00	zand	zwak kleilig, grijs, Zand: zeer fijn (O), matig grote spreiding, Organisch materiaal: hout, Schelpen: veel schelpen, weinig Cerastoderma sp.	120						3
		<i>oude omschr.</i>	<i>[ZAND,***,120,3] zeer fyn, zwak kleihoudend, grys, grote spreiding, VRY veel schelpen O.A. cardium, FYNE houtresten.</i>							
127.00	130.00	zand	grijs, Zand: uiterst fijn (O), Schelpen: spoor schelpen, spoor schelpresten, kleistenen	100						3
		<i>oude omschr.</i>	<i>[ZAND,***,100,3] uiterst fyn, grys, spoor zeer fyn schelpgruis, kleistenen.</i>							
130.00	134.00	zand	grijs, Zand: zeer fijn (O), Schelpen: spoor schelpen, spoor schelpresten	140						3
		<i>oude omschr.</i>	<i>[ZAND,***,140,3] zeer fyn, grys, spoor zeer fyn schelpgruis.</i>							
134.00	135.00	zand	grijs, Zand: matig fijn (O), Schelpen: schelpen, schelpresten, weinig Cerastoderma sp., Macoma sp., Mytilus edulis, Venerupis sp.	210						3
		<i>oude omschr.</i>	<i>[ZAND,***,210,3] matig fyn, grys, schelpresten O.A. venerupis, cardium, macoma EN mytilus.</i>							

### Stratigrafie 1975

Boven	Onder	S	AS	LF	ST	Omschrijving
0.00	2.45	WE				Westland Formatie
2.45	4.35	WEH				Westland Formatie, Hollandveen
4.35	4.80	WE				Westland Formatie
4.80	5.30	WEH				Westland Formatie, Hollandveen
5.30	6.90	WE				Westland Formatie
6.90	7.40	WEH				Westland Formatie, Hollandveen
7.40	14.20	WE				Westland Formatie

14.20	14.45	WEH		Westland Formatie, Hollandveen
14.45	15.70	WE		Westland Formatie
15.70	23.75	KR	EE	Formatie van Kreftenheye of Eem Formatie
23.75	93.00	KE	TE	Formatie van Kedichem of Formatie van Tegelen
93.00	135.00	MS		Formatie van Maassluis

**Stratigrafie 2003**

Boven	Onder	S	AS	LF	ST	Omschrijving
0.00	0.85	AAOM				Antropogeen, omgewerkte grond
0.85	2.30	NAWA				Formatie van Naaldwijk, Laagpakket van Walcheren
2.30	4.35	NIHO				Formatie van Nieuwkoop, Hollandveen Laagpakket
4.35	4.80	EC				Formatie van Echteld
4.80	5.30	NIHO				Formatie van Nieuwkoop, Hollandveen Laagpakket
5.30	6.90	EC				Formatie van Echteld
6.90	7.40	NIHO				Formatie van Nieuwkoop, Hollandveen Laagpakket
7.40	14.20	EC				Formatie van Echteld
14.20	14.45	NIHO				Formatie van Nieuwkoop, Hollandveen Laagpakket
14.45	15.70	KRWY				Formatie van Kreftenheye, Laag van Wijchen
15.70	21.25	KR				Formatie van Kreftenheye
21.25	85.00	WA				Formatie van Waalre
85.00	135.00	MS				Formatie van Maassluis





## Appendix 4. TGA results

labcode	inweeg	105	450	550	800	1000	vocht	LOI (105-1000)	Analyse tijd	Methode	Datum	
unit	gram	%	%	%	%	%	%	%	hh:mm:ss	TGA701		
<b>ise 921</b> (kwaliteits controle ise 921 tga701.xls 12.01.2012)												
average shewhartkaart		2,079	7,074	1,264	4,983	0,073						Opmerkingen
X+3S		3,248	7,808	1,770	5,519	0,316						
X-3S		0,910	6,340	0,758	4,448	-0,171						
ise921	1,2631	1,603	7,225	1,127	4,996	0,058	1,603	13,406	5:48:48	TNO	7-17-14 4:00 PM	
ise921	1,7107	1,772	7,156	1,19	5,026	0,089	1,772	13,461	4:18:32	TNO	7-21-14 5:21 PM	

<b>Samples</b>												
labcode	inweeg	105	450	550	800	1000	vocht	LOI (105-1000)	Analyse tijd	Methode	Datum	Opmerkingen
unit	gram	%	%	%	%	%	%	%	hh:mm:ss	TGA701		
2014010001	3,8485	1,142	2,187	0,404	1,608	0,08	1,142	4,279	5:48:48	TNO	7-17-14 4:00 PM	D90-91
2014010002	3,659	0,297	0,288	0,107	1,67	0,035	0,297	2,100	5:48:48	TNO	7-17-14 4:00 PM	D101-102
2014010003	4,0513	0,777	0,921	0,399	2,639	0,049	0,777	4,008	5:48:48	TNO	7-17-14 4:00 PM	D105-106
2014010004	3,146	2,367	2,038	1,33	7,579	0,1	2,367	11,047	5:48:48	TNO	7-17-14 4:00 PM	D109-110
2014010005	3,1219	1,636	2,167	1,138	6,167	0,096	1,636	9,568	5:48:48	TNO	7-17-14 4:00 PM	D113-114
2014010006	3,3047	3,798	4,164	1,838	4,48	0,605	3,798	11,087	5:48:48	TNO	7-17-14 4:00 PM	D118-119
2014010007	3,4471	1,157	1,094	0,471	2,502	0,057	1,157	4,124	5:48:48	TNO	7-17-14 4:00 PM	D121-122

2014010008	3,7711	0,472	0,614	0,212	2,424	0,046	0,472	3,296	5:48:48	TNO	7-17-14 4:00 PM	D125-126
2014010009	3,1075	0,377	0,682	0,105	1,245	0,024	0,377	2,056	5:48:48	TNO	7-17-14 4:00 PM	D129-130
2014010010	2,6724	0,764	0,873	0,369	1,766	0,052	0,764	3,060	5:48:48	TNO	7-17-14 4:00 PM	D133-134
2014010011	3,7714	1,151	1,6	0,792	4,379	0,061	1,151	6,832	5:48:48	TNO	7-17-14 4:00 PM	D137-138
2014010012	3,0618	1,663	2,316	0,925	3,094	0,085	1,663	6,420	5:48:48	TNO	7-17-14 4:00 PM	D141-142
2014010013	3,7868	0,71	0,826	0,406	2,345	0,071	0,71	3,648	5:48:48	TNO	7-17-14 4:00 PM	D145-146
2014010014	3,0713	0,183	0,333	0,114	1,264	0,029	0,183	1,740	5:48:48	TNO	7-17-14 4:00 PM	D149-150
2014010015	3,3045	2,909	3,479	1,572	4,616	0,135	2,909	9,802	5:48:48	TNO	7-17-14 4:00 PM	D153-154
2014010016	2,0658	0,229	0,561	0,142	1,951	0,025	0,229	2,679	5:48:48	TNO	7-17-14 4:00 PM	D157-158
2014010017	3,3297	1,3	1,447	0,893	4,041	0,077	1,3	6,458	5:48:48	TNO	7-17-14 4:00 PM	D161-162
2014010018	3,7098	0,177	0,183	0,095	1,133	0,029	0,177	1,440	5:48:48	TNO	7-17-14 4:00 PM	D165-166
2014010019	2,2375	0,383	1,115	0,137	2,213	0,031	0,383	3,496	4:18:32	TNO	7-21-14 5:21 PM	D169-170
2014010020	2,8673	0,317	0,264	0,152	1,122	0,04	0,317	1,578	4:18:32	TNO	7-21-14 5:21 PM	D173-174
2014010021	1,5425	1,694	2,017	1,166	3,755	0,104	1,694	7,042	4:18:32	TNO	7-21-14 5:21 PM	D177-178
2014010022	3,2036	1,956	2,192	1,342	2,856	0,102	1,956	6,492	4:18:32	TNO	7-21-14 5:21 PM	D181-182
2014010023	2,0737	0,251	0,486	0,168	8,784	0,022	0,251	9,460	4:18:32	TNO	7-21-14 5:21 PM	D185-186
2014010024	3,2675	2,809	2,651	1,627	2,246	0,322	2,809	6,846	4:18:32	TNO	7-21-14 5:21 PM	D189-190
2014010025	2,8114	2,316	2,176	1,443	6,524	0,103	2,316	10,246	4:18:32	TNO	7-21-14 5:21 PM	D193-194
2014010026	3,6731	1,571	1,507	1,213	6,021	0,079	1,571	8,820	4:18:32	TNO	7-21-14 5:21 PM	D197-198
2014010027	3,2043	0,295	0,199	0,149	1,761	0,036	0,295	2,145	4:18:32	TNO	7-21-14 5:21 PM	D201-202
2014010028	3,1945	1,692	1,722	1,677	6,174	0,122	1,692	9,695	4:18:32	TNO	7-21-14 5:21 PM	D205-206
2014010029	1,7469	1,984	1,363	2,171	7,17	0,119	1,984	10,823	4:18:32	TNO	7-21-14 5:21 PM	D209-210
2014010030	3,7812	2,059	2,318	1,683	6,294	0,151	2,059	10,446	4:18:32	TNO	7-21-14 5:21 PM	D213-214